AD NUMBER
AD382057
CLASSIFICATION CHANGES
TO: **UNCLASSIFIED**
FROM: **CONFIDENTIAL**
LIMITATION CHANGES
TO: **Approved for public release; distribution is unlimited.**
FROM: **Distribution authorized to U.S. Gov't. agencies and their contractors; Critical Technology; MAY 1967. Other requests shall be referred to Air Force Rocket Propulsion Laboratory, Edwards AFB, CA. This document contains export-controlled technical data.**
AUTHORITY
31 MAY 1979, Group 4 per document making, DoDD 5200.10; AFRPL per ltr, 5 Feb 1986

AD 382 057

AUTHORITY: AFRPL
ltr. 5 Feb 86

THIS REPORT HAS BEEN DELIMITED
AND CLEARED FOR PUBLIC RELEASE
UNDER DOD DIRECTIVE 5200.20 AND
NO RESTRICTIONS ARE IMPOSED UPON
ITS USE AND DISCLOSURE.

DISTRIBUTION STATEMENT A

APPROVED FOR PUBLIC RELEASE;
DISTRIBUTION UNLIMITED.

SECURITY MARKING

The classified or limited status of this report applies to each page, unless otherwise marked.
Separate page printouts MUST be marked accordingly.

THIS DOCUMENT CONTAINS INFORMATION AFFECTING THE NATIONAL DEFENSE OF THE UNITED STATES WITHIN THE MEANING OF THE ESPIONAGE LAWS, TITLE 18, U.S.C., SECTIONS 793 AND 794. THE TRANSMISSION OR THE REVELATION OF ITS CONTENTS IN ANY MANNER TO AN UNAUTHORIZED PERSON IS PROHIBITED BY LAW.

NOTICE: When government or other drawings, specifications or other data are used for any purpose other than in connection with a definitely related government procurement operation, the U. S. Government thereby incurs no responsibility, nor any obligation whatsoever; and the fact that the Government may have formulated, furnished, or in any way supplied the said drawings, specifications, or other data is not to be regarded by implication or otherwise as in any manner licensing the holder or any other person or corporation, or conveying any rights or permission to manufacture, use or sell any patented invention that may in any way be related thereto.

AFRPL-TR-67-98

17

(Unclassified Title)
FREE STANDING PYROLYTIC GRAPHITE THRUST CHAMBERS FOR SPACE OPERATION AND ATTITUDE CONTROL

PHASE II: SMALL SCALE TESTING

J.G. Campbell
M.L. Haas
C.D. Coulbert

THE MARQUARDT CORPORATION
Van Nuys, California

MAY 1967

AIR FORCE ROCKET PROPULSION LABORATORY
Research and Technology Division
Air Force Systems Command
Edwards Air Force Base, California

AFRPL-TR-67-98

17

(Unclassified Title)
FREE STANDING PYROLYTIC GRAPHITE THRUST CHAMBERS FOR SPACE OPERATION AND ATTITUDE CONTROL

PHASE II: SMALL SCALE TESTING

J.G. Campbell
M.L. Haas
C.D. Coulbert

THE MARQUARDT CORPORATION
Van Nuys, California

MAY 1967

FOREWORD

(U) This report covers work performed by The Marquardt Corporation under Phase II, Small Scale Testing, of Contract No. AF04(611)-10790, during the period 15 June 1965 to 31 December 1966. The work was sponsored by the Air Force Rocket Propulsion Laboratory, Research and Technology Division, Edwards Air Force Base, California, Air Force Systems Command, United States Air Force, as Air Force Systems Command Project No. 3058, Air Force Program Element Code 6.24.05.18.4. The AFRPL Project Engineer was Captain R. W. Ogershok, RPRRE.

(U) The Project Manager, Mr. C. D. Coulbert, was responsible for the over-all program supervision. The Project Engineer, Mr. J. G. Campbell, was responsible for technical supervision.

(U) The report number assigned to this document by The Marquardt Corporation is 6118.

(U) This technical report has been reviewed and is approved.

Richard W. Ogershok, Captain, USAF
Project Engineer

ABSTRACT

(U) This Phase II report presents the results of a test firing evaluation of small scale (100-pound thrust), free standing, pyrolytic graphite (PG) thrust chambers for application to high energy upper stage and attitude control liquid rocket engines. Propellant combinations used in the test firings were LF_2/BA1014, LF_2/GH_2, and $N_2O_4/0.5N_2H_4$-0.5UDMH. The results of large scale (1000-pound thrust) test firings will be reported in a future final (Phase III) report. The results of previous analyses and material studies conducted prior to the small scale test firings are presented in the Phase I report (Reference 1).

(U) Forty-seven pyrolytic graphite thrust chambers were fabricated in a variety of configurations to evaluate design concepts developed under the Phase I work.

(C) During test firings with $N_2O_4/0.5N_2H_4$-0.5UDMH, eleven sea level PG chambers were tested at 100 psia chamber pressure, with a maximum accumulated duration on one chamber of 300 seconds, including one run of 200 seconds. During some of these tests, the PG chamber wall was film cooled by fuel supplied from orifices in the injector. The erosion rate at the throat during the 200 second run was less than 0.08 mil/sec. The accumulated firing time with sea level chambers was 1022 seconds.

(C) Three altitude PG chambers with 40:1 expansion nozzles each failed after about 16 seconds of test firing with $N_2O_4/0.5N_2H_4$-0.5UDMH. The probable cause of failure was the combined effects of thermal stresses and axial residual stresses on the outside of the throat.

(U) Test firings with LF_2/fuel were made at Marquardt's Magic Mountain Test Facility, using both gaseous hydrogen and a hydrazine blend (BA1014) as fuels. All testing with LF_2/fuel was made with sea level expansion nozzles. All tests were conducted at a chamber pressure of 100 psia, except for two tests made at 300 psia.

(C) Fourteen PG chambers were tested with LF_2/BA1014 for a total accumulated run time of 567 seconds. The longest single duration firing with LF_2/BA1014 was 135 seconds. The erosion rate at the throat was 0.075 mil/sec during the 135 second test. The erosion of the chamber near the injector was greater than the throat erosion. Attempts to eliminate this local erosion by film cooling with BA1014 were unsuccessful.

(C) Eleven PG chambers were tested with LF_2/GH_2 for a total accumulated run time of 305 seconds. The longest single duration run with LF_2/GH_2 was 100 seconds using 50% fuel film cooling. The throat erosion during this run was 0.09 mil/sec.

(U) The temperatures of the outside of the free standing PG chambers during firing were measured photographically by extended range film. These temperatures were about 3800°F when using LF_2/BA1014 or LF_2/GH_2. Oxidation of the outer chamber surfaces, which occurred due to the air environment, would not be a problem for operation in space.

(U) Three thrust chambers with a 40:1 expansion nozzle were vibrated to study the structural integrity of free standing PG chambers when exposed to boost vehicle vibration environments. A structural problem was found to exist at the nozzle throat, caused by high axial residual stresses on the outside surface. One thrust chamber failed at the throat during the vibration tests, but the other portions of the chamber were not damaged.

(U) Additional work was done in studying methods of fabrication which will minimize the residual stresses in the throat region of free standing PG chambers. This work will be reported after the Phase III Large Scale Testing has been completed.

CONTENTS

CONTENTS (Continued)

ILLUSTRATIONS

ILLUSTRATIONS (Continued)

ILLUSTRATIONS (Continued)

TABLES

I. INTRODUCTION

(U) Free standing pyrolytic graphite thrust chambers are being studied for possible use with attitude control and upper stage propulsion systems. Their greatest potential advantage is their extremely light weight. In addition, they may be capable of operating as uncooled thrust chambers over a wide range of duty cycles, and they may have longer operating life than other types of uncooled thrust chambers. The current study is divided into three phases: I. Analysis and Preliminary Design, II. Small Scale Testing, and III. Large Scale Testing. Phase I has been completed and the results are reported in Reference 1. This report presents the results of Phase II. The results of Phase III will be given in the final report of this series.

(U) Free standing pyrolytic graphite thrust chambers are fabricated in a high temperature furnace by deposition of a thin layer of carbon on a graphite mandrel which has the desired shape and dimensions of the final product. The carbon comes from the pyrolysis of a hydrocarbon gas, such as methane, hence the name pyrolytic graphite (PG). The pyrolytic graphite is separated from the mandrel after removal from the furnace, and after minor machining to final dimensions, the thrust chamber is completed. The pyrolytic graphite is highly impervious, and it has very high tensile strength up to at least 5000°F. However, the material is anisotropic, and it therefore is subject to greater residual and thermal stresses than more conventional materials.

(U) During the Phase I analysis and preliminary design (Reference 1), theoretical analyses were made of the temperature and stress distributions to be expected in free standing PG thrust chambers.

(U) The strength of pyrolytic graphite tubes made by a variety of deposition techniques was also investigated during Phase I. During the Small Scale Testing phase reported herein, thrust chambers made by several of these techniques were test fired.

(U) This report presents the results of the test firings, together with discussions of the fabrication and testing problems encountered, which probably were more severe for the small scale tests than they will be for the large scale tests.

II. HARDWARE DESIGN AND FABRICATION

A. Hardware for $N_2O_4/0.5N_2H_4$-0.5UDMH Test Firings

(U) For tests of pyrolytic graphite thrust chambers with $N_2O_4/0.5N_2H_4$-0.5UDMH, three injectors developed for the reaction control system of the Marquardt Apollo Service Module were used. All of the chambers were substrate nucleated (SN) pyrolytic graphite. The PG chambers procured for this program are tabulated in Table I. The nomenclature for the identification of the chambers consists of three numbers: First, the thrust level is designated by C100 for a 100-pound thrust chamber, the second dash number designates the configuration number for that thrust level, and the last number designates the serial numbers for each individual chamber. The individual components and the engine assemblies used in the test firings are described below.

1. C100-1 Pyrolytic Graphite Chambers

(U) The C100-1 chamber configuration had previously been tested at JPL and Marquardt under earlier programs (Reference 2). The throat diameter was 0.75 inch. Some of these chambers were already fabricated and available for testing. They were proof tested to 200 psig before test firing. The C100-1 configuration used end loading on a flared flange for attachment to the injector. An ATJ graphite flange was attached to the PG chamber flange by a phenolic cement, as shown in Figure 1.

2. C100-2 Pyrolytic Graphite Chambers

(U) The C100-2 chamber (Figure 2) had a sea level nozzle with a nominal expansion ratio of 1.8. The chamber was designed for attachment to 100-pound thrust injectors developed for the Apollo SM/RCS. The throat diameter was 0.868 inch. This configuration had a conical tapered end for attachment to a conical seat. This tapered joint depended on close tolerance of the angle of taper for sealing.

3. C100-3 Pyrolytic Graphite Chambers

(U) The C100-3 chamber (Figure 3) had a 40:1 conical expansion nozzle with a 15° half angle. The design was identical to that of the C100-2 configuration between the tapered injector end and the throat.

4. C100-4 Pyrolytic Graphite Chambers

(U) The C100-4 chambers (Figures 4 and 5) were identical to the C100-2 and C100-3 configurations in the combustion chamber, up to the throat. The 40:1 expansion nozzle was of the same configuration as the Apollo Service Module ACS engine, which required a very small radius of curvature (0.527 inch) downstream from the throat.

TABLE I

(U) PROCUREMENT OF PYROLYTIC GRAPHITE CHAMBERS

Chamber No.	Type of PG	Vendor
C100-1-1	Substrate nucleated	Union Carbide (HTM)
-2	Substrate nucleated	Union Carbide (HTM)
-3	Substrate nucleated	Union Carbide (HTM)
-4	Substrate nucleated	Union Carbide (HTM)
-5	Substrate nucleated	Union Carbide (HTM)
-6	Substrate nucleated	Union Carbide (HTM)
-7	Substrate nucleated	Union Carbide (HTM)
C100-2-1	Substrate nucleated	Union Carbide (HTM)
-2	Substrate nucleated	Union Carbide (HTM)
-3	Substrate nucleated	Union Carbide (HTM)
-4	Substrate nucleated	Super Temp Corp.
-5	Substrate nucleated	Super Temp Corp.
-6	Substrate nucleated	Super Temp Corp.
-7	Substrate nucleated	Super Temp Corp.
-8	Substrate nucleated	Super Temp Corp.
-9	Substrate nucleated	Super Temp Corp.
-10	Substrate nucleated	Super Temp Corp.
-11	Substrate nucleated	Super Temp Corp.
C100-3-1	Substrate nucleated	Union Carbide (HTM)
-2	Substrate nucleated	Union Carbide (HTM)
C100-4-1	Substrate nucleated	Union Carbide (HTM)
-2	Substrate nucleated	Union Carbide (HTM)
C100-5-1	Substrate nucleated	Super Temp Corp.
-2	Substrate nucleated	Super Temp Corp.
-3	Substrate nucleated	Super Temp Corp.
-4	Substrate nucleated	Super Temp Corp.
-5	Substrate nucleated	Super Temp Corp.
-6	Substrate nucleated	Super Temp Corp.
-7	Substrate nucleated	Super Temp Corp.

TABLE I (Continued)

Chamber No.	Type of PG	Vendor
C100-5-8	Substrate nucleated	Super Temp Corp.
-9	Substrate nucleated	Super Temp Corp.
-10	Substrate nucleated	Super Temp Corp.
-11	Substrate nucleated	Super Temp Corp.
-12	Substrate nucleated	Super Temp Corp.
-13	Substrate nucleated	Super Temp Corp.
-14	Substrate nucleated	Super Temp Corp.
-15	Substrate nucleated	Super Temp Corp.
C100-6-1	Controlled delaminations	Union Carbide (HTM)
-2	Controlled delaminations	Union Carbide (HTM)
-3	Controlled delaminations	Union Carbide (HTM)
C100-7-1	Boron doped	General Electric Co.
-2	Boron doped	General Electric Co.
-3	Boron doped	General Electric Co.
-4	Boron doped	General Electric Co.
-5	Boron doped	General Electric Co.
-6	Boron doped	General Electric Co.
-7	Boron doped	General Electric Co.

5. T13280 Uncooled Adapter

(U) An uncooled adapter (T13280) was used to connect the C100-1 PG chambers to the Apollo-type injectors, as shown in Figure 6. This adapter was made of L-605 alloy.

6. X22812 Water Cooled Adapter

(U) A water cooled adapter (shown in Figure 7) was made from Berylco 10, a beryllium-copper alloy with high thermal conductivity. The adapter was used to connect the chambers to the injectors.

7. X22830 Film Cooling Adapter

(U) An adapter (X22830) of the same size as the X22812 water cooled adapter was built with 16 film cooling holes (0.007-inch diameter) drilled into the manifold so that fuel jets flowing axially struck the PG wall at an angle of 11°. The fuel film cooling adapter (shown in Figure 8) was made of Berylco 10 alloy.

8. X22835 Metal Sea Level Chamber

(U) A sea level chamber was made from L-605 alloy and instrumented with thermocouples for film cooling tests. The inside contour of this chamber duplicated that of the 100-pound thrust PG chambers. The wall thickness was 0.080 inch. Attachment of the L-605 chamber to the injector and the film cooling adapter is shown in Figure 8.

9. T11549 Uncooled Adapter (Formerly X22805)

(U) The T11549 adapter was made of L-605 alloy. This adapter, the same size as the cooled adapters, was feasible with the Apollo-type injectors because the film cooling jets from the injectors impinged on the adapter, preventing overheating of the L-605 material.

10. 227997 Injector

(U) An 8 on 8 doublet injector (227997) developed for the Apollo SM/RCS Program was used for most of the tests of PG chambers. This injector had 8 film cooling holes which injected 12 percent of the total fuel flow toward the wall.

11. T13747 Injector

(U) An 8 on 8 doublet (T13747) with 27 percent fuel film cooling injected through 16 holes was used for several tests of PG chambers.

12. T9290 Injector

(U) A 12 on 12 doublet injector (T9290) was used for several tests. This injector did not have film cooling.

13. Engine Assemblies

(U) The C100-1 chamber was attached to the Apollo-type injector as shown in Figure 6, using the uncooled adapter T13280. The uncooled adapter was feasible because it was cooled by the film cooling injected from the Apollo-type injector. A seal between the adapter and the PG chamber was obtained by end loading on the edge of the PG chamber and the ATJ graphite flange, using a flat copper gasket.

(U) The C100-2, C100-3, and C100-4 chambers were attached to the Apollo-type injectors with an 11° tapered joint as shown in Figure 7. A split ring and a retaining ring were positioned on the outside surface of the PG chamber and an axial load was applied by six bolts.

B. Hardware for LF_2/BA1014 and LF_2/GH_2 Test Firings

(U) Pyrolytic graphite chambers were tested with six different injector configurations for LF_2/BA1014 firings and two injector configurations for LF_2/GH_2 firings.

1. C100-5 Pyrolytic Graphite Chambers

(U) The C100-5 chambers (Figure 9) were made of substrate nucleated PG with a nominal wall thickness of 0.060 inch in the combustion chamber and 0.045 inch in the throat.

2. C100-6 Pyrolytic Graphite Chambers

(U) The C100-6 chambers (Figure 10) were made from pyrolytic graphite with two controlled delaminations. The nominal wall thickness was 0.120 inch. The three layers were of approximately equal thickness and were very symmetrical throughout the chambers. The delaminations were deliberately caused by interruption of the deposition process. In this way, the overall wall thickness could be deposited to a thickness-to-radius ratio (t/r) greater than that feasible for a single layer.

3. C100-7 Pyrolytic Graphite Chambers

(U) The C100-7 chambers (Figure 11) were made of boron doped PG, containing about 0.5 percent boron. The nominal wall thicknesses were 0.080 inch in the combustion chamber and 0.060 inch in the throat. Figure 12 is a photograph of the C100-5 and C100-7 chambers.

4. X22487 Injector, LF_2/BA1014

(U) The X22487 injector (shown in Figure 13) was a six-element triplet, the center orifice being fluorine in each triplet. Details of the triplet element design are shown in Figure 14. This injector was made of 400 series Monel. The injector was self-cooled by the BA1014 fuel, as were all of the injectors used with BA1014.

5. X22487F Injector, LF_2/BA1014

(U) The X22487F injector was a modification of the X22487 injector, with six 0.011-inch fuel orifices added, one adjacent to each triplet. The extra fuel holes were directed axially. The orifice sizes for this injector are shown in Figure 14.

6. T11459 Injector, LF_2/BA1014

(U) The T11459 injector was similar to the X22487 injector except that the triplet elements were turned 7° outward toward the wall, as shown in Figure 14. This injector was made of 400 series Monel.

7. T14884-1 Injector, LF_2/BA1014

(U) The T14884-1 injector was made of Nickel 200 and used six triplet elements with a zero momentum angle and an impingement diameter of 1.41 inch. The triplet elements were raised above the injector face as shown in Figure 15. The oxidizer orifice diameter was 0.047 inch and the fuel orifice diameters were 0.025 inch.

8. Variable L* Injector (X22861-503), LF_2/BA1014

(U) The X22861-503 injector was made for LF_2/BA1014 firing in the variable L* configuration. This permitted the testing of the C100-5, C100-6, and C100-7 chambers with L* values ranging from 12 to 45 by the use of different length spacers (Figure 16). In this way, fuel film cooling could be injected against the PG chamber wall at various distances from the throat.

(U) The injector was made of Nickel 200, using six triplet elements with a zero momentum angle and an impingement diameter of 1.25 inch. The fluorine orifice diameter was 0.033 inch, the fuel orifice diameters were 0.014 inch, and the injector had twelve 0.010-inch fuel orifices to provide film cooling. The detailed design of the injector head is shown in Figure 17.

9. X22861 Mod Injector, LF_2/BA1014

(U) One test was made with the X22861 Mod injector, which was a modification of the X22861-503 injector with the fuel cooling orifices closed.

10. Fuel Sheet Injector (T13876-502), LF_2/GH_2

(U) The T13876-502 injector was made of copper for use with LF_2/GH_2. This injector had seven elements, each consisting of a fuel sheet surrounding a central oxidizer jet, as shown in Figures 18 and 19. The injector was self-cooled and it was designed to fit interchangeably with chambers and adapters for the T14884 injector. The injector did not have film cooling.

11. Triplet Injector (T14817), LF_2/GH_2

(U) The T14817 injector (formerly X22780) was made for LF_2/GH_2 in the variable L* configuration. This injector (shown in Figures 20 and 21) was made of copper, and consisted of six triplet elements, with GH_2 in the center orifice of each element, a zero momentum angle, and an impingement diameter of 1.25 inch. The fluorine orifice diameters were 0.018 inch, the hydrogen orifice diameters were 0.055 inch, and fuel film cooling orifices, when used, were 0.025 inch in diameter. This injector was used with no film cooling, with 33 percent film cooling (12 film holes), and 50 percent film cooling (24 film holes). The later configuration is shown in Figure 20. The injection velocity of the hydrogen in the 33 percent film cooling configuration was about Mach 0.6, and the fluorine velocity was about 84 ft/sec for a chamber pressure of 100 psia.

12. Fabrication Problems -- Nickel Injectors

(U) Considerable difficulty was encountered in drilling small diameter holes in Nickel 200 during fabrication of the variable L* injectors (X22861).

(U) Early test firing results with copper heat sink chambers had given some evidence that use of fuel injection velocities of about 120 ft/sec would produce 2 to 3 percent increase in performance compared to injection velocities of 60 ft/sec. This evidence was obtained by making tests with various total flow rates, so that the chamber pressure also varied.

(U) It was desired that 33 percent fuel film cooling be included in these injectors.

(U) It was anticipated that drilling of small holes in Nickel 200 would be difficult. Therefore, two basic designs evolved -- one with fuel injection velocities of about 120 ft/sec and the other with injection velocities of about 60 ft/sec -- as described below:

Injector	Approx. Fuel Injection Velocity (ft/sec)	Oxidizer Orifice Diameter (in.)	Fuel Orifice Diameter (in.)	No. of Film Cooling Holes	Film Cooling Orifice Diameter (in.)
X22861-501	120	0.0236	0.010	6	0.010
X22861-503	60	0.033	0.014	12	0.010

The l/d ratio did not exceed 10 for any of the orifices.

(U) The holes were drilled with a Sip Hydroptic-6 Jig Bore. Better results were obtained at 670 rpm than at the machine's maximum speed of 2000 rpm. This jig bore is capable of locating holes within 0.0001 inch. Turpentine was found to be the best lubricant.

(U) The first holes were drilled with high speed steel drills. Water flow of the head showed that many fuel pairs did not impinge very well. Microscopic examination of the holes showed a bellmouth shape near the exit. The exit was countersunk and deburred by hand. This brought some improvement in jet impingement. However, in some cases, the jets did not impinge well even though no burrs or bellmouth exits could be found.

(U) Carbide drills were tried but they broke off repeatedly. A spade drill made of high speed steel was also tried without success.

(U) An order for some 0.010-inch cobalt drills was placed with the Cleveland Twist Drill Co. Delivery was made several months after the order, which was too late for use on this program.

(U) Injector performance tests of the high velocity injector (X22861-501) with a copper heat sink chamber showed that fuel manifold boiling occurred after about 8 seconds of operation. The cause was not determined. Therefore, only the low velocity injector (X22861-503) was used for testing the PG chambers.

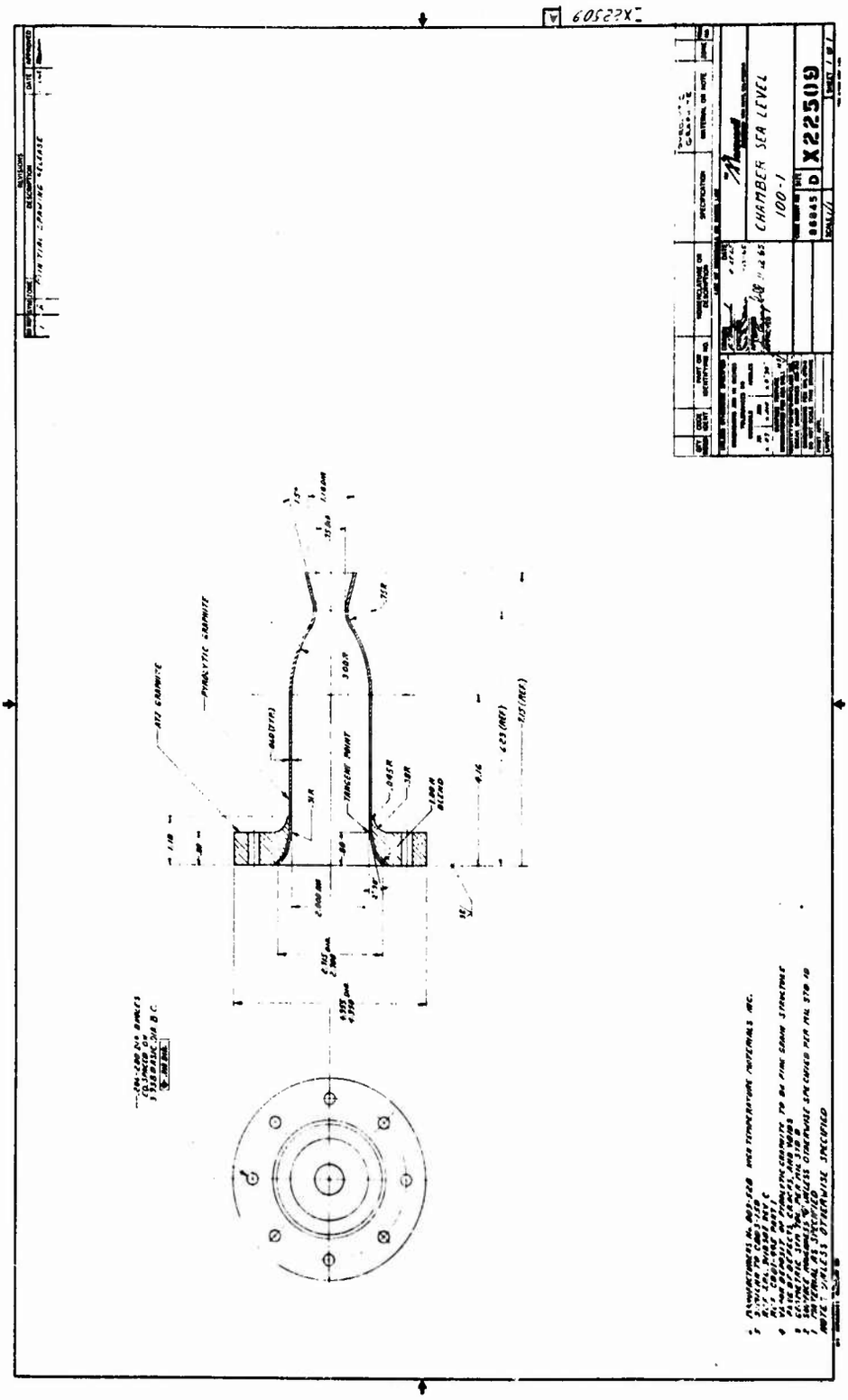

FIGURE 1. (U) Configuration of C100-1 Chamber

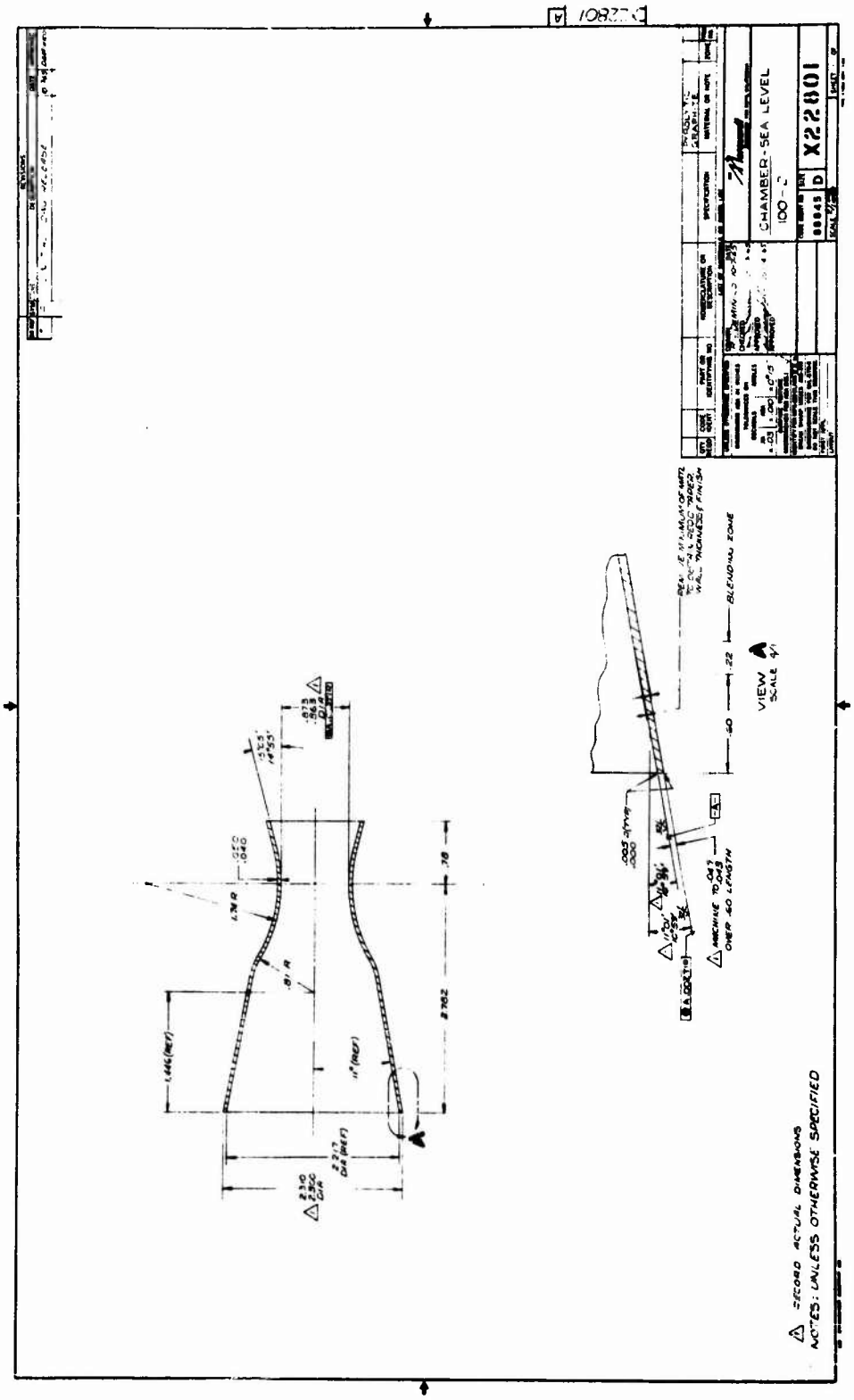

FIGURE 2. (U) Configuration of C100-2 Chamber

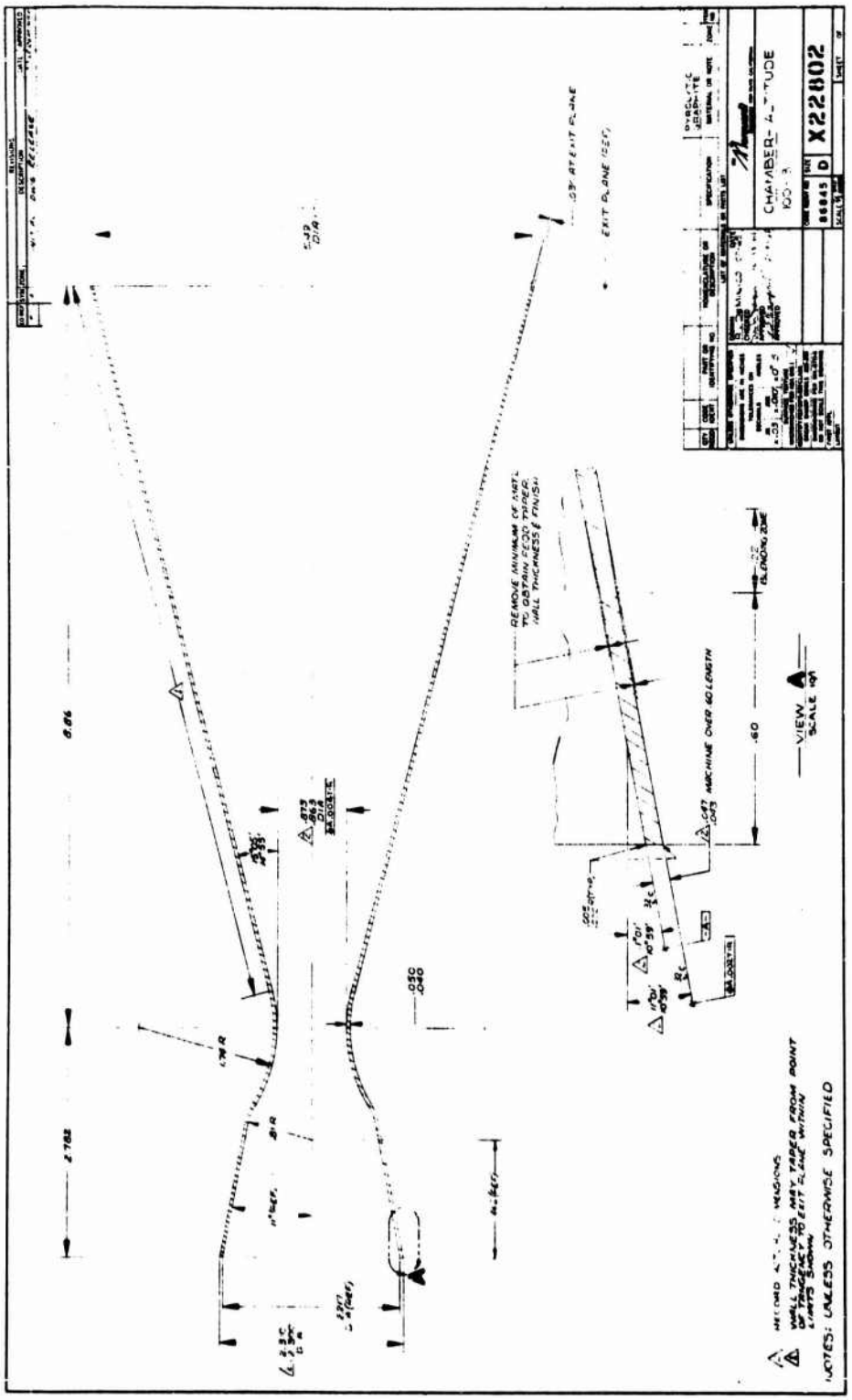

FIGURE 3. (U) Configuration of 7100-3 Chamber

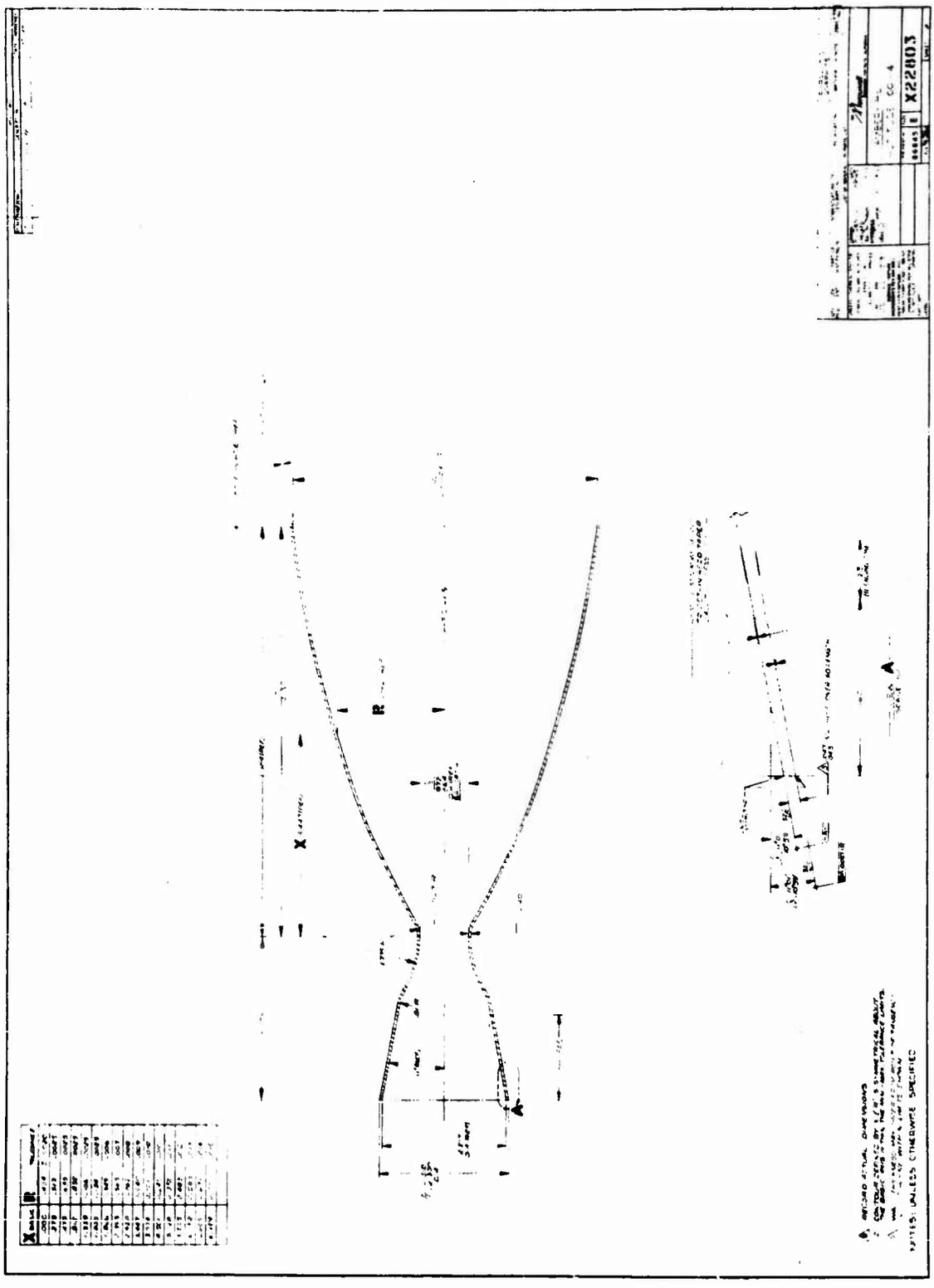

FIGURE 4. (U) Configuration of C100-4 Chamber

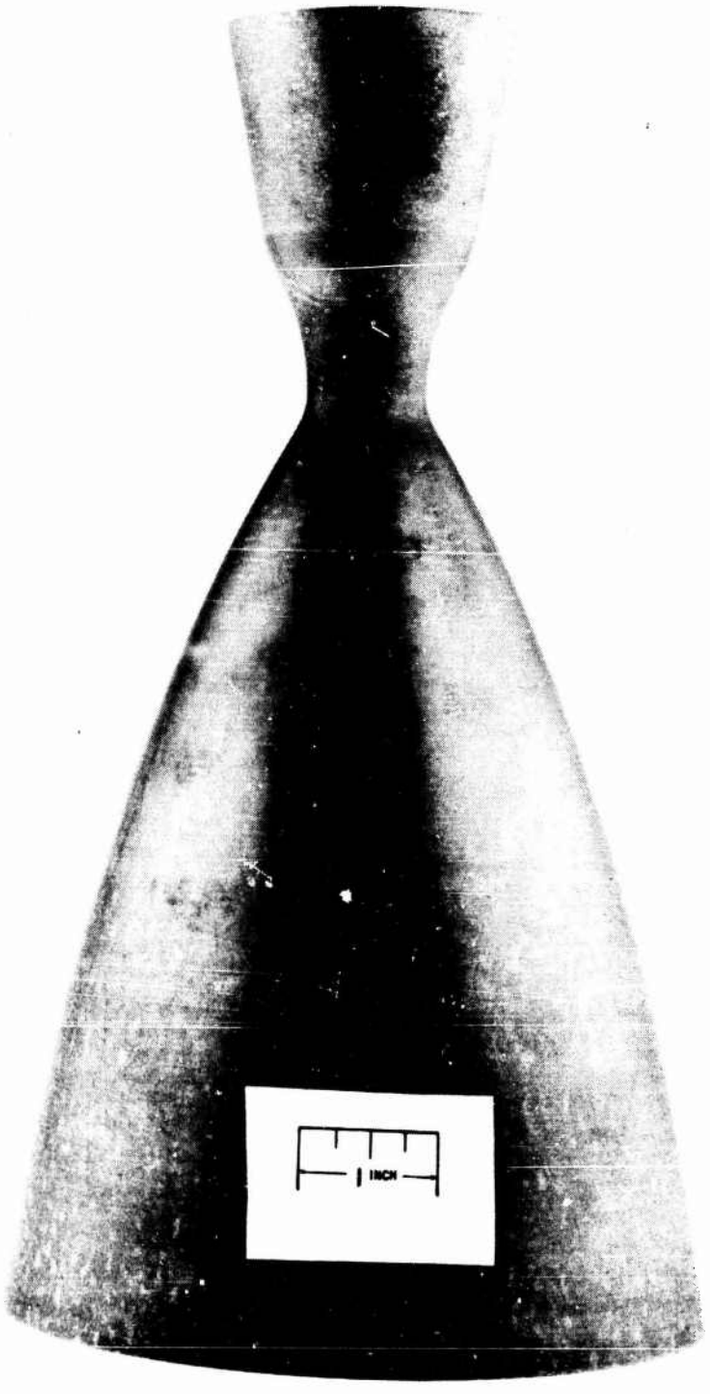

FIGURE 5. (U) C100-4 Chamber

T6015-2

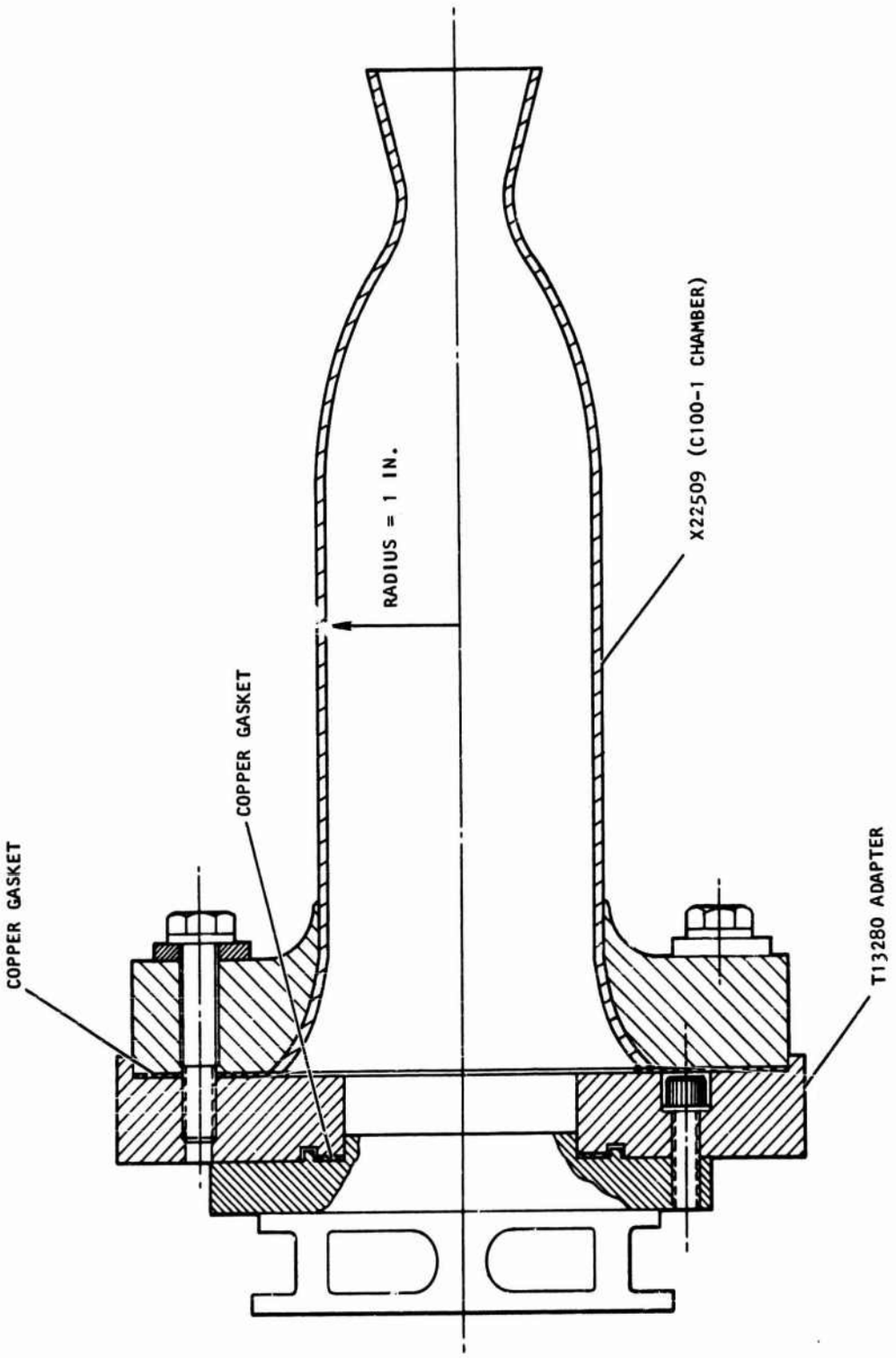

FIGURE 6. (U) Assembly of C100-1 Chamber Engine

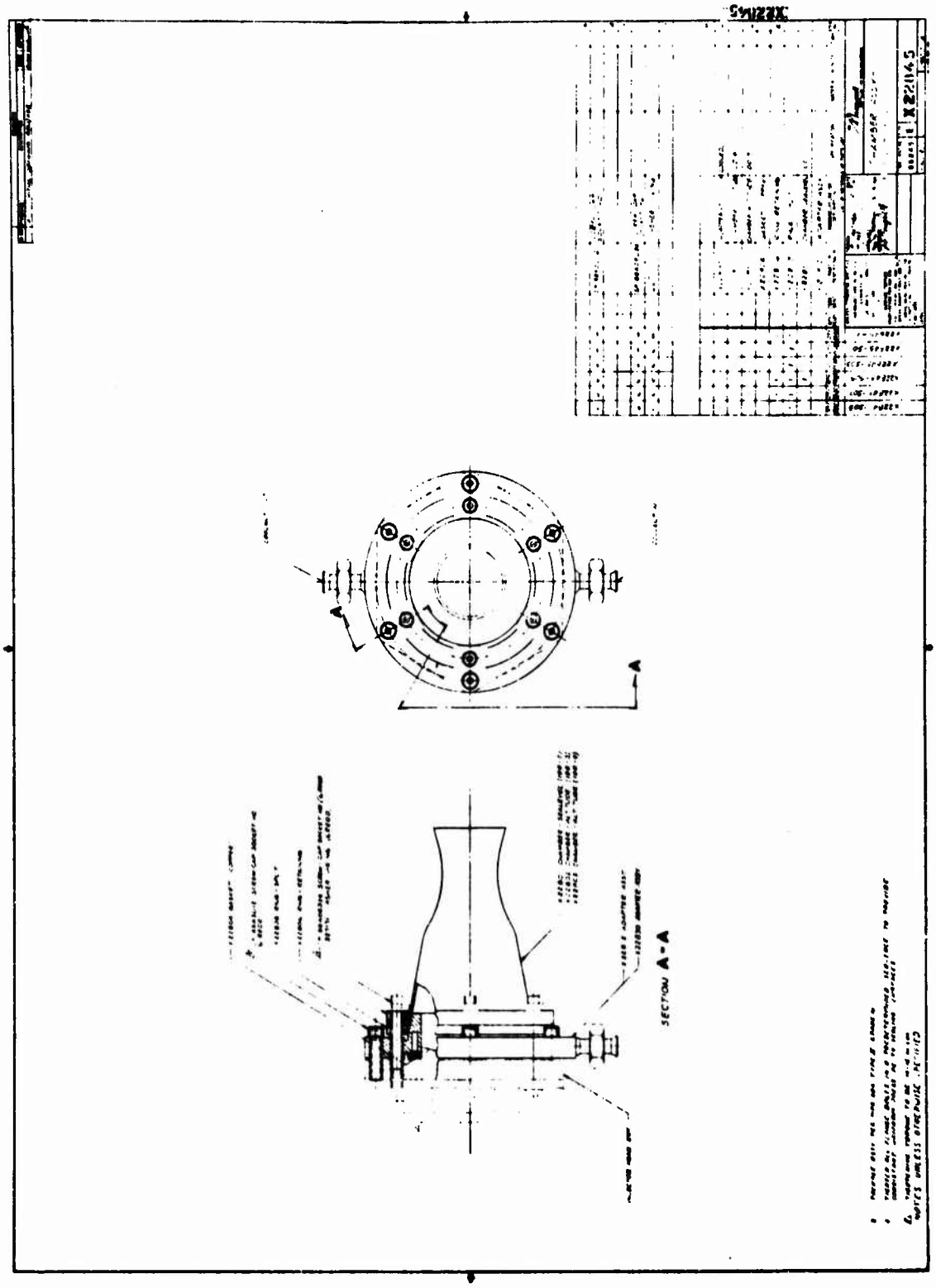

FIGURE 7. (U) Assembly of 100-lb Thrust Tapered Chamber Engine

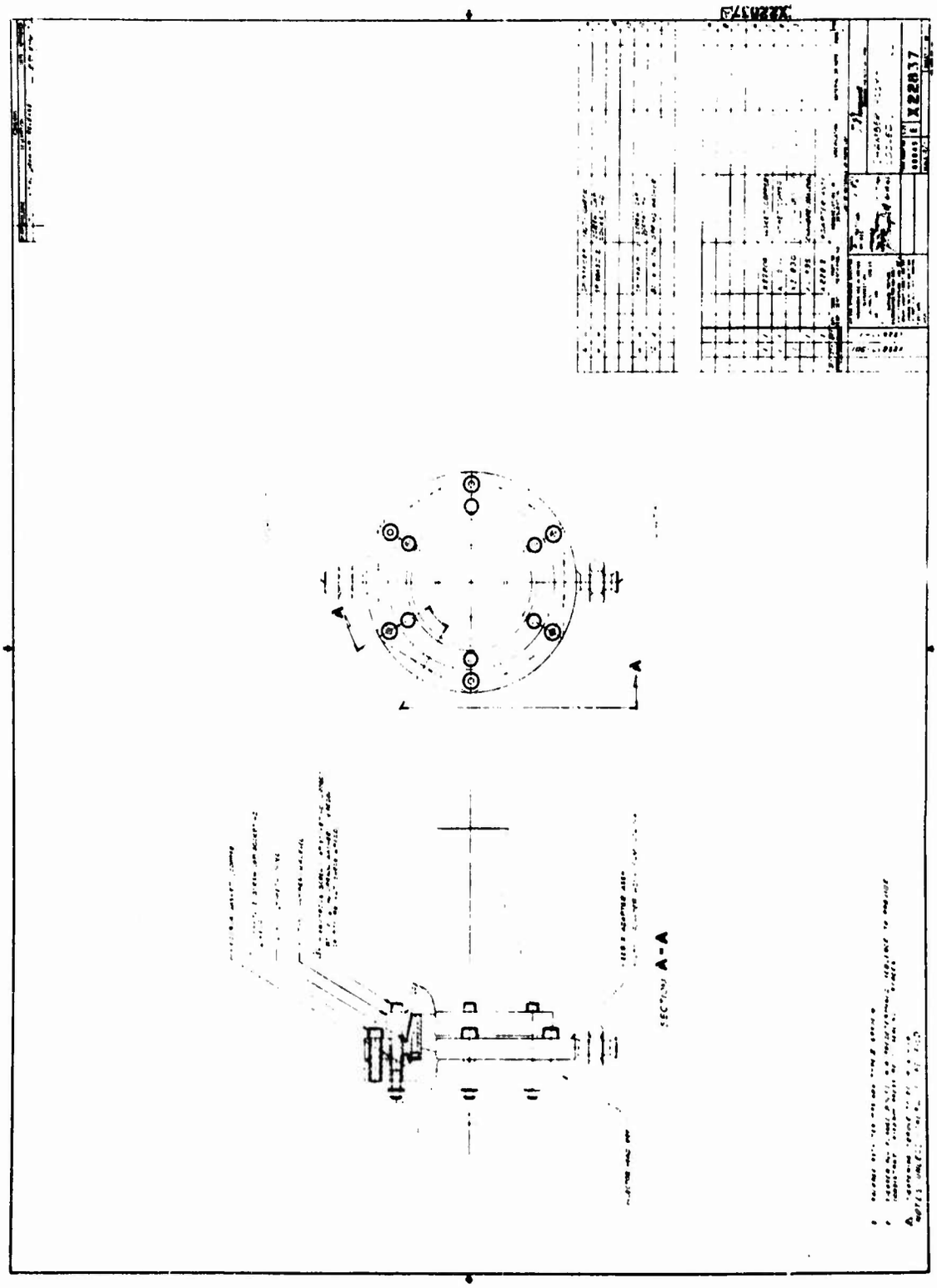

FIGURE 8. (U) Assembly of Film Cooled Chamber Engine

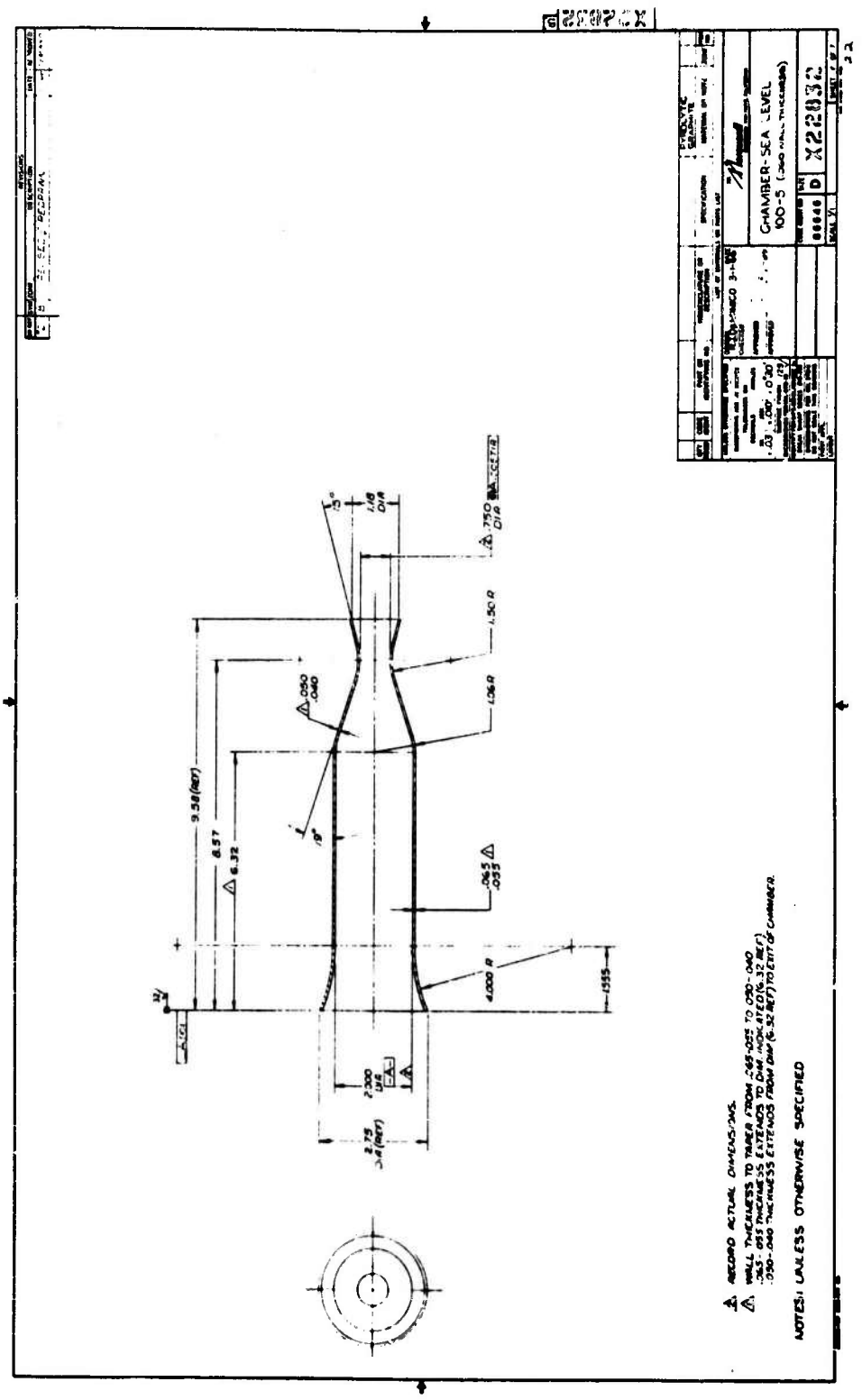

FIGURE 9. (U) Configuration of C100-5 Chamber

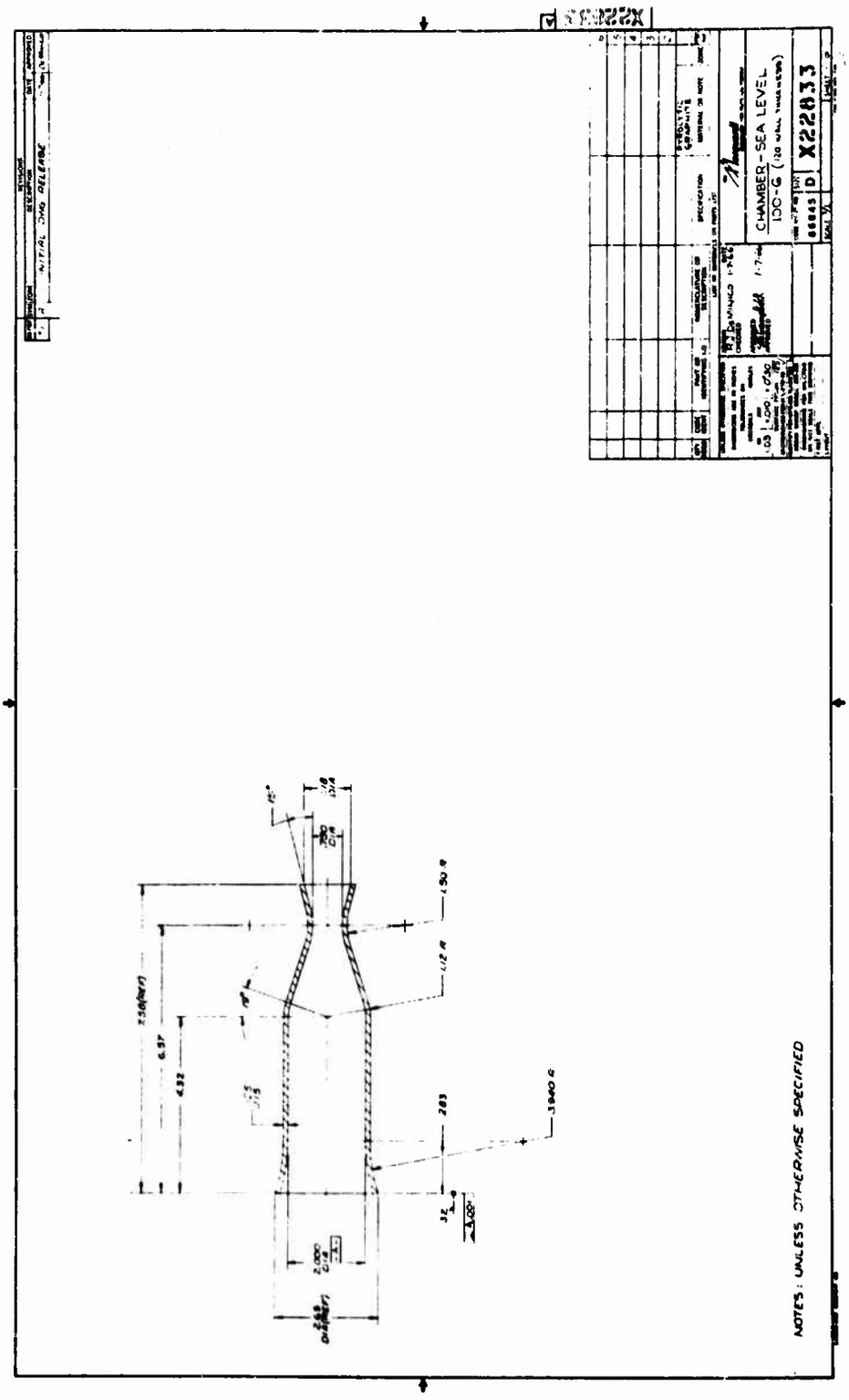

FIGURE 10. (U) Configuration of C100-6 Chamber

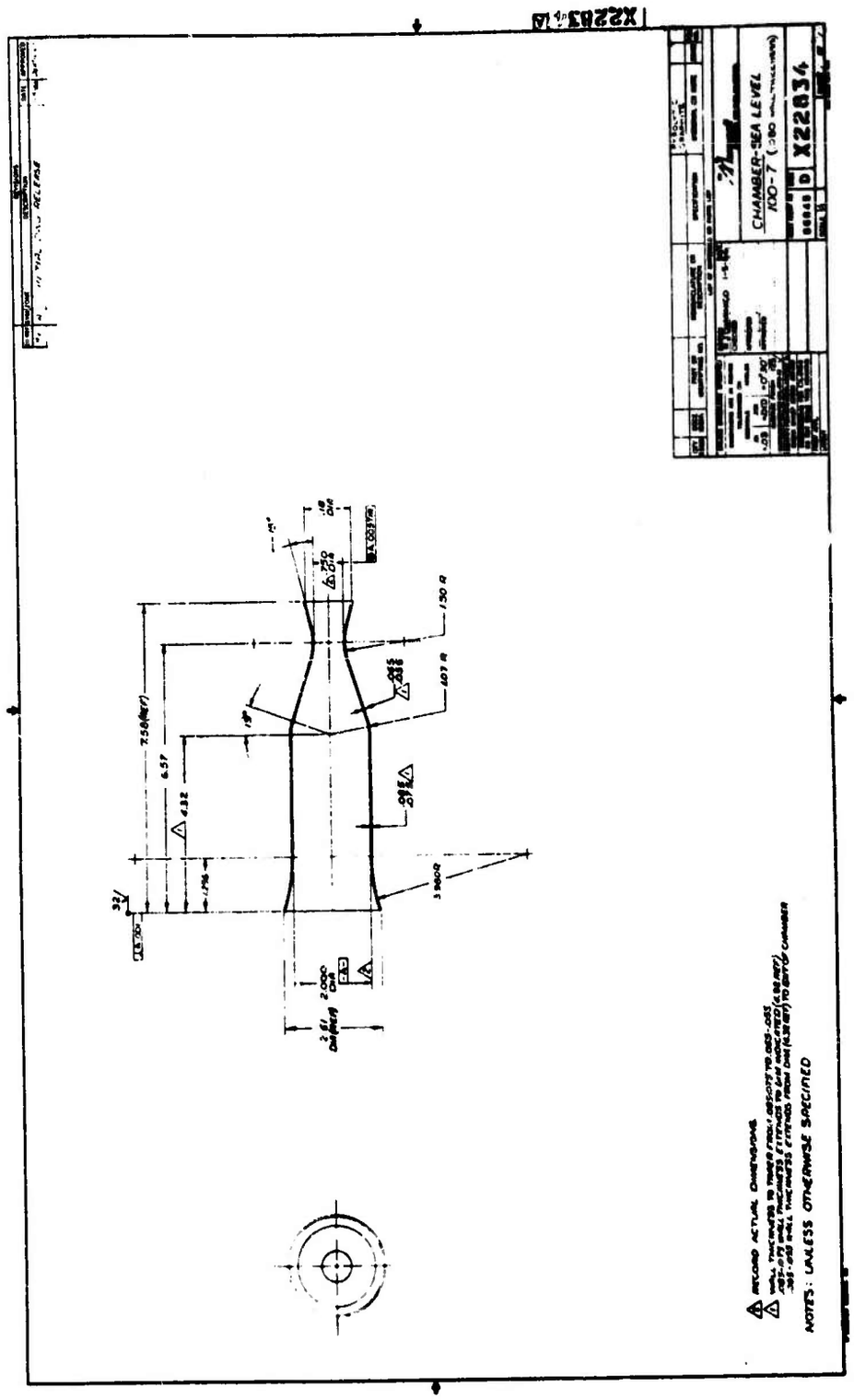

FIGURE 11. (U) Configuration of C100-7 Chamber

8098-1

FIGURE 12. C100-5 and C100-7 Chamber

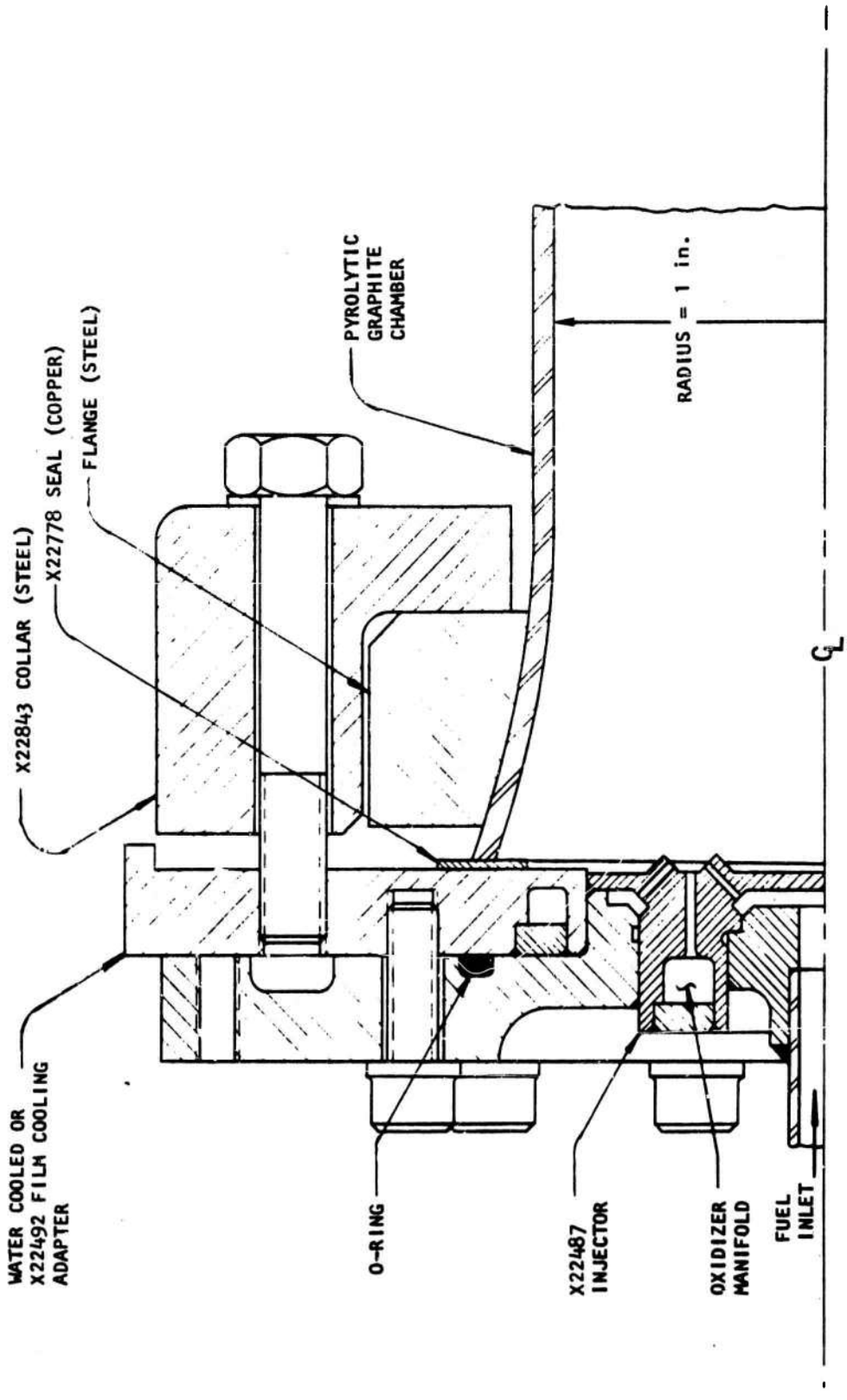

FIGURE 13. (U) Assembly of LF_2/BA1014 Engine, X22487 Injector

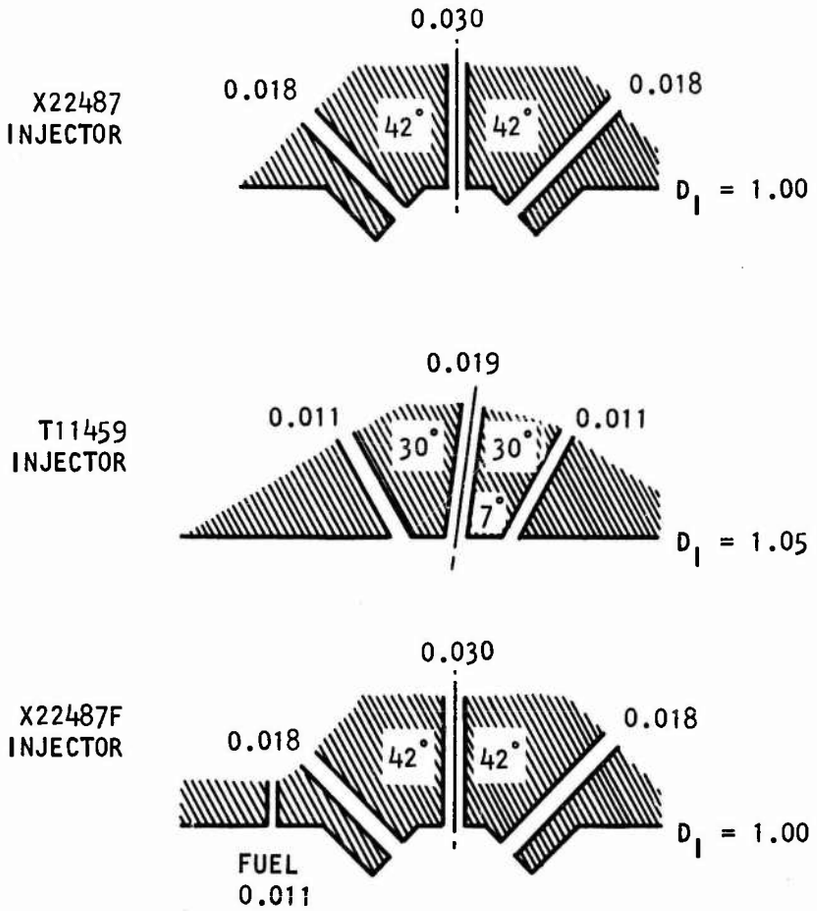

EACH INJECTOR HAS
6 TRIPLE ELEMENTS;
EACH TRIPLET FLOWS
OXIDIZER THROUGH THE
CENTER AND FUEL ON
THE OUTSIDE

FIGURE 14. (U) Triplet Injector Element Designs, LF_2/BA1014

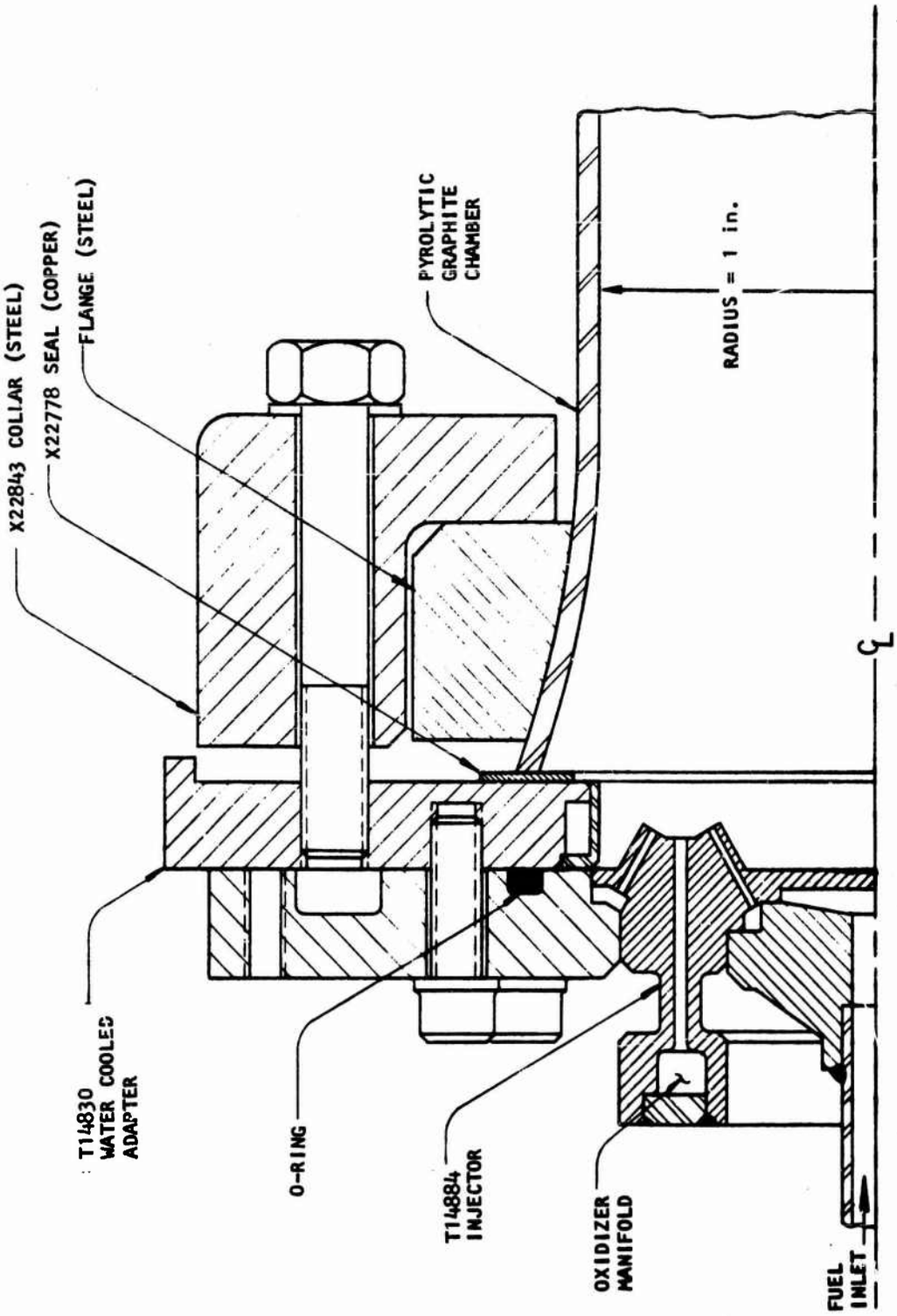

FIGURE 15. (U) Assembly of IF_5/BA1014 Engine, T14884 Injector

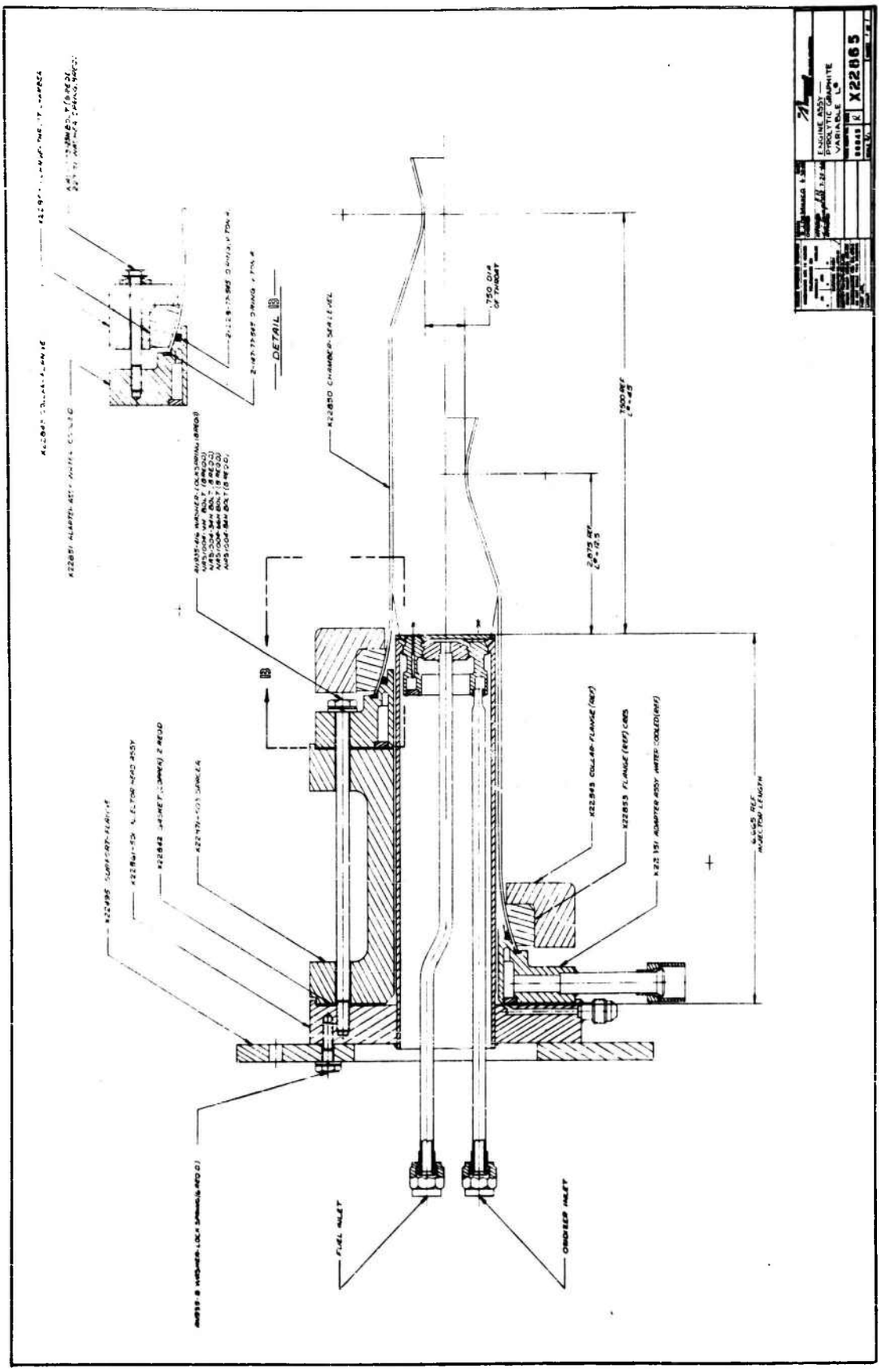

FIGURE 16. (U) Assembly of LF_2/BA1014 Engine, Variable L*

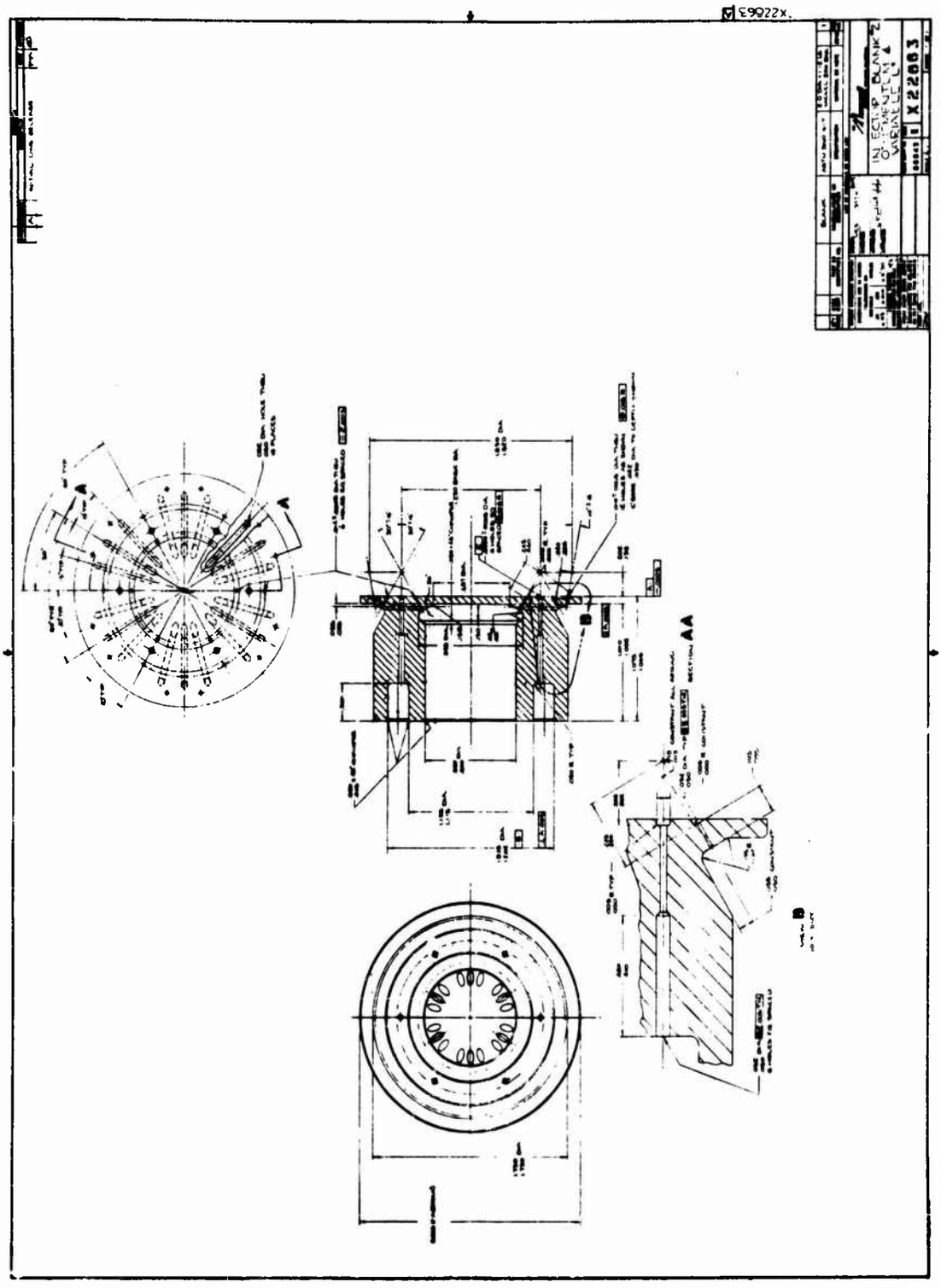

FIGURE 17. (U) Design for X22861-501 Injector Head

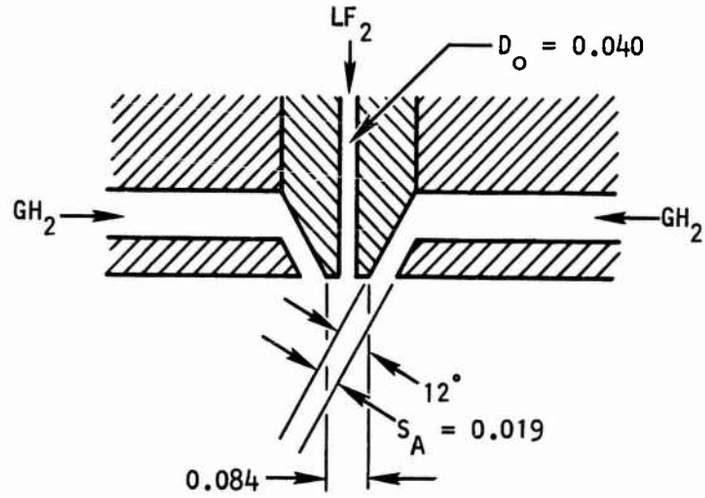

7 COAXIAL ELEMENTS (ONE ELEMENT
IN THE CENTER, THE REMAINING 6
ON A 1.5 in. IMPINGEMENT DIAMETER)

FIGURE 18. (U) Design of T13876-502 Fuel Sheet Injector

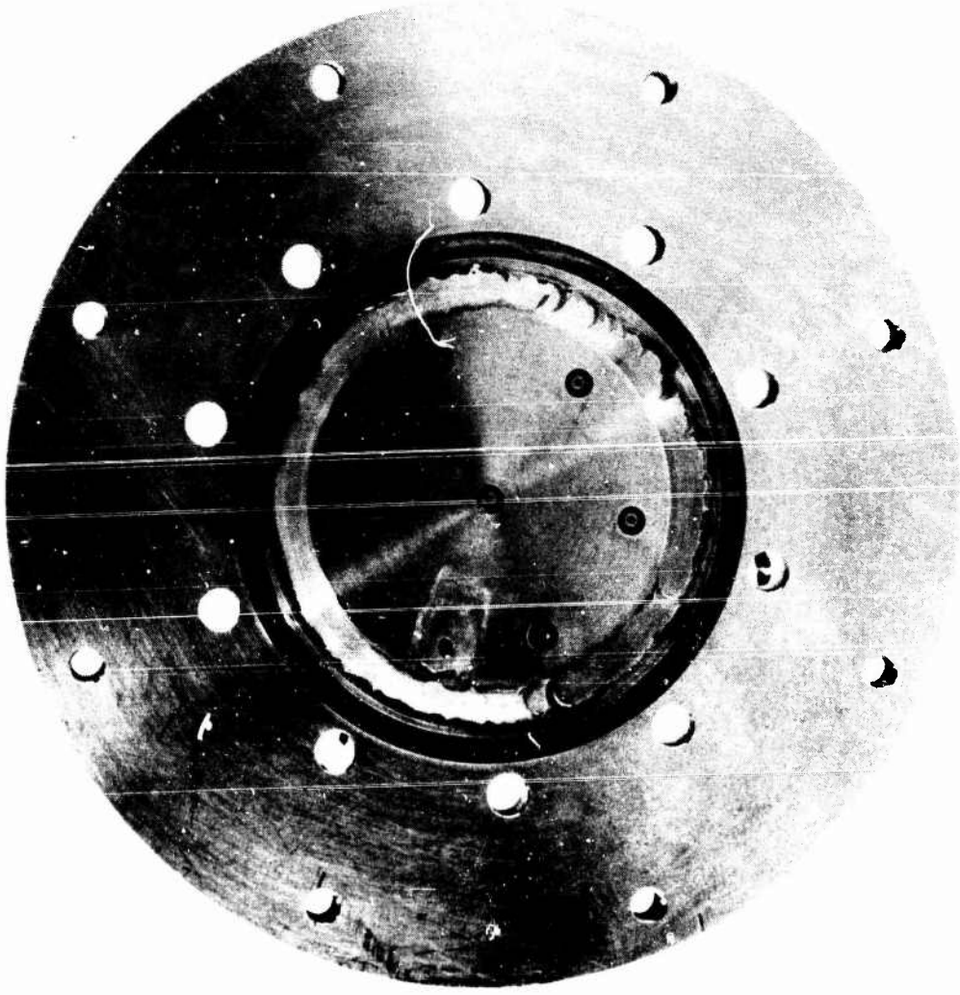

FIGURE 19. (U) T13876-502 Fuel Sheet Injector, LF_2/GH_2

6014-3

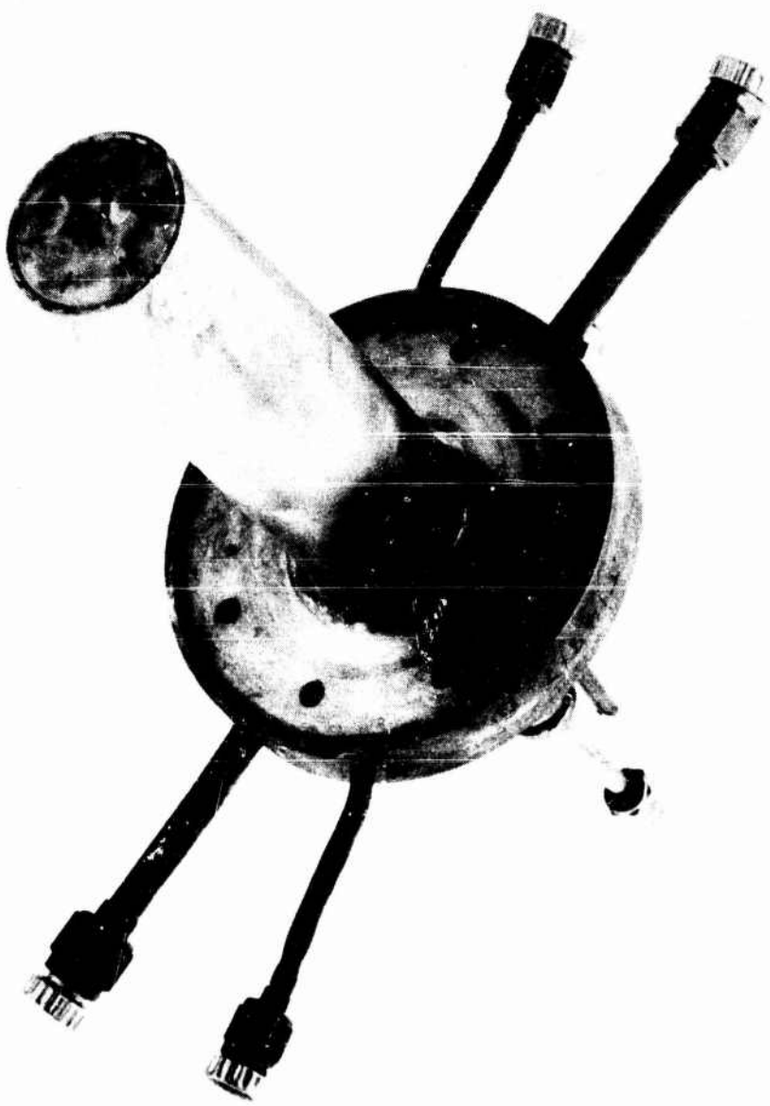

T11314-7

FIGURE 20. (U) LF_2/GH_2 Triplet Injector (T14817)

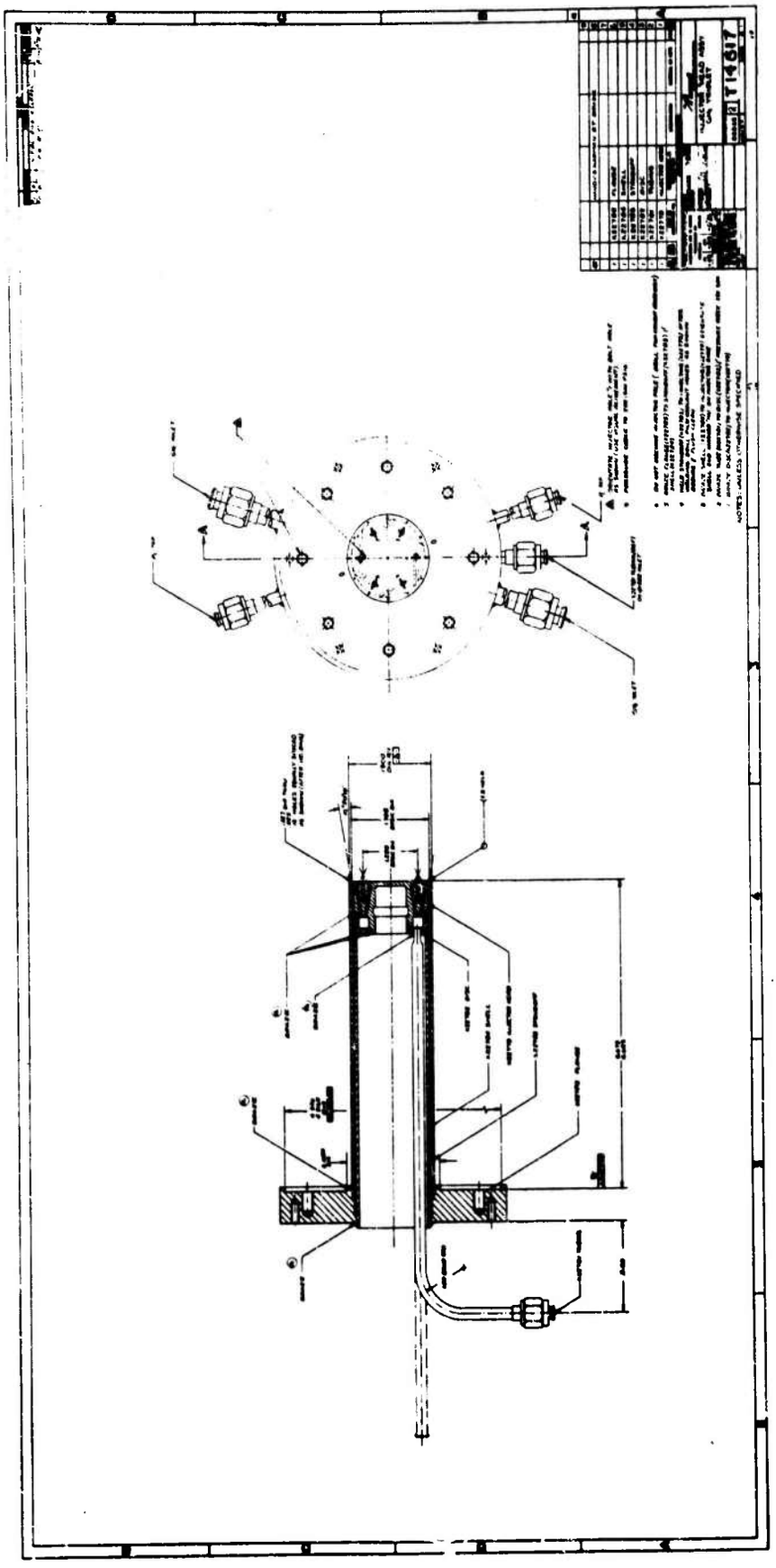

FIGURE 21. (U) Assembly of LF_2/GH_2 Triplet Injector Head (T14817)

III. VIBRATION TESTS

(U) Mechanical vibration tests of 100-pound thrust pyrolytic graphite chambers were performed according to the Boost Vibration Specifications for the Apollo SM/RCS engine. The excitation for this loading is a random vibration that is applied over the frequency interval of 10 to 2000 cps, as follows:

10 to 90 cps	0.055 g^2/cps at 10 cps, increase at 3 decibels (db) per octave to 0.5 g^2/cps at 90 cps
90 to 250 cps	Constant at 0.5 g^2/cps
250 to 2000 cps	0.5 g^2/cps at 250 cps, decrease at 3 db per octave to 0.06 g^2/cps at 2000 cps.

(U) This power spectral density (shown in Figure 22) has a g_{rms} of 19.1. The g_{rms} is a measure of the average power of the power spectral density. Its exact definition is as follows:

$$g_{rms} = \sqrt{\int_{f_1}^{f_2} g_o \, df} \qquad (1)$$

Where

g_o = Power spectral density, g^2/cps

f = Frequency, cps

$f_{1,2}$ = Limit frequencies for power spectral density (10 and 2000 in this case)

A. C100-1-1 Chamber

(U) The C100-1-1 chamber was vibrated for 5 minutes in both the longitudinal and transverse directions. X-rays were then taken of the chamber. Since the transverse mode of vibration was determined to be the most critical, the chamber was vibrated for an additional 30 minutes in this mode. X-rays were again taken and no damage could be detected from visual observation or from the X-ray photographs.

(U) A photograph of the C100-1-1 chamber attached for transverse vibration is shown in Figure 23.

B. C100-3-1 Chamber

(U) Vibration tests were performed on PG altitude chambers of the C100-3 and C100-4 configurations using a test fixture which could be

used for proof testing of the chamber and also could attach directly to the shaker. This permitted a leakage check of the tapered joint before and after vibration.

(U) A vibration test of the C100-3-1 chamber was performed. Before vibrating, a 300 second pressure check with a water and oil mixture at 200 psig showed no leakage through the tapered joint. X-rays of the chamber, taken previous to this pressure check, revealed no delaminations and visual observations likewise revealed no irregularities other than some nodules.

(U) The fixture and attached chamber were assembled on the shaker and vibrated for 300 seconds in the longitudinal mode. A visual inspection of the chamber after this vibration revealed no cracks or other irregularities. The fixture-chamber combination was reassembled on the shaker in the transverse mode (Figure 24) in preparation for a 300 second vibration test according to the same Apollo Boost Vibration Specification. Approximately 15 seconds after the power build-up started, but before the full power spectral level was reached, the chamber failed abruptly at the throat section. The bell section was thrown about 3 feet horizontally and fell about 3 feet to the floor, landing on the exit end. A few local chips were observed at the exit end, but no other damage was caused by this impact.

(U) It was estimated that the power input level reached at the time of failure was about 15 g_{rms}, compared to a planned power input level of 19.1 g_{rms}.

(U) Visual inspection of the chamber and bell portions revealed that these two large sections comprised essentially the entire chamber. That is, there were no small pieces missing from the throat region. However, on both broken sections, the material in the area of the throat was heavily delaminated. A few axial cracks extending less than an inch from the failure section could also be seen. A photograph of this chamber after failure is shown in Figure 25.

C. C100-4-1 Chamber

(U) The C100-4-1 chamber (bell nozzle) was attached to the shaker in the transverse mode and shaken first with a slow 1 g sinusoidal frequency sweep and then at some low random vibration levels for a total of 8.2 minutes.

(U) Strain gages were attached to the outside surface of the chamber as follows:

Gage No. 1: Axial at throat

Gage No. 2: Circumferential, 4 in. from exit

Gage No. 3: Axial, 4 in. from exit

Gage No. 4: Circumferential, 1 in. from exit

Gage No. 5: Axial, 1 in. from exit

(U) The 1 g sinusoidal sweep resulted in the determination of one natural frequency in the 0 to 2000 cps range of about 185 cps ±10 cps. The natural frequency showed up in the recording of Gage No. 1. The other gages read at such low levels throughout the test that any accurate readings were impossible, indicating that the only critical region is the throat. The maximum reading of Gage No. 1 at resonance was about 1375 x 10^{-6} in./in. Assuming E = 4.42 x 10^{6} psi, and ignoring the effect of circumferential strain, which was probably small, the axial stress at the throat was 6077 psi.

(U) Several runs were also made at low random levels of vibration. These runs were at 1, 2, 3, 4, 5, and 6 g_{rms}, with a minimum of 60 seconds at each level. The random vibration spectrum was similar to the requirement in the Apollo Boost Specification, but at lower levels. (The g_{rms} for the Apollo Boost Specification is 19.1 g_{rms}.)

(U) A frequency of 181 cps was clearly visible in the strain gage trace (Gage No. 1) and it is assumed that this is the natural frequency of the first bending mode. A nearly linear relationship between the g_{rms} level and the peak axial strain at the throat was observed as shown in Table II.

TABLE II

(U) THROAT AXIAL STRESS AND STRAIN DURING VIBRATION OF THE C100-4-1 CHAMBER

Input (g_{rms})	Measured Strain (10^{-6} in./in.)	Actual Stress (psi)	Maximum Load Factor ($n_{3\sigma}$)	Predicted Stress Using Equation (3) (psi)
1	312	1379	23.3	907
2	625	2763	46.5	1815
3	1000	4420	69.8	2722
4	1187	5247	93.1	3629
5	1500	6630	116.3	4537
6	1750	7735	139.6	5444

(U) A static test was run on Chamber C100-4-1 to check the accuracy of the recording instrumentation. Weights up to 20 pounds were attached near the end of the chamber. The indicated stress and the predicted stress agreed within about 30 percent and most of this discrepancy was probably due to the loading distribution during the static test.

D. C100-3-2 Chamber

(U) The C100-3-2 chamber (conical nozzle) was attached to the shaker for vibration testing in the transverse mode. Only one strain gage was attached to the chamber at the throat in the axial position, since the vibration tests of the C100-4-1 chamber had shown negligible vibration stresses elsewhere in the nozzle.

(U) The chamber was subjected to random vibration according to the Apollo Boost Vibration Specification at input levels of 1, 2, and 3 g_{rms} instead of the full 19.1 g_{rms}. The recorded and predicted stress and strain at the throat of the C100-3-2 chamber are given in Table III.

TABLE III

(U) THROAT AXIAL STRESS AND STRAIN DURING VIBRATION OF THE C100-3-2 CHAMBER

Input (g_{rms})	Measured Strain (10^{-6} in./in.)	Actual Stress (psi)	Predicted Stress Using Equation (3) (psi)
1	344	1519	1227
2	688	3039	2454
3	1125	4973	3681

(U) The natural frequency as taken from the random trace was 137 cps, compared to a calculated value of 181 cps.

E. Vibration Analysis

(U) The vibration analysis included analysis prior to testing as well as analysis of test results. The analysis consisted of two main parts:

1. A determination of the loading due to a prescribed vibration environment
2. A determination of the stresses in the chamber from a known loading

(U) To determine the response of a chamber subjected to a random vibration in the transverse mode, it was assumed that the chamber acted as a cantilever beam with a single degree of freedom so that the maximum load factor for a standard deviation of 3σ can be obtained from the following equation:

$$n_{3\sigma} = 3\sqrt{\frac{\pi}{2} f_n (g_o)_{f_n} A.F.} \quad (2)$$

Where

f_n = Natural frequency, cps

$(g_o)_{f_n}$ = Power spectral density at f_n, g^2/cps

A.F. = Amplification factor

$n_{3\sigma}$ = Maximum load factor for a standard deviation of 3σ

(U) The predicted maximum stress, which will not be exceeded more than 1 percent of the time, is obtained from the following equation for the primary bending mode:

$$\sigma = n_{3\sigma} \sigma_s \quad (3)$$

Where

σ_s = Stress under static load, psi

σ = Maximum stress, psi

$n_{3\sigma}$ = Maximum load factor

(U) A stress analysis of the throat of free standing PG thrust chambers under transverse acceleration or first bending mode vibration was made. The throat is the critical region under this loading because the section modulus is minimum at that location. The following assumptions were used:

1. The wall thickness is constant throughout the chamber.
2. Transverse acceleration occurs only along one axis.
3. The chamber is cantilevered from the injector, with no side supports.

(U) The results of this analysis show that, for a given load factor, and for geometrically similar chambers, the bending stress at the throat will be directly proportional to the throat diameter. Also, it was found that the bending stresses in a given size chamber are independent of wall thickness, as long as the wall thickness is constant throughout the nozzle. One remedy for the high bending stresses would be to use a thinner wall in the expansion nozzle than in the throat region.

(U) To analyze the vibrations of the PG chambers, a computer program (Marquardt Program No. 4016, Dynamic Analysis of Beams) was used to determine directly the natural frequencies and mode shapes and indirectly to calculate the bending moments and stresses to which the chamber would be subjected for certain vibration environments.

(U) Table IV shows the calculated natural frequencies of three actual 100-pound thrust chambers and three design chambers (100, 1000, and 5000-pound thrust) with conical nozzles and a constant wall thickness for each chamber of 0.045 times the throat radius. For the actual engines, the wall thickness was not constant and the value in the table is the local thickness at the throat. The natural frequencies of the actual chambers were used to compare with the test results. It can be seen from Table IV that the fundamental frequency and each corresponding higher frequency decreases with increasing chamber size.

TABLE IV

(U) CALCULATED NATURAL FREQUENCIES OF PYROLYTIC GRAPHITE CHAMBERS

Thrust (lbs)	Chamber	Throat Dia. (in.)	Nozzle Configuration	t/R_*	t (in.)	Natural Frequency (cps)		
						First Mode	Second Mode	Third Mode
100	C100-4-1 (Used for amplification tests)	0.867	Bell	0.10	0.043	276	>3000	>3000
100	C100-3-1 (Failed vibration test)	0.828	Cone	0.142	0.059	179	2242	>3000
100	C100-3-2 (Used in random vibration test)	0.868	Cone	0.094	0.041	181	~2200	>3000
100	Nominal design configurations, 40:1 expansion	0.868	Cone	0.045	0.020	177	2444	>3000
1000		2.6	Cone	0.045	0.059	48	554	2026
5000		5.85	Cone	0.045	0.13	25	373	1359

(U) Table V shows predicted throat bending stresses (axial stress) for each design chamber of the conical nozzle configuration. The stresses were calculated using the natural frequencies found by the computer program described above (Marquardt Program No. 4016) and an assumed amplification factor of 150.

TABLE V

(U) PREDICTED THROAT BENDING STRESSES
Apollo Boost Random Loading
Conical 40:1 Expansion Nozzles

Thrust (lbs)	Throat Diameter (in.)	Stress Under Static Load (psi)	Natural Frequency (cps)	$(g_o)_{f_n}$ (g^2/cps)	Maximum Load Factor ($n_{3\sigma}$)	Maximum Stress (psi)
100	0.868	62.3	177	0.5	433.2	26,988
1000	2.6	192.8	48	0.268	165.3	31,841
5000	5.85	435.4	25	0.14	86.1	37,488

(U) It can be seen from Table V that although the maximum load factor decreases with increasing thrust level, the static stress at the throat increases at a higher rate, giving a slightly increasing maximum stress with increasing thrust level.

(U) Calculations were also made which showed that the static stress levels of chambers with bell nozzles are less than those with conical nozzles of the same thrust level, while the natural frequencies are higher. The total effect is probably such that the maximum stresses at each thrust level are similar for either a bell or a conical nozzle.

(U) For the C100-4-1 chamber, an analysis prior to the test predicted a natural frequency (first mode) of 276 cps and an axial stress at the throat under static load of 39 psi. Using the results of the 1 g sinuscidal sweep on this chamber, it would appear that the amplification factor at this resonance was 6077/39 = 156. If this were correct, it would indicate practically no damping. Possible explanations of the difference in calculated (276 cps) and measured natural frequency (181 cps) include the following:

1. Nonrigid support, i.e., the joint holding the chamber to the shaker was not completely fixed, but had some flexibility. However, this would tend to reduce the amplification factor.

2. Inaccuracies in the lumped parameter method of calculating the natural frequency. This error is probably not very great.

(U) Analysis for the random vibration tests of the C100-4-1 chamber resulted in predicted load factors at each vibration level and corresponding stress values, which are shown in Table II. A sample calculation using Equation (2) is shown here:

For the 6 g_{rms} input,

$$n_{3\sigma} = 3\sqrt{\frac{\pi}{2} \times 181 \times 0.5 \times \left(\frac{6}{19.1}\right)^2 \times 156}$$

$$n_{3\sigma} = 139.6$$

Using Equation (3),

$$\sigma = 139.6 \times 39$$

$$\sigma = 5444 \text{ psi}$$

(U) Using Equation (2) for the C100-3-1 chamber and using a calculated natural frequency of 179 cps and a representative amplification factor of 150, a maximum load factor of 342 $n_{3\sigma}$ was calculated at the time of failure of the C100-3-1 chamber, giving an axial stress at the throat section of 23,000 psi.

F. Conclusions

(U) It appears that the combination of axial residual stresses at the throat and the vibration induced stresses in altitude PG chambers causes a local stress which, at typical Apollo boost vibration levels, is an important structural problem. While the stress levels reached are above the nominal strength of PG, the strength of PG subjected to vibration may be different from this nominal value.

(U) Possible means of alleviating the problem include the following:

1. Reducing the wall thickness of the expansion nozzle
2. The use of external supports on the nozzle
3. The use of a relatively flexible engine mounting between the injector head and the spacecraft structure
4. The attainment of higher strength pyrolytic graphite
5. The use of PG with controlled delaminations to improve internal damping
6. Revision of the severity of the vibration environment

(U) One objective of the vibration tests was to determine whether PG would suffer unusual delaminations or cracking under vibration. The test results show that this is not a problem.

(U) Evaluation of the vibration problem of larger size chambers is not possible with certainty. However, larger chambers may be exposed to different vibration environments than the Apollo Boost Vibration Specification, which is appropriate for the 100-pound thrust reaction control engines.

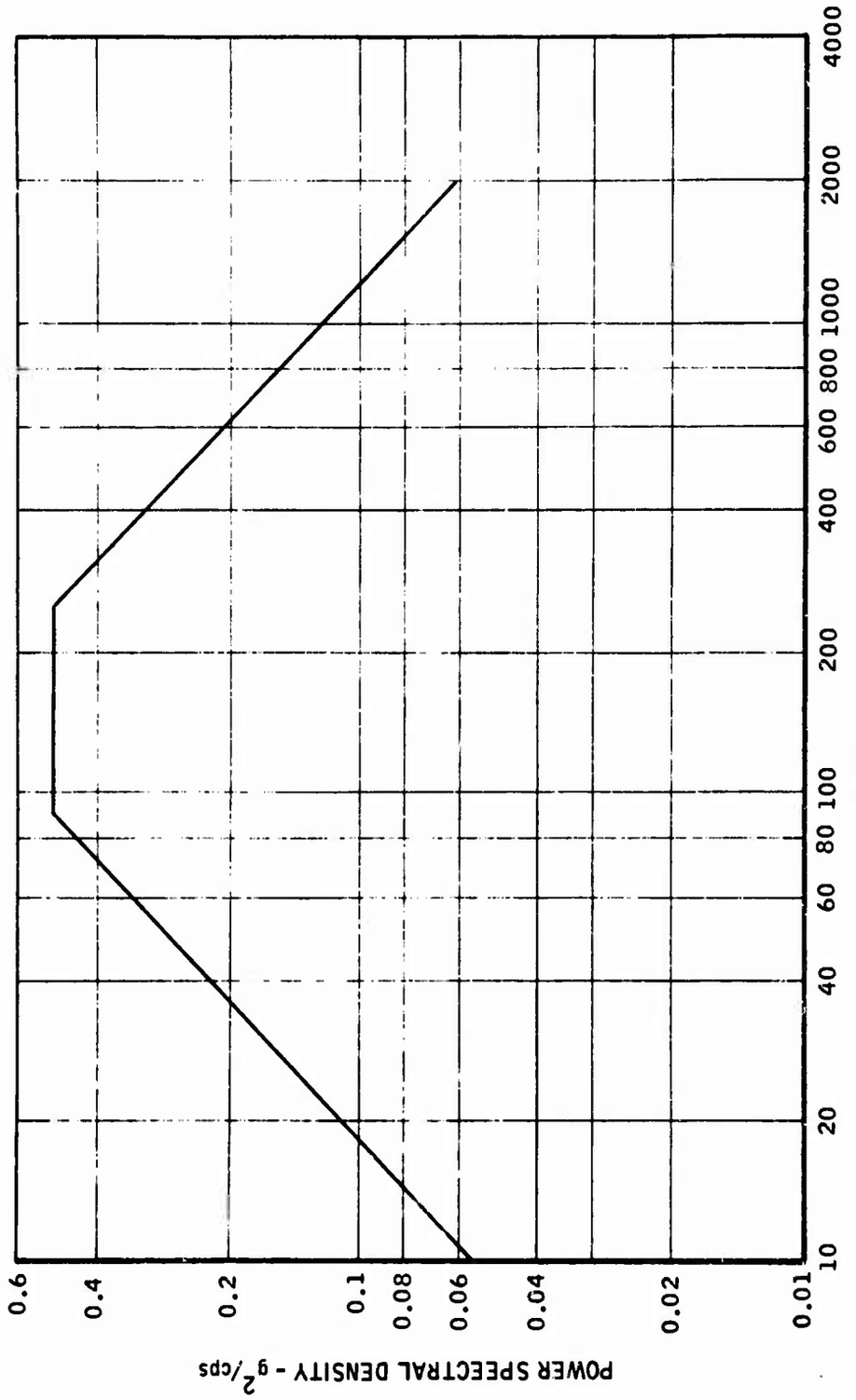

FIGURE 22. (U) Power Spectral Density for Vibration Tests

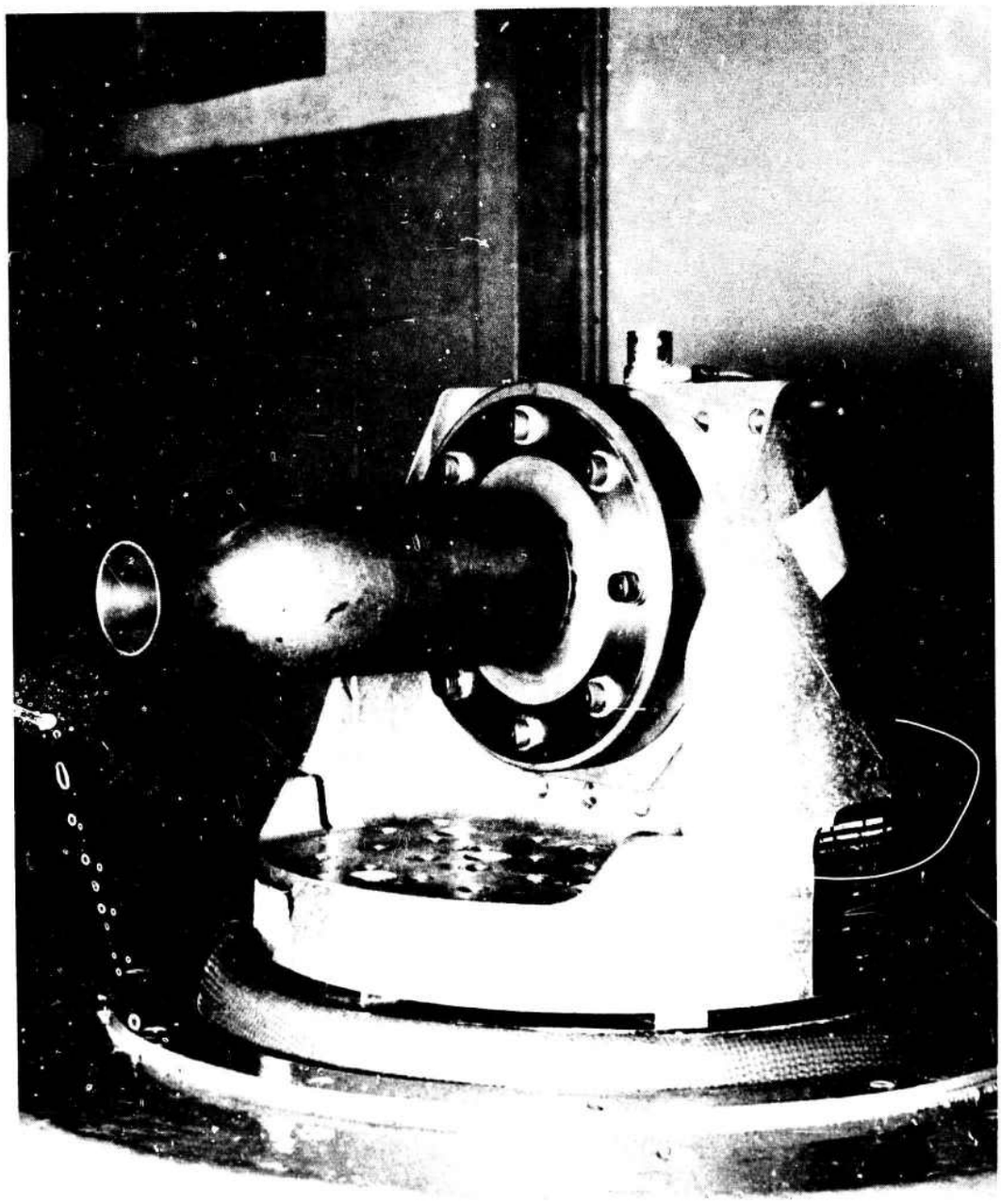

T11261-2

FIGURE 23. (U) Setup for Vibration Test of C100-1-1 Chamber in Transverse Mode

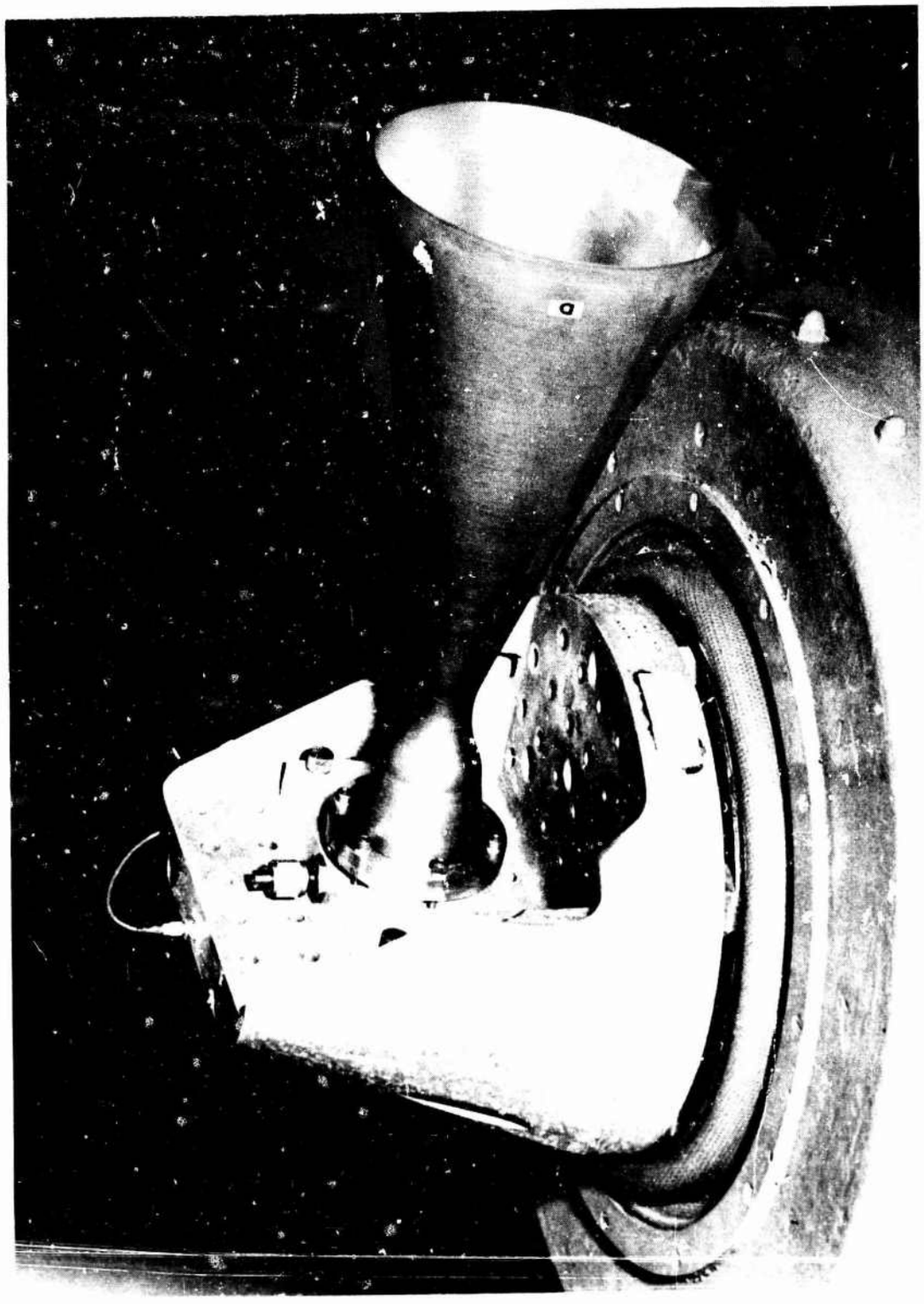

FIGURE 24. (U) Setup for Vibration Test of C100-3-1 Chamber in Transverse Mode

F11280-1

FIGURE 25. (U) C100-3-1 Chamber after Vibration Test

T11280-2

IV. TEST FIRINGS WITH $N_2O_4/0.5N_2H_4$-0.5UDMH

(U) Test firings of 100-pound thrust PG chambers with $N_2O_4/0.5N_2H_4$-0.5UDMH were made in two phases. During the first phase (10 to 16 December 1965) over 600 seconds of firing time were accumulated, using two chambers of the C100-1 configuration and two chambers of the C100-2 configuration. All tests were performed at sea level ambient pressure, a nominal chamber pressure of 100 psia, and an O/F of 2.0. The two injectors used were similar to the injectors developed for the Apollo SM/RCS. One injector (227997) was an 8 on 8 doublet with 12 percent of the fuel impinging on the wall for film cooling. The other injector (T9290) was a 12 on 12 doublet with no film cooling. The test firings are summarized in Table VI and the results for the various test configurations are discussed below:

A. 227997 Injector, 12% Film Cooling, C100-1-4 Chamber (L* = 40)

(C) The 227997 injector (8 on 8, 12 percent film cooling) was tested with the C100-1-4 PG chamber during Runs 4 and 6, with the configuration shown in Figure 6. The erosion rate of the PG wall at the throat was a minimum of 0.19 mil/sec and a maximum of 0.24 mil/sec, indicating nonuniform erosion. Erosion rates have been calculated under the assumption that no erosion occurred during trim runs of 3 seconds or less.

B. 227997 Injector, 12% Film Cooling, Short Chamber (L* = 12)

(C) The 227997 injector with 12 percent film cooling was tested with a tapered C100-2-4 chamber during Runs 11, 12, and 21. This configuration is shown in Figure 7. The overall erosion rate for Runs 11, 12, and 21 ranged from a minimum of 0.059 mil/sec to a maximum of 0.076 mil/sec. Measurements of the diameter and wall thickness of the C100-2-4 chamber before testing and after Run 21 are given in Table VII. A total firing time of 306 seconds was accumulated on the C100-2-4 chamber. After these tests, the wall thickness at the throat ranged from 0.032 to 0.037 inch, and the chamber appeared to be capable of additional testing. However, although the erosion rate for this configuration was lower than for the longer C100-1-4 chamber, it was not as low as hoped, and it was decided that additional film cooling would be required. Therefore, fabrication of the film cooling adapter shown in Figure 8 was begun.

(C) Run 24 was intended to be a long duration run with the configuration shown in Figure 7 using the C100-2-1 chamber. However, the chamber failed after 210 seconds. The cause of the failure is not known.

C. T9290 Injector, No Film Cooling, C100-1-5 Chamber (L* = 40)

(U) The T9290 injector (12 on 12, no film cooling) was tested with the C100-1-5 PG chamber during Runs 17 and 28, for a total duration of 37 seconds. The test configuration is shown in Figure 6. Both of these runs were stopped prematurely because of smoke around the chamber flange. It was later concluded that the smoke was caused by decomposition of the phenolic cement between the graphite flange and the chamber flange.

TABLE VI

(U) SUMMARY OF TESTS OF 100-lb THRUST CHAMBERS, $N_2O_4/0.5N_2H_4$-0.5UDMH

10 to 16 December, 1965

Run No.	Chamber	Injector	L*	Film Cooling (%)	Run Time (sec)	P_c (psia)	O/F	C* Eff.	Increase in Throat Diam. (in.)	Throat Erosion Rate mil/sec	Remarks
4	C-100-1-4	227997	40	12	10	100.7	1.88	94.	--	See Run 6	Preceded by 3 trim runs (9 sec total).
6	C-100-1-4	227997	40	12	30	101.7	1.87	94.5	0.019 max. 0.015 min.	0.24 max. 0.19 min. Runs 4, 6	Preceded by a 2 sec run. Removed because of excessive erosion.
11	C-100-2-4	227997	12	12	30	97.0	2.06	92.5	--	See Run 21	Preceded by 4 trim runs (16 sec total).
12	C-100-2-4	227997	12	12	60	97.6	1.91	92.7	--	See Run 21	Removed for inspection and measurement of erosion
17	C-100-1-5	T9290	40	0	10	--	1.82	--	--	See Run 28	Removed because of suspected leak and possible fire. No P_c or thrust readings. 4 trim runs (11 sec total).
21	C-100-2-4	227997	12	12	200	93.6	2.08	91.2	0.044 max. 0.034 min.	0.076 max. 0.059 min. Runs 11,12,21	Removed for inspection. 3 trim runs (9 sec total). Chamber in good condition.
24	C-100-2-1	227997	12	12	210	95.6	2.05	91.9	--	--	Engine rupture at 210 sec. 2 trim runs (4 sec total).
28	C-100-1-5	T9290	40	0	27.0	100.6	2.08	95.2	0.014 max. 0.008 min.	0.19 max. 0.11 min. Runs 17, 28	Stopped run due to a possible fire around outside of chamber. Chamber after removal looked okay. 3 trim runs (6 sec total).

TABLE VII

(U) INSPECTION DIMENSIONS BEFORE AND AFTER TEST FIRING OF THE C100-2-4 CHAMBER

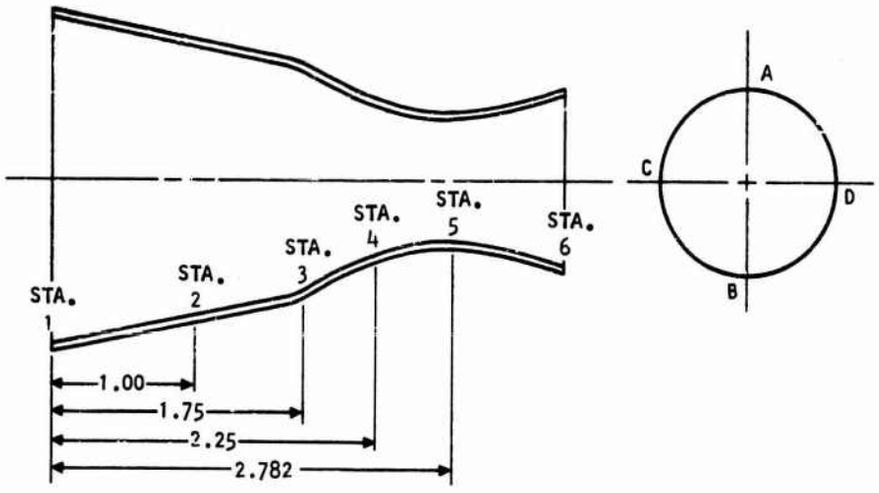

PRERUN MEASUREMENTS (ins.)

Sta.	I.D. A-B	I.D. C-D	O.D. A-B	O.D. C-D	Wall Thickness			
					A	B	C	D
1	2.213	2.214	2.305	2.306	0.046	0.046	0.046	0.046
2	1.821	1.821	1.928	1.930	0.054	0.053	0.054	0.054
3	1.5035	1.5045	1.6135	1.6145	0.055	0.055	0.055	0.055
4	1.035	1.0355	1.145	1.455	0.055	0.055	0.055	0.055
5	0.847	0.847	0.955	0.9555	0.054	0.054	0.054	0.054
6	1.140	1.140	1.246	1.246	0.053	0.053	0.053	0.053

POSTRUN MEASUREMENTS (ins.)

Sta.	I.D. A-B	I.D. C-D	O.D. A-B	O.D. C-D	Wall Thickness			
					A	B	C	D
1	--	--	2.305	2.305	0.046	0.046	0.046	0.046
2	--	--	1.930	1.930	0.053	0.054	0.053	0.054
3	--	--	1.614	1.614	0.052	0.053	0.049	0.051
4	--	--	1.145	1.139	0.044	0.046	0.040	0.040
5	0.884*	0.887*	0.955	0.951	0.034	0.037	0.032	0.032
6	--	--	1.244	1.244	0.046	0.044	0.043	0.044

* Calculated

(C) The throat erosion rate ranged from a maximum of 0.19 mil/sec to a minimum of 0.11 mil/sec. This amount of erosion was slightly lower than the erosion of the throat of a long (C100-1) chamber tested with the 227997 injector with 12 percent film cooling. This again showed that film cooling of the throat of the long chamber was quite ineffective. The fact that the erosion with the 12 on 12 (T9290) injector was lower than for the 8 on 8 (227997) injector was probably due to the differences in the injector propellant distribution.

(U) During the second phase of testing with $N_2O_4/0.5N_2H_4$-0.5UDMH, a film cooling adapter was used to inject additional fuel against the wall, as shown in Figure 8. The results of this phase of the testing (which occurred during March 1966) are given in Table VIII. The total accumulated testing time for all of the $N_2O_4/0.5N_2H_4$-0.5UDMH testing was 1140 seconds. Most of these tests were made with the 227997 injector (8 on 8, 12 percent film cooling) used earlier, but some tests were made with the T13747 injector, which was similar to the 227997 injector except that 27 percent fuel film cooling was injected through 16 film cooling orifices.

D. Metal Chamber, Film Cooling Tests, 227997 Injector

(U) A chamber made of L-605 alloy was used in the configuration shown in Figure 8 to investigate the relationship between chamber temperature and the amount of film cooling. The 227997 injector (12 percent film cooling) was used, and additional film cooling was introduced by the X22830 film cooling adapter. During Runs 3356 through 3367, the mixture ratio of the injector was kept constant at 2.0. The additional fuel through the adapter lowered the overall O/F ratio as shown in Table VIII. It was found that no loss in performance resulted from adapter film cooling up to 24.8 percent of the total fuel flow, at which point the throat temperature, measured by thermocouples, was 1510°F after 5 seconds, but still rising. It was anticipated that a wall temperature of about 2000°F or less would be required to get very long runs with the PG chambers with the oxidizing $N_2O_4/0.5N_2H_4$-0.5UDMH.

(C) These test runs revealed that steady state throat temperatures, within the limits of the L-605 chamber (around 2000°F) could not be obtained with up to 25 percent of the total fuel flow through the film cooling adapter. This is in addition to the 12 percent of the injector fuel flow for film cooling that is built into the injector. At these conditions, the C* efficiency was about 92 percent of the theoretical efficiency.

(U) Higher film cooling rates were not tried since the chamber was damaged during Test 3367. The damage -- a hole in the throat opposite the thermocouple -- evidently occurred due to a hot spot since the maximum thermocouple reading was only 1940°F. However, it was possible to repair the chamber and it was used for subsequent tests.

(U) The throat thermocouple response of the L-605 chamber for several runs is presented in Figure 26. It is believed that the correlation between the film cooling rates and the wall temperature was somewhat inconsistent because of the nonuniform cooling.

TABLE VIII

(U) SUMMARY OF TESTS OF 100-lb THRUST CHAMBERS $N_2O_4/0.5N_2H_4$-0.5UDMH

7 to 25 March, 1966

Run No.	Run Time (sec)	Chamber	Injector	Adapter	Injector Film Cooling (%)	Adapter Film Cooling (%)	Test Cell Condition	Throat Erosion (mil/sec)	O/F Total	Chamber Pressure (psia)	C* Efficiency (%)	Maximum Outside Throat Temperature (°F)	Remarks
3356	5.2	L-605	227997	Film cooling	12	12.4	Sea level		1.76	98.2	92.5	1400	Trim run
3357 to 3363		L-605	227997	Film cooling	12	See Remarks	Sea level						Wrong flow meter constants used for Runs 3357 to 3363; therefore P_c = 70 to 71 psia, C* efficiency = 73 to 78.
3364	5.1	L-605	227997	Film cooling	12	20.0	Sea level		1.63	99.8	92.3	1560	Correct flow meter constants.
3365	7.1	L-605	227997	Film cooling	12	20.1	Sea level		1.65	100.1	92.6	1960	
3366	5.0	L-605	227997	Film cooling	12	24.8	Sea level		1.52	101.8	92.3	1510	Increase adapter film cooling flow rate.
3367	11.2	L-605	227997	Film cooling	12	N.A.	Sea level					1940	Burned hole in chamber wall.
3368	0	C100-2-5	227997	Film cooling	12	N.A.	Altitude						Chamber failed on start, altitude conditions probably due to ignition overpressure.
3369	7.4	C100-2-6	227997	Film cooling	12	43.6	Sea level		1.59	109.3	95.0		Values from quick look data.
3370	7.2	C100-2-6	227997	Film cooling	12	35.7	Altitude		1.59	108.5	94.3		Heat injector head to 100°F and start with back pressure for all following altitude runs.
3371	7.1	C100-2-6	227997	Film cooling	12	35.0	Altitude		1.48	109.9	93.3		
3372	7.1	C100-2-6	227997	Film cooling	12	25.7	Altitude		1.56	107.9	93.9		Decrease adapter film cooling flow rate
3373	7.3	C100-2-6	227997	Film cooling	12	21.9	Altitude		1.62	106.9	94.0		
3374	7.0	C100-2-6	227997	Film cooling	12	N.A.	Altitude						No recorders this run.
3375	7.0	C100-2-6	227997	Film cooling	12	13.7	Altitude		1.72	104.9	92.3		
3376	5.2	C100-2-6	227997	Film cooling	12	41.1	Altitude		1.42	109.9	91.7		Attempt long run; chamber failed.
3377	7.3	C100-2-7	227997	Film cooling	12	26.6	Sea level		1.48	111.8	95.4		Trim run.
3378		C100-2-7	227997	Film cooling	12	27.6	Sea level		1.56	109.8	95.7	1910**	Planned 30 second run; chamber failed on 21.4 seconds.
3379	5.0	C100-2-8	T13747	Water cooled	27	0	Sea level		2.26	98.9	92.0		Trim run.
3380	14.6	C100-2-8	T13747	Water cooled	27	0	Sea level	0.059	2.03	104.5	97.5		Remove chamber high throat erosion, high chamber erosion in several spots.

N.A. = Not available.

TABLE VIII (Continued)

Run No.	Run Time (sec)	Chamber	Injector	Adapter	Injector Film Cooling (%)	Adapter Film Cooling (%)	Test Cell Condition	Throat Erosion (mil/sec)	O/F Total	Chamber Pressure (psia)	C* Efficiency (%)	Maximum Outside Throat Temperature (°F)	Remarks
3381	5.0	L-605	T13747	Film cooling	27	61.5	Sea level		1.21	104.3	88.4	1540	Adapter film cooling flow rates from quick look data.
3382	5.0	L-605	T13747	Film cooling	27	46.0	Sea level		1.60	103.3	89.0	1630	
3383	5.1	L-605	T13747	Film cooling	27	48.9	Sea level		1.75	102.5	87.9	1430	
3384	5.0	L-605	T13747	Film cooling	27	49.9	Sea level		1.81	100.0	85.9	1260	
3385	5.0	L-605	T13747	Film cooling	27	53.8	Sea level		1.99	96.8	82.9	950	
3386	9.0	L-605	T13747	Film cooling	27	53.7	Sea level		1.97		87.4		No recorders - values from quick look data.
3387	20.4	L-605	T13747	Film cooling	27	56.8	Sea level		1.96	98.5	82.8		Temperature measurement erratic.
3388	18.2	L-605	T13747	Film cooling	27	64.0	Sea level		1.87	100.1	82.9	1380 (Steady state)	
3389	24.5	L-605	T13747	Film cooling	27	63.0	Altitude		1.94	96.0	80.4	1500	
3390	16.8	L-605	T13747	Film cooling	27	56.6	Altitude		1.95	96.0	93.1	1120	Temperature measurement could be in error - thermocouple was found open at end of run - burned hole in chamber near throat.
3391	5.1	C100-2-2	227997	Uncooled	12	0	Sea level		1.89	100.8	95.0		Trim run.
3392	15.3	C100-2-2	227997	Uncooled	12	0	Sea level	0.220	2.00	98.0	93.2	1750**	Remove chamber - low erosion in chamber and throat.
3393	16.5	C100-4-1	227997	Uncooled	12	0	Altitude		1.90	97.7	94.0	2100**	Planned 30 second run - chamber failed in 16.5 seconds.
3394	15.1	C100-3-2	227997	Uncooled	12	0	Altitude	0.050	1.97	97.2	93.3	2180**	Remove chamber.
3395	30.2	C100-2-3	227997	Uncooled	12	0	Sea level	0.051	2.0	98.6	94.3	1960** (Steady state)	Chamber removed.
3396	30.2	C100-2-9	227997	Uncooled	12	0	Sea level	0.008	2.0	103.2	94.2	Below 1600**	Chamber removed.
3397	19.2	C100-4-2	227997	Uncooled	12	0	Altitude		2.0	101.1	92.7	1850**	Planned 30 second run - chamber failed 19.2 seconds.
3398	0	C100-3-2	227997	Uncooled	12	0	Altitude						Chamber failed on start, this was second time chamber was run.
3399	90.2	C100-2-9	227997	Uncooled	12	0	Sea level	0.0820	1.99	101.5	93.7	1760** (Steady state)	Throat erosion measured.
3400	0	C100-2-9	227997	Uncooled	12	0	Sea level						Chamber failed on start.
3401	90.5	C100-2-3	227997	Uncooled	12	0	Sea level	0.104	1.98	96.8	93.3	2070** (Steady state)	Throat erosion measured.
3402	101.6	C100-2-3	227997	Uncooled	12	0	Sea level		2.00	94.6	94.1	2180 at 30 sec 2380 at 100 sec	Temperature rising slowly-planned run until chamber failure - chamber failed 101.6 seconds.

** Photographic pyrometry

E. PG Chamber Film Cooling Tests

(U) During Runs 3368 to 3375, PG chambers were used to get additional data on the effect of various amounts of film cooling on engine performance, using the 12 percent film injector and the film cooling adapter. The mixture ratio of the injector was kept at 2.0, so that the overall O/F ratio was less than 2.0. Erosion data were not obtained during these short performance runs.

(U) For the PG chambers, the outside wall temperatures were measured by a Therm-o-scope (two-color pyrometer) and by photographic pyrometry (extended range film). The inside wall temperatures were somewhat hotter because of the low c-direction conductivity. An estimate of the temperature rise across the wall (for steady state temperatures only) is shown in Figure 27.

(U) The results of the photographic pyrometry measurements are shown in Figures 28 to 30. The Therm-o-scope was used only on one firing and the results are compared with the photographic measurements in Figure 28. The Therm-o-scope could not measure temperatures below 1900°F, and the photographic technique could not detect temperatures below 1700°F. The two techniques agreed within about 80°F.

(C) During the first test of a 1.8:1 expansion sea level chamber (C100-2-5) at altitude conditions, the chamber failed at the start, probably due to ignition overpressure. Experience has shown that ignition overpressures would not occur for heated fuel and chamber pressure above about 3.0 psia. Therefore, on all of the subsequent altitude tests, the injector head was heated to 100°F and the chamber pressure was built up to about 2.5 psia (the maximum possible) prior to the start. In spite of these measures, there were several subsequent failures of chambers at ignition, probably due to pressure spikes.

(C) During these runs, it was found that engine performance was not reduced by film cooling from the adapter of as much as 43.6 percent of the total fuel flow. During Run 3376, an attempted long duration firing was terminated by the failure of the C100-2-6 PG chamber after 5 seconds of operation. At this time, the chamber had accumulated a total firing duration of about 55 seconds in 8 runs.

(C) On Run 3378, another attempt to make a long duration run on a PG chamber with adapter film cooling was terminated by failure of the C100-2-7 PG chamber after 21 seconds of operation. There was no evidence that the failures of the sea level chambers were due to residual stress in the throat, which was the cause of the failures of the 40:1 altitude chambers.

(C) The short chamber life during these tests is not in agreement with the much longer life obtained with similar chambers during previous tests using the same 12 percent film injector without additional film cooling. It appears that the injection of additional fuel cooling along the wall from the 16-hole adapter caused some chemical or heat transfer condition which was more destructive of the PG chamber than the injector by itself. It is also

possible that uneven film flow rates might have caused uneven heating. The liquid streams from the adapter were observed to be quite parallel before the motor test firings, but steadily diverged in a random pattern as the testing progressed. There was also a continual change in the flow rate-pressure drop relationship of the adapter, and some of the 16 holes were observed to enlarge in diameter. The most likely explanation of this is chemical attack of the Berylco 10 by the fuel.

F. PG Chamber, T13747 Injector, 27% Film Cooling

(C) During Runs 3379 and 3380, the C100-2-8 PG Chamber was tested with the T13747 injector (27 percent fuel film cooling) and a water cooled adapter. After Run 3380, inspection of the PG chamber (with only 19.6 seconds of testing) showed severe erosion in the combustion chamber, particularly in the contraction region. This was an unexpected result, since other tests of this injector had shown that chamber temperatures were somewhat lower with the T13747 injector (27 percent film cooling) than when using the 227997 injector. The reason that this method of film cooling did not prove satisfactory is probably that the injector doublet elements had to be operated at a high mixture ratio (and hence a high momentum angle) in order to keep the overall mixture ratio near the target value of 2.0. It is probable that the high momentum angle of the injector resulted in mixing an oxidizer-rich stream along the wall, resulting in an unfavorable chemical environment near the wall of the PG chamber. The solution to this problem would be an injector design tailored to the special requirements of minimizing the chemical erosion of PG.

G. Metal Chamber, Film Cooling Tests, T13747 Injector

(U) Runs 3381 through 3390 were made with the repaired L-605 chamber, the T13747 injector (27 percent film cooling), and the film cooling adapter. In these tests, it was attempted to keep the overall O/F ratio around 2.0, using higher adapter film cooling flow rates than those previously tried. Steady state throat temperatures were obtained with about 64 percent of the total fuel flowing through the adapter. During Test 3390, the chamber was again damaged. The fuel valve leads had burned through on this run, causing the valve to close. As a result, only oxidizer had been injected into the chamber for several seconds.

(C) During these tests with the T13747 injector and the film cooling adapter, much greater loss in engine performance was experienced than when making similar tests (Runs 3364 to 3366 and 3369 to 3378) with the 227997 injector. The only exception was Run 3390, which gave a C* efficiency of 93.1 percent. However, this performance value was probably in error, since it differed so greatly from the nine preceding runs.

H. PG Chamber, 227997 Injector, 12% Film Cooling

(U) The C100-2-2 PG chamber was tested during Runs 3391 and 3392 with an uncooled adapter and the 227997 injector (12 percent film cooling). Inspection of the chamber after the 5 second and 15 second runs showed much

lower erosion than had been experienced with the T13747 injector during Runs 3379 and 3380. This configuration had also shown relatively low erosion during the previous tests in December 1965.

(U) It was concluded that none of the combinations of adapter film cooling were more advantageous for extended duration runs than the 12 percent film cooling provided by the 227997 injector. Therefore, the remainder of the testing was done with this injector, using an uncooled adapter. The uncooled adapter was feasible because the film cooling fuel jets struck directly on the adapter.

I. C100-4-1 Altitude PG Chamber

(C) Two PG chambers with a 40:1 bell expansion nozzle failed during short firings. During Run 3393, the C100-4-1 chamber failed after 16.5 seconds of firing, at which time the throat temperature was approaching the steady state condition. The expansion bell was recovered intact (as shown in Figure 31) as well as large pieces of the chamber, indicating that the failure had probably occurred at the throat.

(C) The other bell chamber, C100-4-2, failed during Run 3397 after 19.2 seconds of firing. No large pieces of this chamber were recovered. However, considering the similarity of the firing life of these two chambers, plus the failure at the throat of the C100-3-1 chamber during transverse vibration, it seems probable that the failure was caused by high residual stresses at the throat. No residual stress measurements were available for this exact configuration. However, it is likely that the residual stresses were even higher, because of the small (0.527-inch) radius of curvature, than the 8300 psi measured in the throats of the C100-2 configuration (Reference 1).

J. C100-3-2 Altitude PG Chamber

(C) The C100-3-2 altitude chamber was successfully tested for 15.1 seconds during Run 3394. Inspection of the chamber after the run showed a low throat erosion rate of 0.05 mil/sec. The erosion in the contraction region was not measured but it appeared to be nominal.

(C) The chamber failed at ignition of Run 3398. No large pieces were recovered. Although the possibility of ignition overpressure cannot be proven, it seems likely. A warm injector and a chamber pressure of about 2.5 psia were used on this test in an attempt to eliminate ignition spiking.

K. Sea Level PG Chambers

(U) A series of test firings were made with two PG chambers made by different vendors to investigate possible differences in erosion rates. The erosion rate data are summarized in Table IX, and the estimated inside chamber throat temperatures are summarized in Table X.

TABLE IX

(U) SUMMARY OF PG CHAMBER EROSION RATES
Chambers Tested 7 to 25 March 1966

Chamber No.	Run Time (sec)	Increase in Throat Diameter (Measured) (ins.)	Average Throat Erosion Rate (mil/sec)
C-100-2-8 Super Temp	5.0 14.6 Total 19.6	Total 0.0023	0.059
C100-2-2 HTM	5.1 15.3 Total 20.4	Total 0.0090	0.220
C100-3-2 HTM	15.1 0.0 Total 15.1	Total 0.0015	0.050
C100-2-3 HTM	30.2 90.5 101.6 Total 222.3	0.0031 0.0188 Total 0.0219 for 120.5 sec	0.091 for 120.5 sec
C100-2-9 Super Temp	30.2 90.2 0.0 Total 120.4	0.0005 0.0148 Total 0.0153 for 120.4 sec	0.064 for 120.4 sec

TABLE X

(U) ESTIMATED INSIDE CHAMBER THROAT TEMPERATURES

Run No.	Chamber No.	Measured Outside Wall Temperature (°F)	Estimated Wall Thickness (in.)	Temperature Drop** ΔT (°F)	Estimated Inside Wall Temperature (°F)	Time After Ignition (sec)
3392	C100-2-2	1750	0.0435	180	1930	15
3395	C100-2-3	1960	0.0412	250	2210	30
3399*	C100-2-9	1760	0.0430	190	1950	80
3401	C100-2-3	2070	0.0397	290	2360	30
3402	C100-2-3	2180	0.0318	250	2430	30

* = Wall thickness from measured value after Run 3399
** = From Figure 27.

(U) For the longer runs (90 to 100 seconds), throat erosion was calculated from the chamber pressure and propellant flow rates. It was assumed in the calculations that the characteristic velocity (C*) remained constant throughout the test. The calculated as well as the measured throat erosion rates are presented in Figure 32.

(C) Chamber C100-2-3, made by HTM, was tested for 30, 90, and 101 seconds, the third test (Run 3402) ending in failure of the chamber. The erosion rate measured over 120 seconds was 0.091 mil/sec.

(C) Chamber C100-2-9, made by Super Temp Corp. was tested for 30 and 90 seconds. The chamber failed at ignition of the third run, probably due to a pressure spike. The erosion rate measured over 120 seconds was 0.064 mil/sec.

(U) The erosion rates of the HTM chambers were always higher than those for the Super Temp chambers for short run times up to 30 seconds. For 120 seconds, however, the erosion rates of the two vendor's chambers (C100-2-3 and C100-2-9) were similar.

(U) It was concluded that no significant differences in erosion of the two vendor's PG had been demonstrated, since precise measurement of small amounts of erosion, probably nonuniform, is difficult.

L. Conclusions

(C) Test firing of 100-pound thrust altitude chambers showed that a structural problem exists, probably due to high axial residual stresses near the throat. This problem was probably intensified by the small radius of curvature downstream from the throat of the bell nozzles. It is probable that other configurations than the bell nozzle are more likely to be successful. For example, many steady state tests of sea level chambers were made with no indication of a structural failure near the throat. The sea level chambers had a large radius of curvature downstream from the throat, the same as the conical altitude nozzle. The stresses downstream from the throat during operation are almost entirely due to the residual and anisotropic thermal stresses (in the absence of vibrations) and these stresses were probably very similar, at the same station, in both the sea level and altitude versions of the conical nozzle.

(C) Unfortunately, the demonstration of a long run with the conical altitude nozzle was not achieved because of failure on the second ignition. At that time, the thermal stresses had not been incurred, and the failure was probably due to a pressure spike. However, it appears that further studies of the effects of different nozzle configurations, deposition techniques, and types of PG are required to solve the residual stress problem.

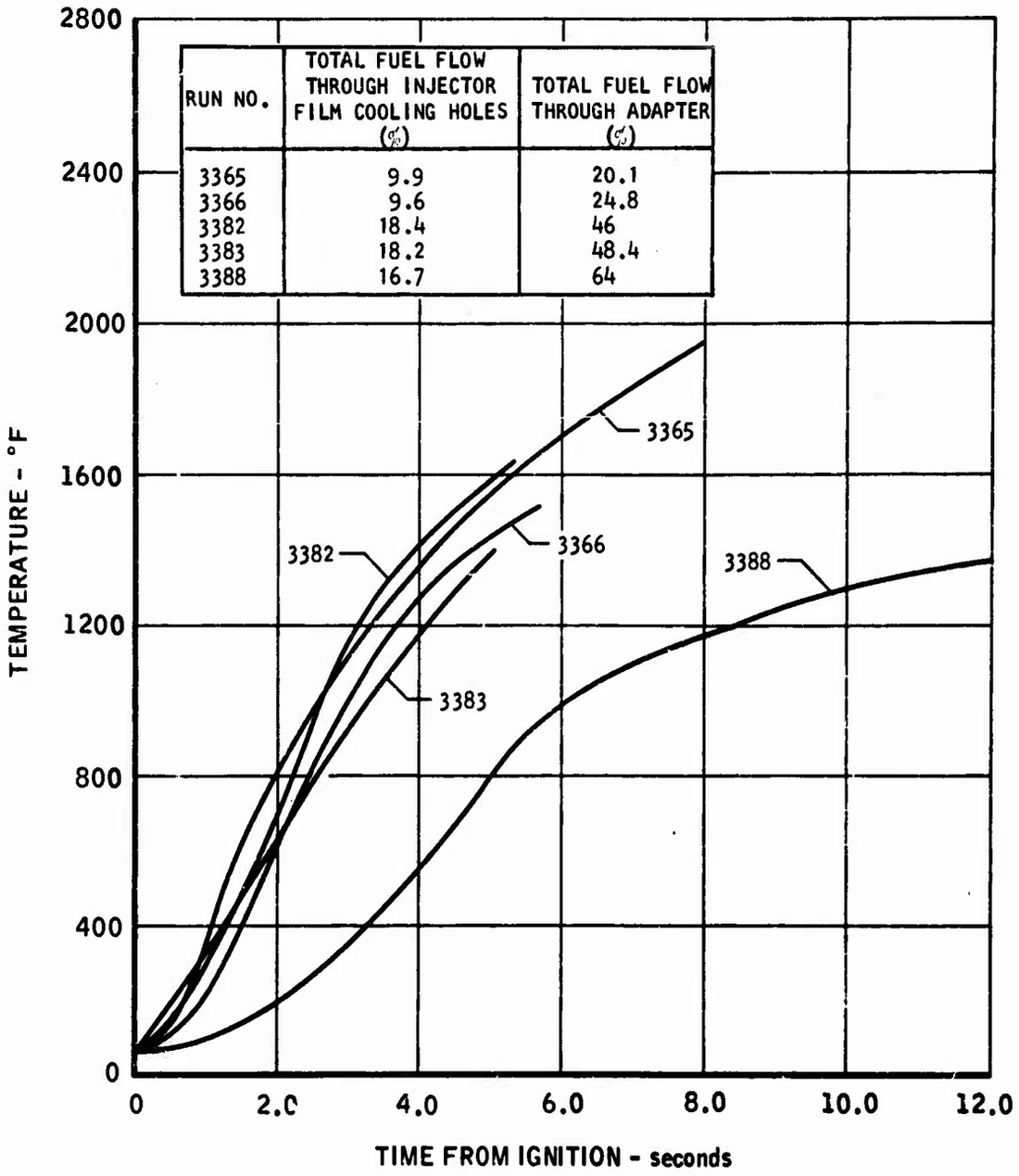

FIGURE 26. (U) Temperature Response of the Thermocouple Located at the Throat of the L-605 Chamber

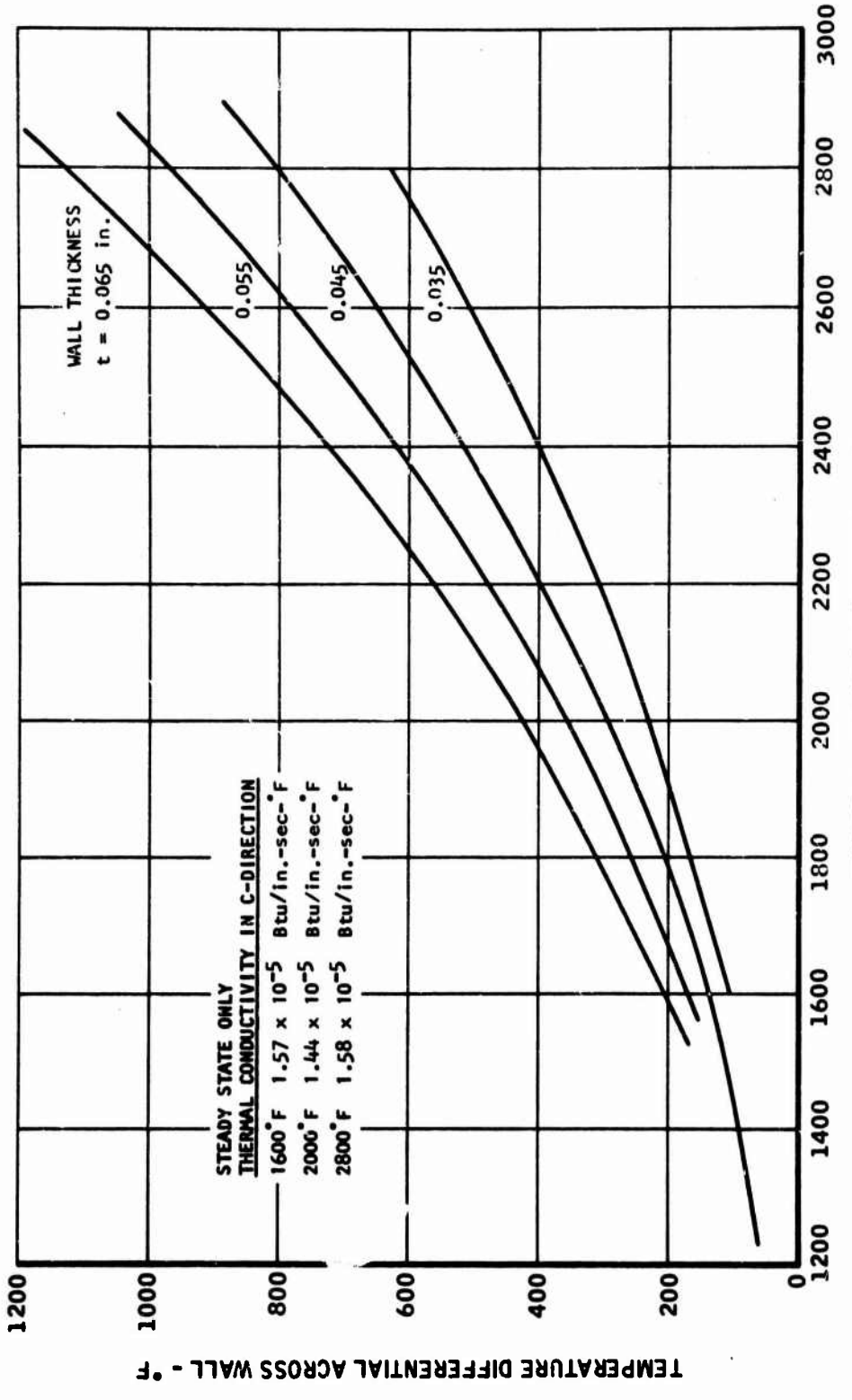

FIGURE 27. (U) Temperature Drop Across Various Thickness Pyrolytic Graphite Chamber Walls

5016-120

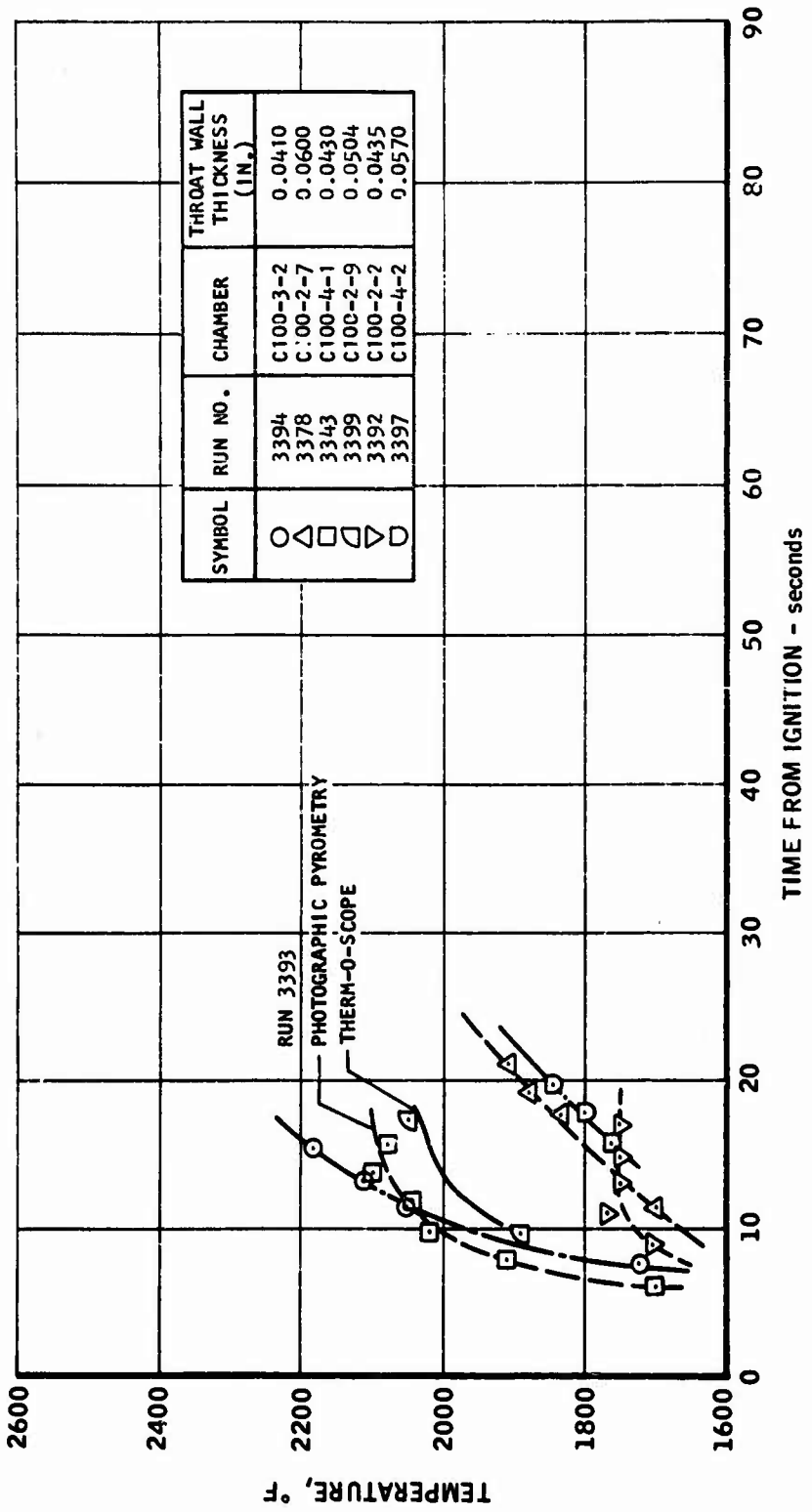

FIGURE 28. (U) Throat Temperatures of PG Chambers Tested 17 to 26 March 1966

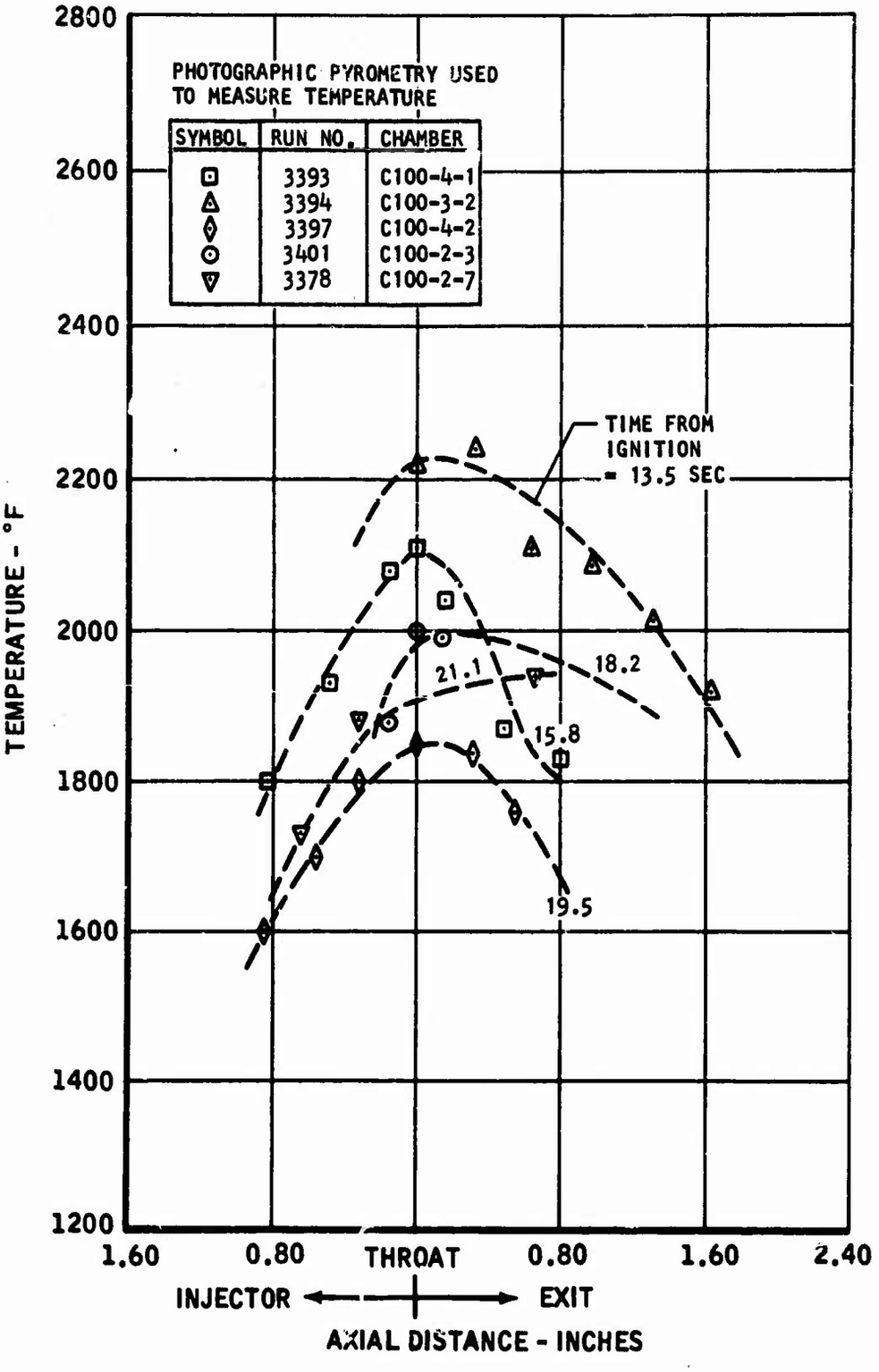

FIGURE 29. (U) Throat Temperatures of PG Chambers Tested 17 to 26 March 1966

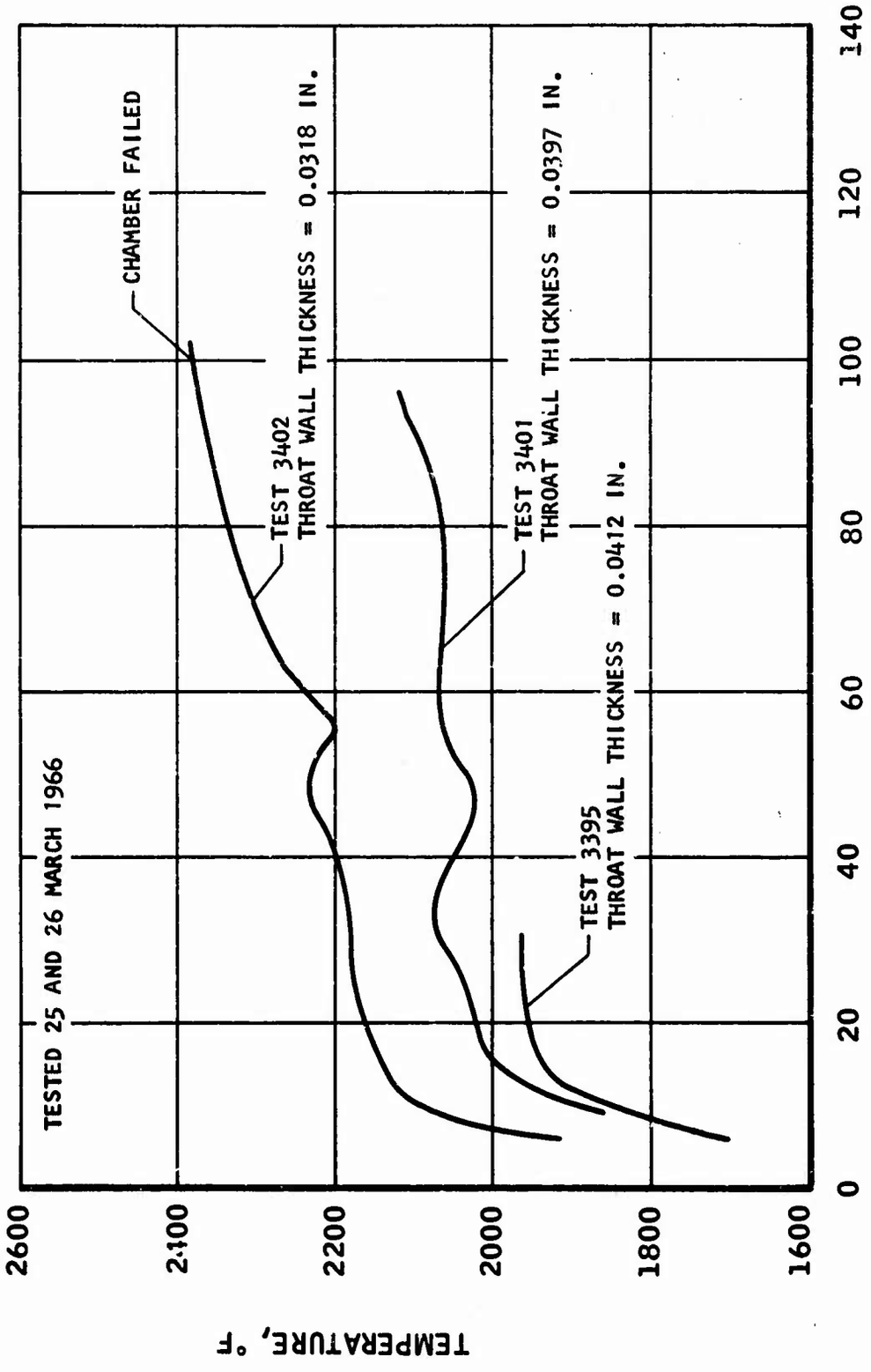

FIGURE 30. (U) Throat Temperatures of C100-2-3 Chamber

FIGURE 31. (U) Exit Cone of C100-4-1 PG Altitude Chamber

8090-1

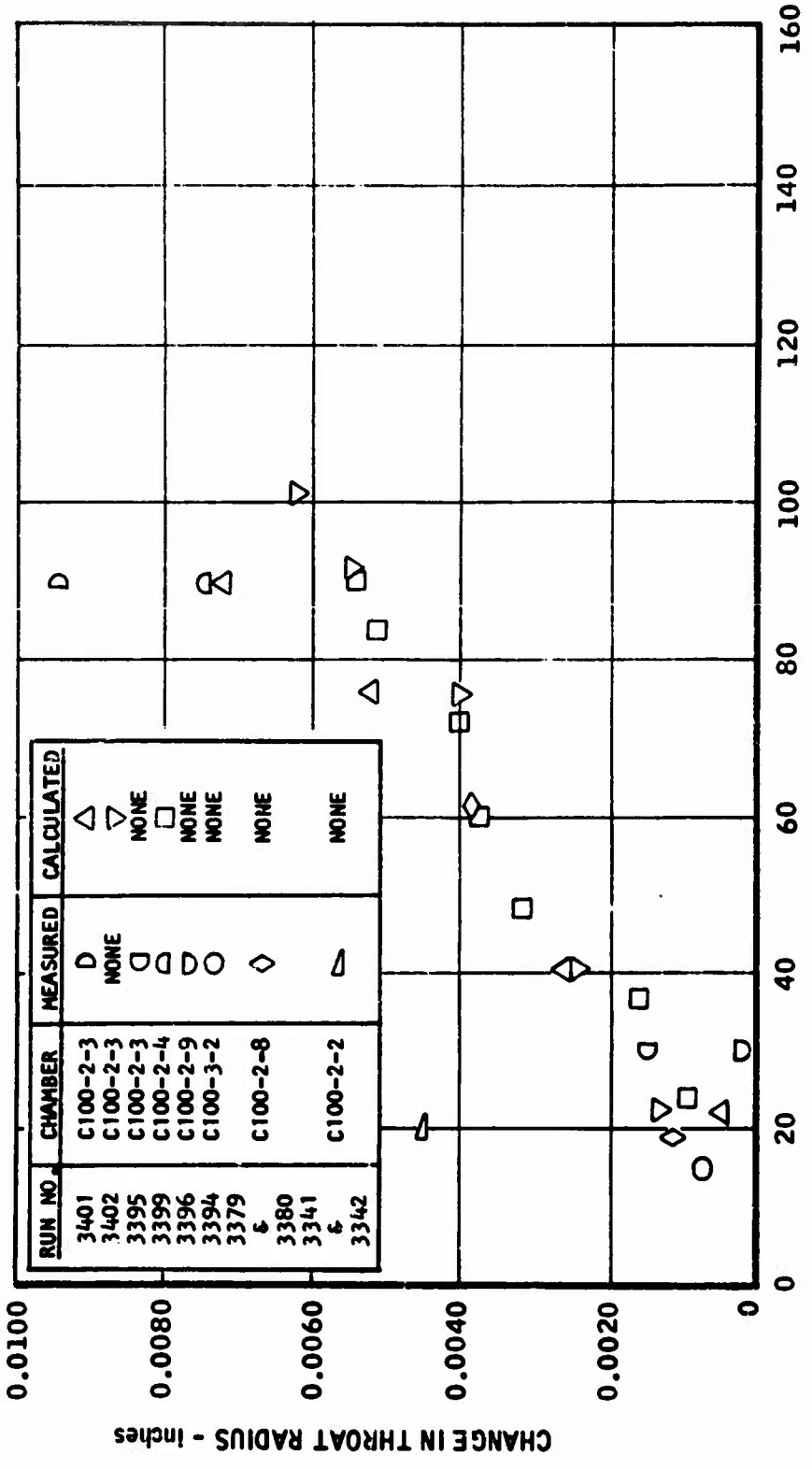

FIGURE 32. (U) Change in Throat Radius of PG Chambers Tested 17 to 26 March 1966

V. TEST FIRINGS WITH LF_2/BA1014

(U) Test firings with LF_2/BA1014 and LF_2/GH_2 were performed at the Marquardt Magic Mountain test site, using Pad M-2. All tests were made at the ambient pressure (12.3 psia) of the Magic Mountain test sites, and all of the thrust chambers had a nominal expansion ratio of 2.5:1. The test results are summarized in Table XI.

A. X22487 and T11459 Injectors

(C) The first test firings of pyrolytic graphite chambers with LF_2/BA1014 were made in March 1966. During these early tests, both the X22487 injector and the T11459 injector were found to give marginal performance, about 90% C* efficiency, at the target mixture ratio of 2.0. Details of the injector designs and test configurations are given in Section III. It was found that the C100-1 chamber configuration was developing a crack in the PG flange during short runs. The 400 series Monel injectors were found to suffer some chemical attack by the combustion gases, and the center of the injector face was bulging out, evidently due to overheating. The throat erosion rates with the T11459 injector were rather high (about 0.45 mil/sec) during Runs 27 and 29. In addition, the erosion was not uniform.

B. X22487F Injector

(C) Six additional fuel orifices were added to the X22487F injector as shown in Figure 14. Tests during Runs 32 through 35 showed that sealing of the controlled delamination chambers (Configuration C100-6) by end loading on copper seals was not satisfactory. Chamber C100-6-2 suffered a partial shear failure of the end of the chamber near the copper seal when assembled to the X22487F injector as shown in Figure 13. Chamber C100-6-3 was tested with the X22487F injector for 4.7 seconds after a previous 5 second test with the T11459 injector. The two outer lamina of the chamber were spalled off after the test. The inner layer was intact and in good condition. Leakage and partial burnout of the steel flange and the copper seal indicated that a seal failure might have permitted combustion gas to enter between the layers, causing failure. Another possible explanation for the failure might have been a shear failure near the end of the outer layer as was experienced with the C100-6-2 chamber.

(U) At the conclusion of these tests (Runs 21 through 42), testing was discontinued while new injectors were fabricated. All of the new injectors were made of Nickel 200. The higher thermal conductivity (about twice that of 400 Monel) was expected to alleviate the overheating of the injector face and it was expected that nickel would have greater resistance to chemical corrosion by the combustion gases than Monel. One new design also introduced the variable L* configuration.

C. Injector Plugging

(U) Test firings with LF_2/BA1014 were resumed in July 1966, using copper heat sink chambers. Numerous instances of oxidizer orifice

TABLE XI

(U) SUMMARY OF TESTS OF 100-LB THRUST CHAMBERS, LF_2/FUEL
March to December 1966

Run No.	Chamber	Injector	Fuel	L* (in.)	Film Cooling (%)	Run Time (sec)	P_c (psia)	O/F	C* Eff. (%)	I_{sp} Eff. (%)	Throat Erosion Rate (mil/sec)	Remarks
21	C100-1-3	X22487	BA1014	37	0	12.	154.9	1.94	91.0	89.1		Chamber failure, injector explosion
27	C100-1-7	T11459	BA1014	37	0	6.	111.9	2.05	89.4	85.3	0.42	Crack in chamber flange
28	C100-1-6	T11459	BA1014	37	0	5.5	101.8	1.86	89.1	89.3		
29	C100-1-6	T11459	BA1014	37	0	7.2	91.1	1.48	92.8	91.6	0.45	Crack in chamber flange; inj. face bulging
30	C100-1-5	T11459	BA1014	37	0							Insufficient oxidizer lead
31	C100-1-9	T11459	BA1014	37	0	12.	121.8	1.34	95.2	86.		Chamber failure, injector explosion
32	C100-6-2	X22487F	BA1014	37	0							Injector failure at oxidizer inlet
33	C100-6-2	T11459	BA1014	37	0	0						No fuel flow. Chamber seal leaks
34	C100-6-3	T11459	BA1014	37	0	5.	65.3	1.59	84.7	87.1		Fuel orifices partially plugged
35	C100-6-3	X22487F	BA1014	37	0	4.7	104.2	1.5	86.	83.4		Outer chamber layers failed
38	C100-7-1	X22487F	BA1014	37	0	4.9	103.9	2.47	88.4	84.7		
39	C100-7-1	X22487F	BA1014	37	0	4.3	106.1	2.0	91.5	85.6		
40	C100-7-1	X22487F	BA1014	37	0	4.2	99.8	1.74	92.	86.4		
41	C100-7-1	X22487F	BA1014	37	0	5.2	102.	1.64	92.5	86.2		
42	C100-7-1	X22487F	BA1014	37	0	5.7	98.9	1.43	93.1	86.9		
78	C100-7-2	T13876-502	GH_2	48	0	5.5	91.	11.5	99.5	96.5	0.36	
79	C100-7-2	T13876-502	GH_2	48	0	5.8	89.	13.0	95.2	93.1	0.17	
80	C100-7-2	T13876-502	GH_2	48	0	20.1	86.	12.4	100.1	96.3	0.37	0.57 mil/sec in erosion streak
81	C100-5-1	T13876-502	GH_2	62	0	15.1	88.	11.4	104.	99.4	0.63	
82	C100-5-1	T13876-502	GH_2	62	0	0						Chamber failed at ignition
133	C100-5-10	T14884-1	BA1014	62	0	10.2	110.	1.98	97.7	91.7		
134	C100-5-10	T14884-1	BA1014	62	0	10.6	109.	1.96	98.3	95.7		
138	C100-5-10	T14884-1	BA1014	62	0	5.8	109.	2.00	97.1	94.2		Seal leaked
149	C100-5-7	X22861-503-1	BA1014	24	33	10.4	99.6	2.03	89.4	83.6		
150	C100-5-7	X22861-503-1	BA1014	24	33	20.	99.6	1.98	89.2	80.3		
151	C100-5-7	X22861-503-1	BA1014	24	33	9.3						Chamber failed
152	C100-5-13	T14884-1	BA1014	62	0	40.5	98.8	2.03	97.6	93.5	0.1	Water cooled adapter failed
153	C100-5-12	X22861-503-1	BA1014	24	33	20.2	103.5	1.97	91.0	85.5		
154	C100-5-13	T14884-1	BA1014	62	0	41.9	94.4	2.08	95.4	91.8	0.075	
158	C100-5-9	X22861 Mod.	BA1014	24	0	19.8	103.5	2.06	93.4	84.5		Fuel manifold leak

TABLE XI (Continued)

Run No.	Chamber	Injector	Fuel	L* (in.)	Film Cooling (%)	Run Time (sec)	P_c (psia)	O/F	C* Eff. (%)	I_{sp} Eff. (%)	Throat Erosion Rate (mil/sec)	Remarks
159	C100-7-5	T14884-1	BA1014	48	0	40.	100.	2.0	96.6	93.5	0.11	
160	C100-7-5	T14884-1	BA1014	48	0	80.	103.5	1.99	99.8	95.2	0.07	
163	C100-7-7	T14817	GH_2	24	33	10.2	105.1	11.7	100.5			Conflicting throat erosion data
164	C100-7-7	T14817	GH_2	24	33	20.5	101.8	10.4	99.5	99.	0.20	Chamber delamination on outside
165	C100-5-6	T14817	GH_2	24	33	35.[a]	100.[b]	12.[b]				Chamber failure during fourth cycle
166	C100-6-1	T14884-1	BA1014	52	0	137.	97.3	1.97	96.7		0.075	
167	C100-5-11	T14817	GH_2	24	50	21.8	97.4	12.1	97.6	93.	0.125	
168	C100-5-15	T14817	GH_2	12	50	21.7	97.	12.	93.4	91.5	0.10	
169	C100-5-15	T14817	GH_2	38	0	21.7	104.8	12.1	103.6	104.4		Chamber failure at end
170	C100-5-11	T14817	GH_2	38	0	0	100[b]	12[b]				Chamber failure at ignition
171	C100-5-14	T14817	GH_2	38	0	0	100[b]	12[b]				Chamber failure at ignition
172	C100-7-6	T14817	GH_2	24	0	10.3	99.9	12.6	95.8	96.7		Conflicting throat erosion data
173	C100-7-6	T14817	GH_2	24	0	20.5	100.6	11.2	103.	104.6	0.20	
174	C100-6-2	T14817	GH_2	24	0	16.8	102.6	11.5	100.4	102.9	0.15	Seal leak
177	C100-5-10	T14817	GH_2	24	50	101.	98.1	12.1	97.1	97.1	0.09	
179	C100-7-4	T14884-1	BA1014	52	0	3.	299.	2.[b]				Seal leak
180	C100-7-4	T14884-1	BA1014	52	0	1.7	302.5	2.				Seal leak

(a) 10 sec on, 20 sec off, 10 sec on, 10 sec off, 10 sec on, 5 sec off, 5 sec on at failure

(b) Nominal

plugging were encountered, such as had occurred sporadically in the earlier testing. In some cases, a solid particle could be found in the oxidizer orifice, but in other cases, the injector orifices would be clear after the run.

(U) It was decided that further testing should be discontinued until the causes of injector plugging could be identified and eliminated. During the first week of August 1966, cold flow tests of LF_2 through a bent tube with a small hole (0.018 inch) again encountered sporadic plugging. In one case, a solid particle was found in the hole. In most other cases, the hole was clear upon inspection after the run.

(U) Investigation of this problem led to the conclusion that much of the oxidizer orifice plugging was caused by frozen contaminants (HF, CO_2) in the LF_2. The fluorine system being used at Pad M-2 consisted of a 25 gallon LF_2 tank in an LN_2 bath. Fluorine was cryopumped into the tank from gaseous fluorine containers. At that time, the specification for gaseous fluorine supplied by Allied Chemical allowed as much as 0.5% concentrations of both HF and CO_2. Both HF (M.P. = -117°F) and CO_2 (M.P. = -70°F) will be solid at LF_2 temperatures near -320°F. It was learned that other organizations had had plugging problems caused by frozen HF. In one case, a 1/2-inch line had been plugged repeatedly.

(U) Other sources of HF were identified as follows:

1. Water in the helium and nitrogen pressurization systems

2. Ingestion of atmospheric moisture into LF_2 system

Any water coming in contact with F_2 would form HF.

(U) The use of filters for the LF_2 system was considered. However, screen type filters were known to have a short operational life in LF_2. A small disk type filter was obtained from Vacco Valve Co., and cold flowing of LF_2 through this filter showed rapid buildup of pressure differential, probably caused by frozen HF. A larger filter was later obtained, but cold flow tests were not performed because the filter did not pass a leakage check.

(U) The following steps were taken to solve the oxidizer system plugging problem:

1. All LF_2 lines, valves, and other components were disassembled and thoroughly cleaned. During cleaning and inspection of the Annin valve in the LF_2 run line, it was found that an area inside of the valve port was deteriorated, with numerous small chips of metal in a granulated condition. This area had been welded during attachment of a male AN connection. The area had poor accessibility for cleaning and inspection. This corroded weld area was probably the source of most or all of the solid particle plugging which had been experienced.

2. A silica gel dryer was installed in both the gaseous helium and gaseous nitrogen pressurization systems.

3. A continuous purge on fluorine lines was used at any time when atmospheric moisture might diffuse into the system during engine mounting and between runs.

4. A distillation procedure was used to separate the HF and other frozen gases from the fluorine. After the fluorine had been cryopumped into the run tank, the LN_2 bath was emptied. Within 24 hours, the run tank temperature had risen to about -150°F. At this point, all of the fluorine was gas, but the HF and CO_2 were still frozen. The valve between the run tank and the fluorine storage containers was closed and the vent valve was opened. As the HF and CO_2 became gaseous, they vented into the atmosphere. In this manner, most of the contaminants were removed from the fluorine.

(U) After the above steps were taken, sixty-five test firings were performed without a single instance of oxidizer orifice plugging.

D. T14884-1 Injector

(U) The T14884 injector was designed for operation at a chamber pressure of 300 psia, thereby requiring three times as much propellant flow as the other injectors. The orifice diameters were made larger to avoid excessive injector pressure drop. Tests with copper heat sink chambers showed that this injector had very high performance, both at the design point of 300 psia and also at a chamber pressure of 100 psia. Therefore it was used extensively to test PG chambers. All tests were conducted at a nominal chamber pressure of 100 psia and a nominal mixture ratio of 2.0, with the exception of two short runs made at a chamber pressure of 300 psia.

1. Runs 133, 134, 138

(U) The C100-5-10 PG chamber was tested for two 10 second runs. Inspection after the run showed that the inside of the chamber was in very good condition, with no visible evidence of having been fired. The outside surface of the chamber had been oxidized, and the surface had a slightly rough appearance. The engine assembly was as shown in Figure 15 except that the X22872 water cooled adapter was placed next to the T14830 adapter. The L* was 62. The copper seal was replaced by a 0.015-inch thick Grafoil seal and the joint was packed inside and out with C9 graphite cement. This seal was leaking during the first leak check before Run 133, but the leak was stopped by increasing the torque on the bolts connecting the chamber to the adapter. Run 138 was an attempted long duration firing but it was terminated after 5.8 seconds because of a combustion gas leak past the Grafoil/C9 cement seal. The C9 cement had almost completely disappeared, and the Grafoil was sheared through.

2. Runs 152, 154

(U) The C100-5-13 PG chamber was given two 40 second test firings with the T14884-1 injector. The chamber was sealed to the X22851 adapter with a Viton A O-ring, and a PG sleeve and some Grafoil packing were used to protect the O-ring from overheating. This configuration was similar to that shown in Figure 33 except that the T15360 adapter was replaced by the T14830 adapter.

(U) The inside surface of the chamber was in excellent condition after these runs. The PG sleeve near the injector, which was about 2 inches long, was badly eroded in spots, indicating that injector streaking would be a problem near the injector. However, the erosion at the throat was very uniform, with no visible or measurable streaks.

(U) The outside surface temperatures of the chamber were measured photographically by extended range film. The temperature distribution is shown in Figures 34 and 35. The hottest region was the throat, which had an outside surface temperature of 3845°F. The corresponding inside surface temperature, for the wall thickness of about 0.034 inch, was about 5700°F.

(U) Separation occurred in the exit and at a lower expansion ratio than that which was predicted. The erosion in the separated region shown in Figure 36 was much deeper, probably due to oxidiation by recirculating air. The oxidized exterior of the chamber after Run 154 is shown in Figure 37. This oxidation would not be a problem for operation in space.

3. Runs 159, 160

(C) The C100-7-5 boron doped PG chamber was tested on Runs 159 and 160 for 40 and 80 seconds, respectively. The engine assembly was as shown in Figure 33, except that the T15360 adapter was replaced by the T14830 adapter. A PG sleeve and Grafoil packing were used to protect the O-ring. The erosion in the throat was 0.11 mil/sec during Run 159, and the chamber was in excellent condition. About 0.20 inch in length was cut off the chamber exit before Run 160 to eliminate the separation problem.

(C) The throat erosion rate during the 80 seconds duration of Run 160 was 0.07 mil/sec. Spalling occurred on the outside surface near the throat, and oxidation appeared to be severe at one spot outside of the exit, as shown in Figure 38.

4. Run 166

(U) The C100-6-1 PG chamber, which was made with two controlled delaminations, was tested for 137 seconds, using the configuration shown in Figure 33.

(U) No PG sleeve was used for this run. The test was terminated at 137 seconds, instead of the target of 200 seconds, because of failure of the O-ring seal. Some melting of the lip of the X22851 adapter occurred, but it was usable for further tests.

(C) Most of the chamber was in excellent condition after the test. However, local injector streaking, probably caused by fluorine-rich zones between the triplets of the T14884 injector, was found just past the location of the adapter lip. This is shown in Figure 39. The region of separation in the exit is shown in Figure 40. The outside surface temperature of the chamber, measured by extended range film, did not exceed 3100°F. As a result, the oxidation of the outside surface was not very great. The throat erosion rate during Run 166 was 0.075 mil/sec.

(U) This test showed that the controlled delamination PG chamber may be a good method of extending the strength and wall thickness of free standing pyrolytic graphite thrust chambers.

5. Runs 179, 180

(C) Runs 179 and 180 were made at a chamber pressure of 300 psia, using the C100-7-4 PG chamber and the engine configuration shown in Figure 33. The O-ring seal failed a few seconds after ignition on both runs. The PG chamber was in good condition, with no sign of erosion except on the edge near where the seal failed.

E. Variable L* Injector

(C) The variable L* injector (X22861-503) was used to test PG chambers with LF_2/BA1014 using some of the BA1014 to film cool the PG chambers. The test configuration was as shown in Figure 16. The L* was 24, and the distance from the injector face to the throat was 4.5 inches. After Runs 149 and 150, of 10 and 20 seconds duration, respectively, the C100-5-7 chamber was removed from the stand and inspected. The throat wall thickness had eroded an average of 0.10 mil/sec. However, there was one narrow streak where the erosion rate was 0.33 mil/sec. The appearance of the inside of the combustion chamber was very good.

(C) The C100-5-7 chamber was reassembled to the injector for Run 151, which was terminated by failure of the chamber after 9 seconds of operation. No sizeable fragments of the chamber were recovered.

(C) The C100-5-12 chamber was test fired for 20 seconds during Run 153, using the same configuration as that used for the 10 second test of Run 149 and the 20 second test of Run 150. Careful measurement of the wall thickness in the chamber after the test revealed a deep erosion streak just downstream from the impingement point of each of the twelve film cooling jets. The wall thickness was as thin as 0.004 inch in these grooves. In fact, several measurements of this streaking by a wall thickness gage caused the gage points to puncture the wall, as shown in Figure 41. Some of the erosion streaks are also shown in Figure 41. The deepest erosion occurred about

1/2 inch downstream from the injector face. It is probable that similar erosion occurred in the C100-5-7 chamber, but it was not noticed during the inspection between Runs 150 and 151.

(C) It was concluded that unreacted water from the BA1014 used for film cooling was responsible for the deep erosion streaks in the PG walls, since it is known that H_2O reacts with graphite at temperatures as low as 2000°F (Reference 3). No further attempts to film cool the PG with BA1014 were made.

F. Modified X22861 Injector

(U) A 20 second test firing with LF_2/BA1014 was made using the Modified X22861 injector with the film cooling orifices peened closed. The fuel in the injector evidently boiled, probably because there was less fuel going to the outer edge of the injector. Leaks developed in the injector fuel manifold and the test results were not considered significant.

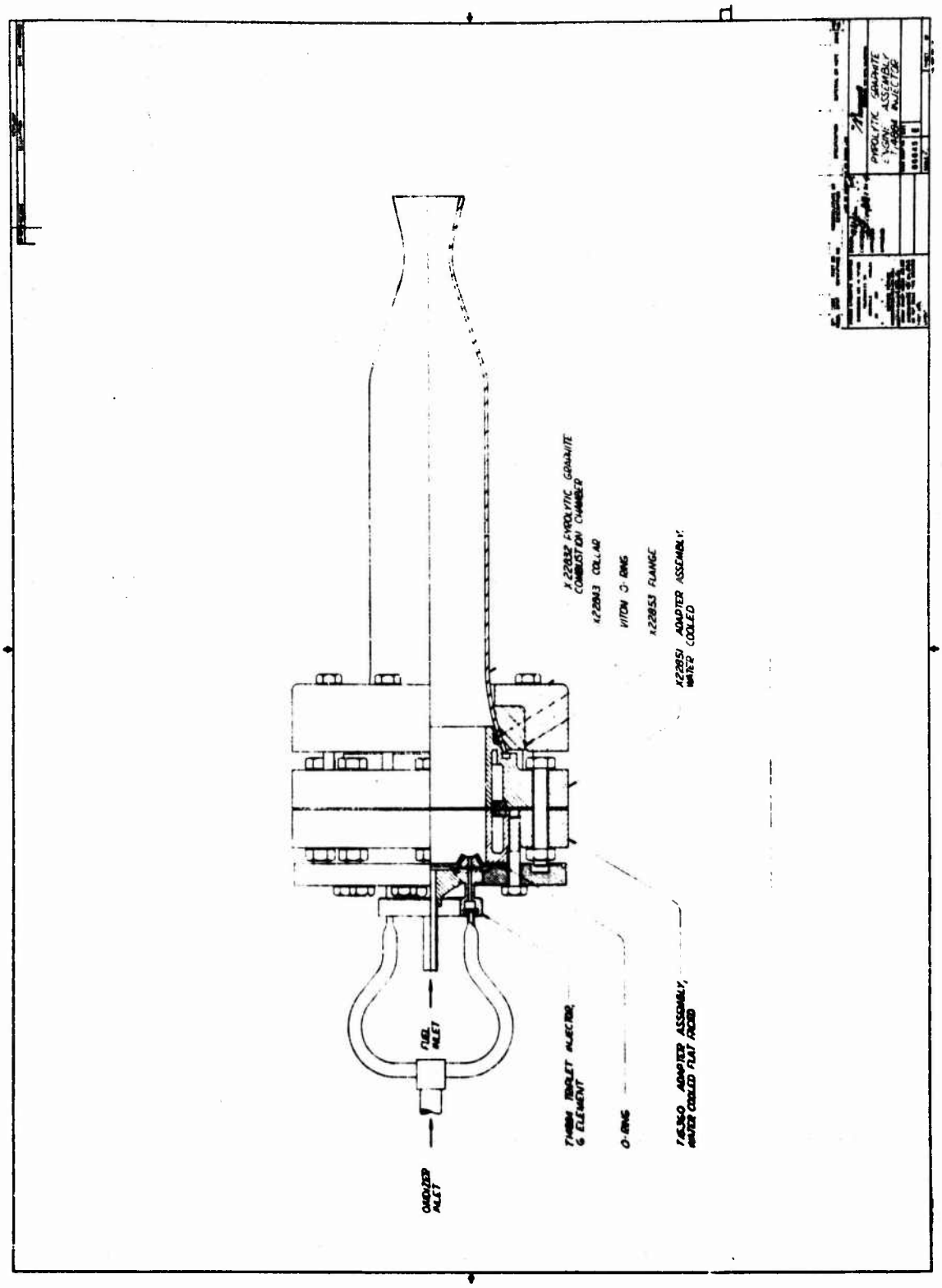

FIGURE 33. (U) Assembly of PG Engine, T14884 Injector

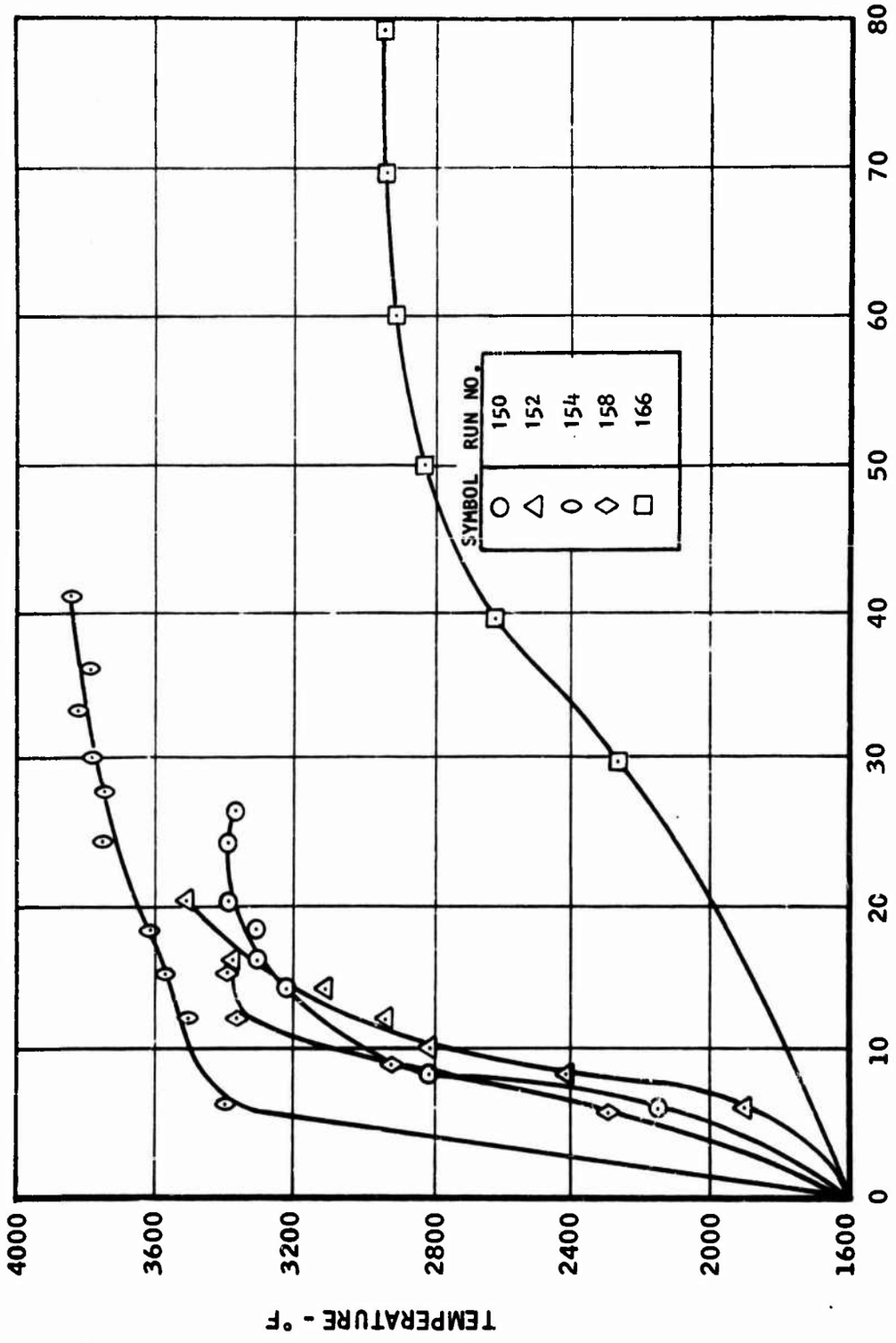

FIGURE 34. (U) Outside Throat Temperatures During IF_5/BA1014 Test Firings

5016-189

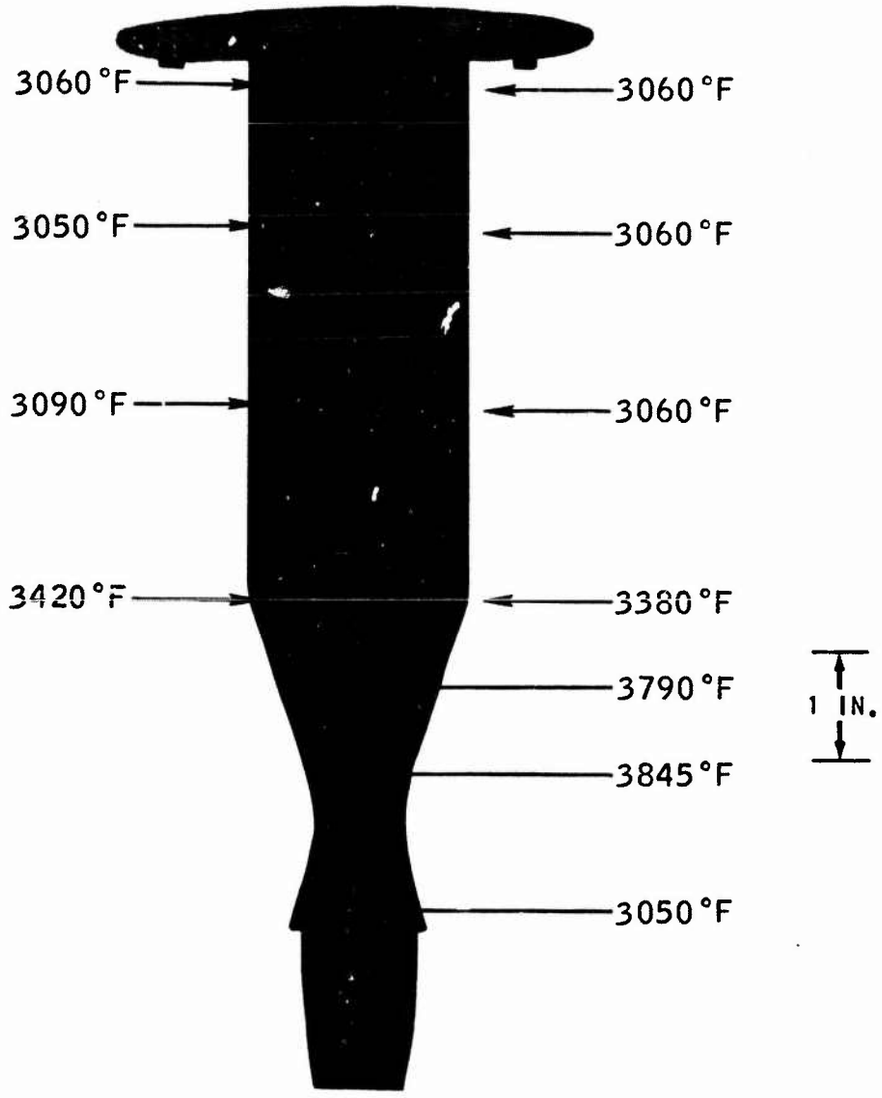

- CHAMBER C-100-5-13
- INJECTOR T14884-1
- RUN NUMBER 154
- P_c = 96.5 PSIA
- MEASURED WITH XR FILM
- O/F = 2.04
- L^* = 62
- (APPROX.) STEADY STATE, 41 SECONDS AFTER IGNITION

CT6015-8CN

FIGURE 35. (U) Temperatures of 100-lb Thrust PG Chamber During LF_2/BA1014 Test Firing

FIGURE 36. (U) Exit Nozzle of C103-5-13 Chamber

T6015-4

T6015-3

FIGURE 37. (U) C100-5-13 Chamber after Test Firing Run 154

FIGURE 38. (U) C100-7-5 Chamber after Test Firing Run 160

T11314-6

T6015-18

FIGURE 39. (U) Inlet of C100-6-1 Chamber after Test Firing Run 166

T6015-19

FIGURE 40. (U) Exit of C100-6-1 Chamber after Test Firing Run 166

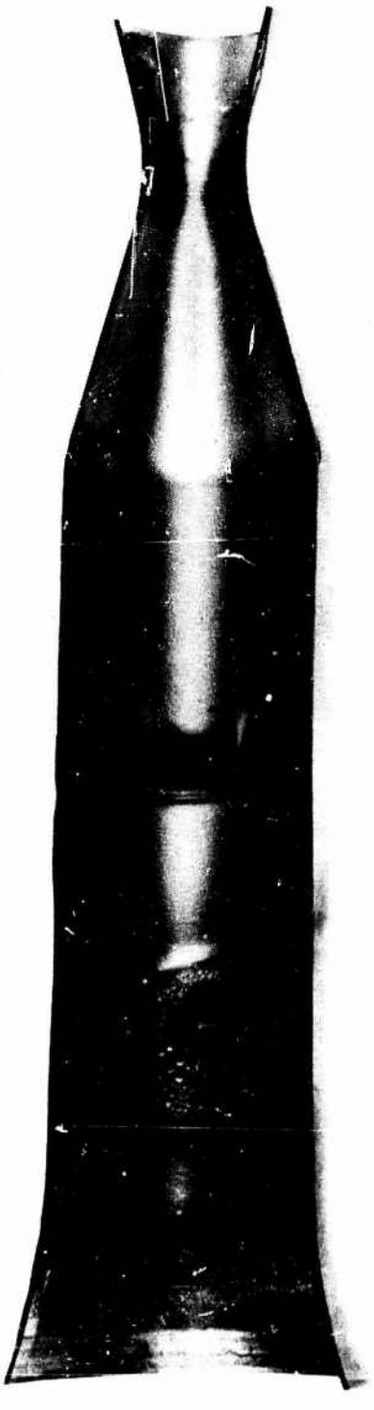

T6015-16

FIGURE 41. (U) Inside Surface of C100-5-12 Chamber after Test Firing Run 153

VI. TEST FIRINGS WITH LF_2/GH_2

(U) Test firings of pyrolytic graphite chambers with LF_2/GH_2 were all made at a nominal chamber pressure of 100 psia and a nominal mixture ratio of 12. All tests were made at the ambient pressure (12.3 psia) of the Magic Mountain test site.

A. Fuel Sheet Injector, No Film Cooling

(C) The fuel sheet injector (T13876-502) was tested with PG chambers in April 1966. The PG chambers were attached to the injector by a method similar to that shown in Figure 13. This injector did not have provisions for film cooling.

(C) The C100-7-2 chamber was tested during Runs 78, 79, and 80 for 5.5, 5.8, and 20 seconds, respectively. Throat erosion during these tests was nonuniform and rather high, about 0.35 mil/sec. However, there was one very bad erosion streak in the throat. After Run 80, the wall thickness in the streak measured 0.052 inch, compared to the original wall thickness of 0.070 inch, indicating an erosion rate in the streak, for the three runs, of 0.57 mil/sec.

(C) The C100-5-1 chamber was tested for 15 seconds on Run 81. The throat erosion was 0.63 mil/sec. At ignition of Run 82, the chamber failed. Engine performance with this injector was very high, the C* efficiency being close to 100 percent. It was concluded that long run times would not be possible with the fuel sheet injector because of the high and nonuniform erosion rates in the PG chambers. Therefore, fabrication of the T14817 triplet injector was begun, using the variable L* configuration and integral film cooling.

B. Triplet Injector, 33% Film Cooling

(C) The tests of PG chambers with the triplet injector (T14817) were made in December 1966. The performance of this injector was very high, approaching a C* value of 100 percent for most runs. The tests with 33 percent film cooling are described below.

1. Runs 163, 164

(C) The C100-7-7 chamber was tested on Runs 163 and 164 for 10 and 20 seconds, respectively. An L* of 24 and 33 percent film cooling was used. The throat erosion rates during Run 163 were difficult to interpret. There was no measured change in wall thickness (0.061 inch) but the throat diameter measured from 0.745 to 0.749 inch, compared to an original diameter of 0.742 inch. The maximum outside temperature after 18 seconds of firing on Run 164 is shown in Figure 42 to be 3850°F. The outside surface temperatures during Run 164 are also shown in Figure 43. The severe delaminations which occurred during this run are visible in this photograph which was taken with extended range film. This was the second boron doped PG chamber to delaminate on the outside surface during test firings. The

other delamination was on the C100-7-5 chamber during Run 160. No delaminations occurred during any of the test firings with substrate nucleated PG chambers.

(C) The wall thickness after Run 164 was 0.055 inch and it was uniform all around the throat. This would indicate a throat erosion rate, for Runs 163 and 164 combined, of 0.2 mil/sec. The outside diameter of the throat measured 0.864 inch, compared to the original outside diameter of 0.863 inch. This increase might indicate growth of the boron PG, or might have been influenced by the outside delamination which extended around part of the throat.

2. Run 165

(C) A cyclic test firing was made of the C100-5-6 chamber during Run 165. Ten second firing cycles were separated by decreasing off times of 20, 10, and 5 seconds. The chamber failed midway in the fourth firing, after three hot starts and a total of 35 seconds of firing.

(C) Motion pictures of the test showed that the burnout had occurred near the injector face. An oxidizer purge was used to clear about 3 feet of 1/4 inch oxidizer line between firings. The purge pressure was reduced to a minimum during this run in order to eliminate excessive cooling of the chamber by the purge pressure gas. As a result, the purge of fluorine was probably very slow, and probably caused fluorine to be purged onto the hot chamber for several seconds between runs, causing excessive local erosion. This condition was avoided by using a 3 second hydrogen fuel lag on other runs.

C. Triplet Injector, No Film Cooling

(C) Tests of the triplet injector (T14817) with the film cooling holes closed were made to determine the effectiveness of the hydrogen film cooling. During these tests, which took place during a 4 day period, data reduction indicated engine performance slightly over 100 percent C* efficiency on three out of four runs. The data are given in Table XI. The reason for these erroneous data has not been discovered.

1. Run 169

(C) The C100-5-15 chamber was tested for 20 seconds during Run 169. The chamber failed just before the test was to be terminated. The maximum outside surface temperature after 18 seconds of firing was 3845°F, as shown in Figure 44. This test was made with an L* of 38.

2. Runs 170 and 171

(U) The PG chambers failed at ignition during Runs 170 and 171. It was decided that a PG sleeve which had been inserted between the chamber and injector to offset possible overheating of the injector barrel had been too tight, building up stresses in the PG chamber wall. This sleeve was not used in subsequent runs, and no heating problem was encountered.

3. Runs 172 and 173

(U) The C100-7-6 PG chamber was tested during Runs 172 and 173 for 10 and 20 seconds, respectively, with no film cooling from the triplet injector, using an L* of 24.

(C) The throat erosion after Run 172 was difficult to determine accurately. The wall thickness was 0.048 to 0.049 inch, compared to an original thickness of 0.051 inch. The most severe erosion had occurred in the combustion chamber, near the injector. Here the original wall thickness of 0.066 inch had diminished to 0.052 inch.

(C) After Run 173, the wall thickness at the throat was 0.045 inch, indicating an erosion rate, for Runs 172 and 173 combined, of 0.2 mil/sec. The erosion of the chamber near the injector was again severe, with a minimum wall thickness of 0.005 inch.

4. Run 174

(C) The C100-6-2 controlled delamination chamber was tested for 16 seconds with no film cooling. The test was terminated by leakage of combustion gas past the O-ring seal. The chamber was in good condition after the run. The throat erosion was 0.15 mil/sec.

D. Triplet Injector, 50% Film Cooling

(U) The triplet injector (T14817) was modified to provide 50% fuel film cooling by using a total of 24 film cooling holes. This configuration was found to give excellent engine performance and low throat erosion of the PG chambers and, in addition, the local chamber erosion near the injector was largely eliminated.

1. Run 167

(C) The C100-5-11 PG chamber was tested for 20 seconds. The throat erosion rate was 0.125 mil/sec. The inside surface of the chamber was in excellent condition, with no visible effects of the firing. The L* for this test was 24, and the C* efficiency was 97.6 percent. The maximum outside surface temperature during this run, shown in Figures 42 and 45, was 3200°F.

2. Run 168

(C) The C100-5-15 PG chamber was tested for 20 seconds on Run 168. The L* was 12 and the C* efficiency was 93.4 percent. The throat erosion rate was 0.10 mil/sec. The chamber was in excellent condition after this test. The maximum outside temperature was 3300°F, as shown in Figures 42 and 46. This was about 100°F hotter than the C100-5-11 chamber on the previous run. However, the wall thickness was thinner, 0.049 inch compared to 0.056 inch for the C100-5-1 chamber.

3. Run 177

(C) The C100-5-10 PG chamber was tested for 100 seconds on Run 177. The L* was 24 and C* efficiency was 97.1 percent. The throat erosion was very uniform, at a rate of 0.09 mil/sec. Considerable oxidation occurred on the outside surface, as shown in Figure 47. The inside surface was in excellent condition after the run, as shown in the cutaway view in Figure 48.

(C) The outside surface temperature increased as the run progressed, as shown in Figure 42, due to the gradual decrease in wall thickness. The inside surface temperature can be estimated from Figure 49 if the outside surface temperature is known. Measurements of the outside diameter at the throat showed that the oxidation rate of the outside surface was about 0.10 mil/sec.

(U) The axial residual stress on the outside of the throat of the C100-5-10 chamber was measured after the test firing to be 4500 psi, with a wall thickness of about 0.035 inch, compared to a stress of 8500 psi in the C100-5-3 chamber which was never test fired and which had a wall thickness at the throat of 0.055 inch.

(U) The microstructure of the throat of the C100-5-10 chamber after firing is compared with the as-deposited microstructure of the C100-5-3 chamber in Figure 50. The inside surface of the C100-5-10 chamber after firing showed the formation of tiny growth cones. It is not clear whether any changes had occurred in most of the structure.

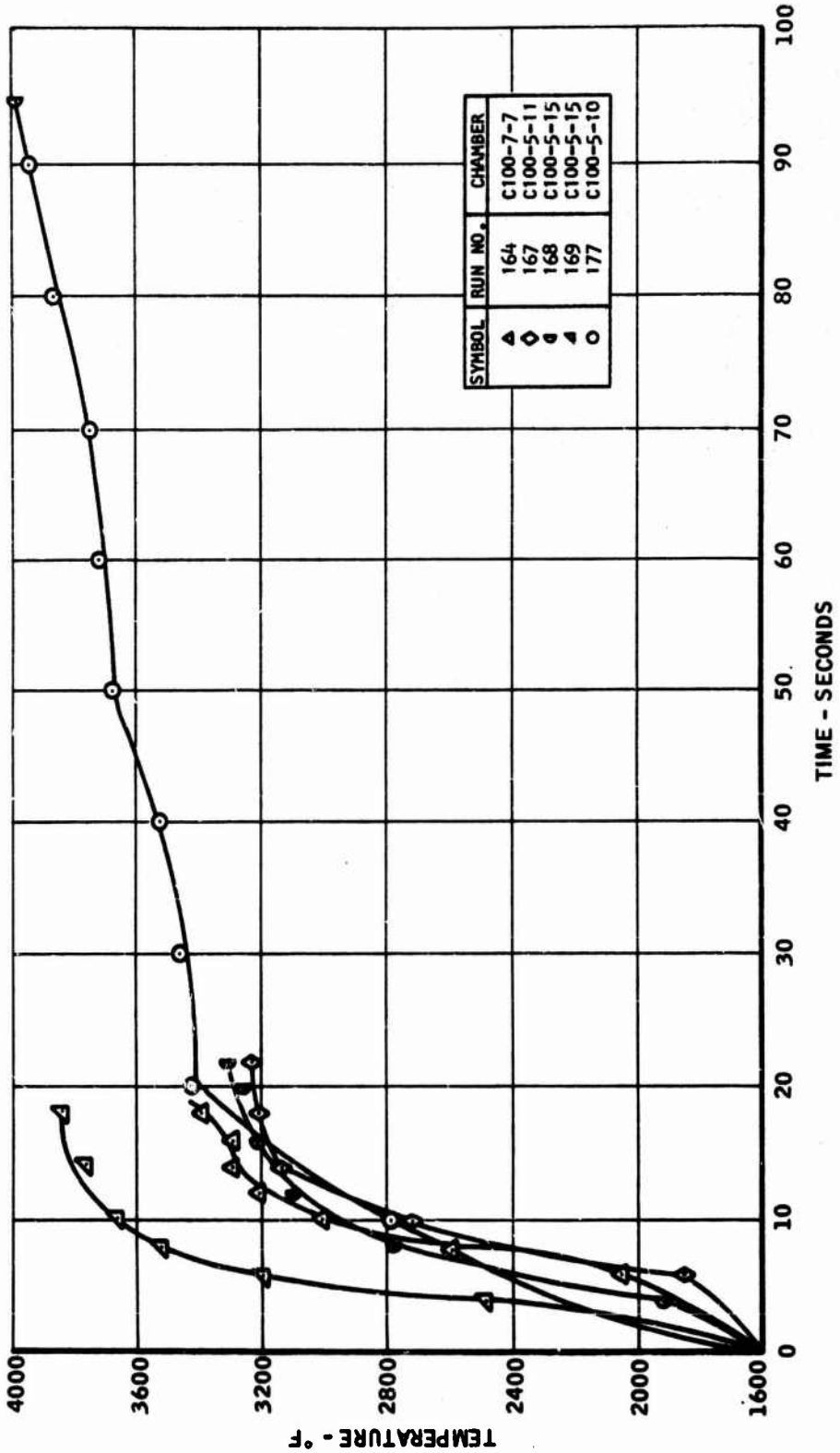

FIGURE 42. (U) Outside Throat Temperatures During LF_2/GH_2 Test Firings

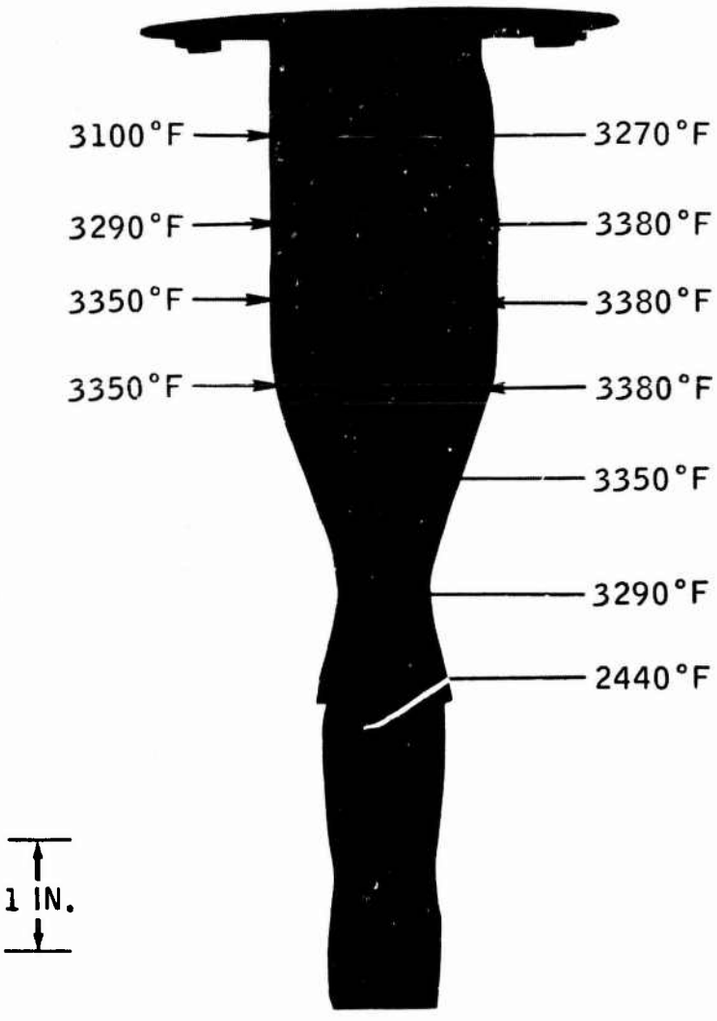

- CHAMBER C-100-7-7
- INJECTOR T14817
- RUN NO. 164
- P_c = 100
- O/F =12
- L*=24

(APPROX) STEADY STATE, 18 SECONDS AFTER IGNITION

- MEASURED WITH XR FILM

CT6015-10CN

FIGURE 43. (U) Temperatures of 100-lb Thrust PG Chamber During LF_2/GH_2 Test Firing, 33% Fuel Film Cooling

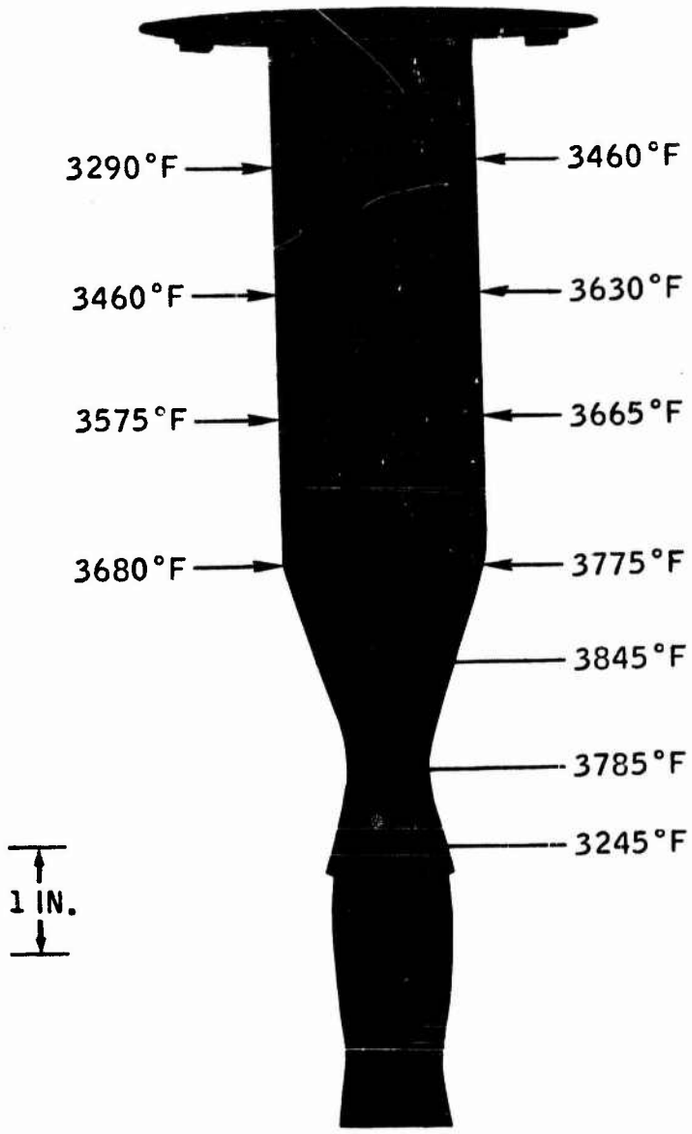

- CHAMBER C100-5-15
- INJECTOR T14817
- RUN NO. 169
- P_c = 100
- O/F = 12
- L*=38

(APPROX) STEADY STATE, 18 SECONDS AFTER IGNITION

- MEASURED WITH XR FILM

CT6015-14CN

FIGURE 44. (U) Temperatures of 100-lb Thrust PG Chamber During LF_2/GH_2 Test Firing, No Fuel Film Cooling

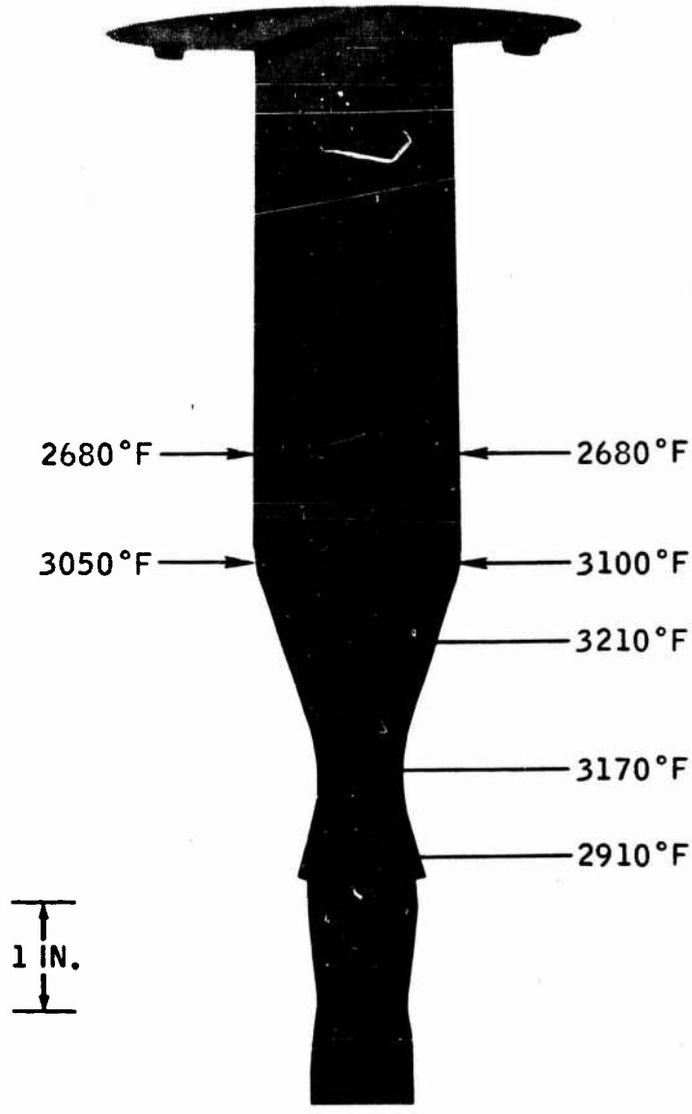

- CHAMBER C100-5-11
- INJECTOR T14817
- RUN NO. 167
- P_c = 100
- O/F =12
- L* = 24

(APPROX) STEADY STATE, 20 SECONDS AFTER IGNITION

- MEASURED WITH XR FILM

CT6015-12CN

FIGURE 45. (U) Temperatures of 100-lb Thrust PG Chamber During LF_2/GH_2 Test Firing, 50% Fuel Film Cooling

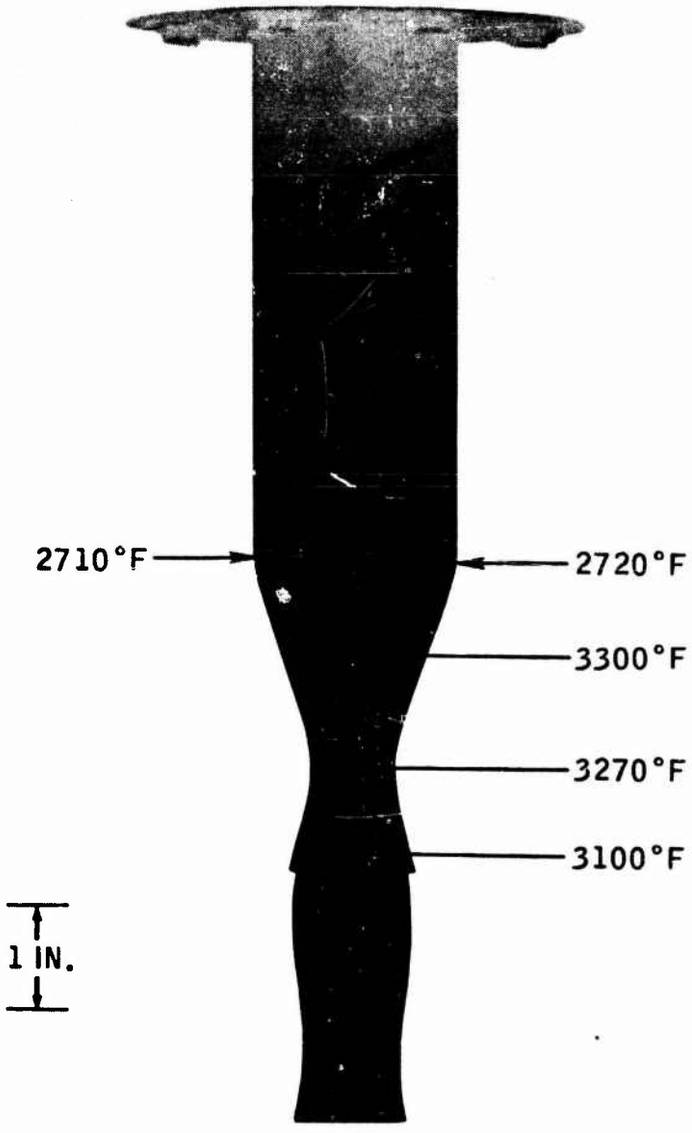

- CHAMBER C100-5-15
- INJECTOR T14817
- RUN NO. 168
- P_c = 100
- O/F = 12
- L*=12.5

(APPROX) STEADY STATE, 22 SECONDS AFTER IGNITION

- MEASURED WITH XR FILM

CT6015-13CN

FIGURE 46. (U) Temperatures of 100-lb Thrust PG Chamber During LF_2/GH_2 Test Firing, 50% Fuel Film Cooling

T6015-17

FIGURE 47. (U) C100-5-10 Chamber after Test Firing Run 177

FIGURE 48. (U) Inside of C100-5-10 Chamber after Test Firing Run 177

8512-1

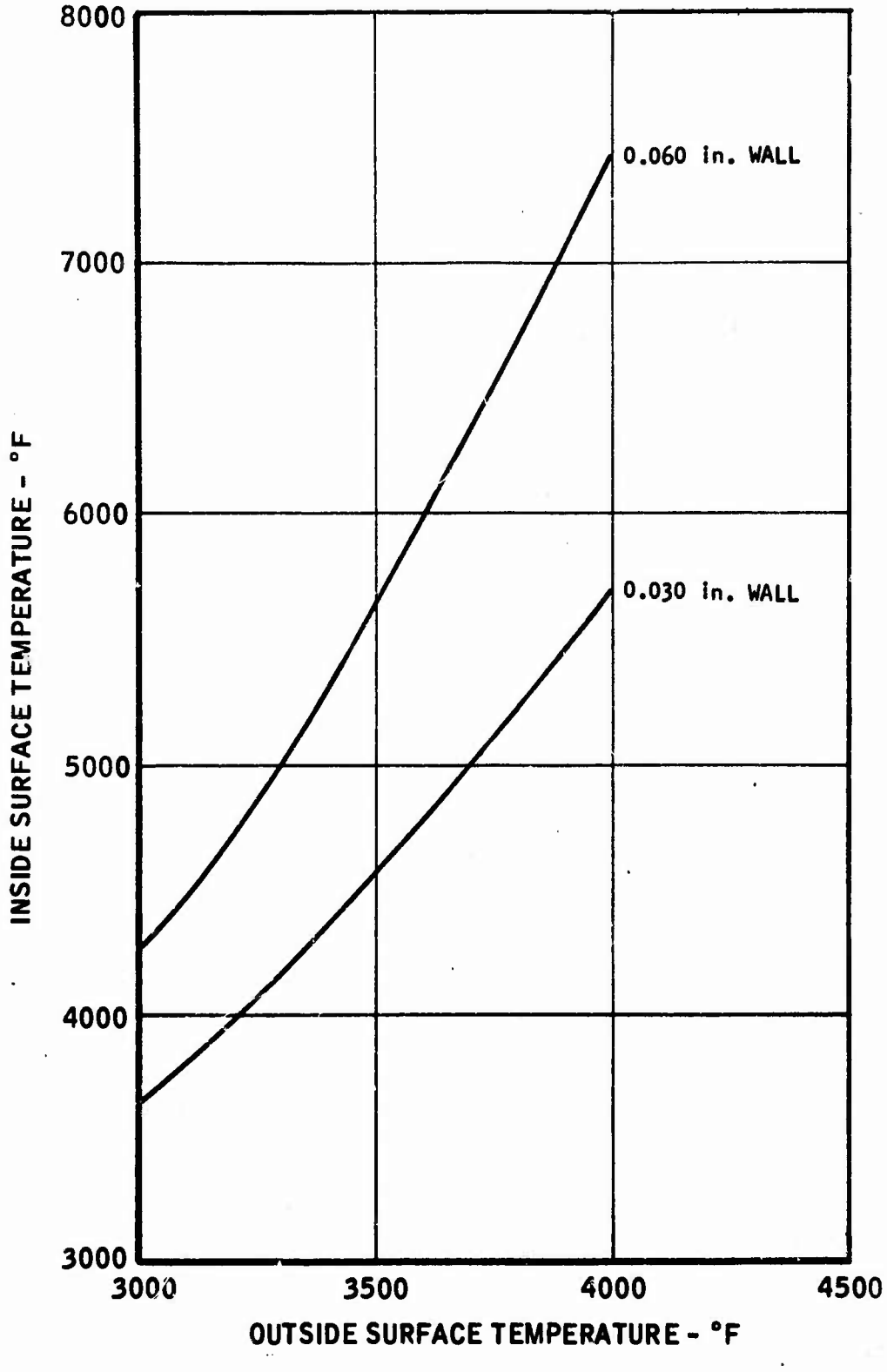

FIGURE 49. (U) Wall Temperatures of PG Chambers with 0.030 and 0.060-inch Thick Walls

5016-191

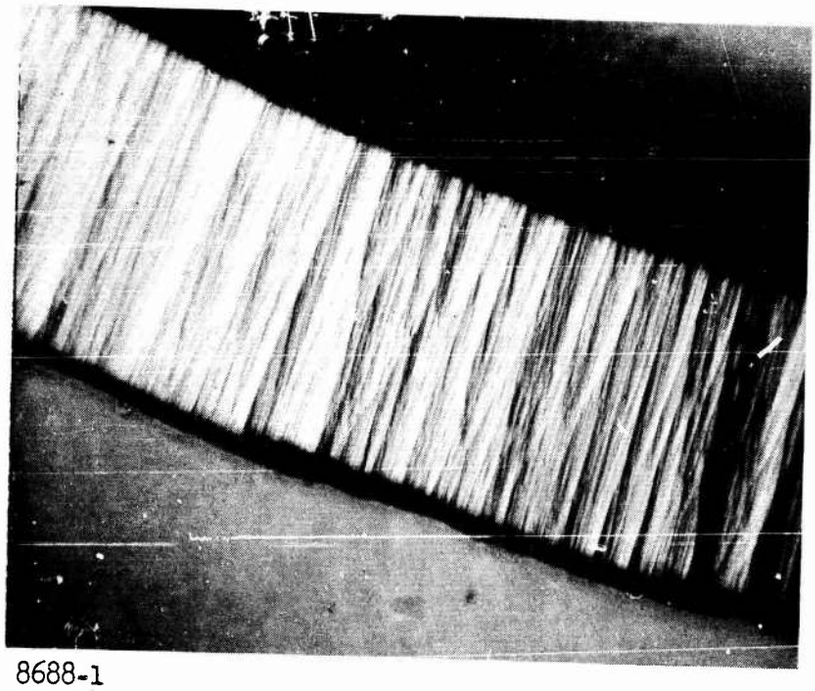

8688-1

A. C100-5-3 Chambers, as Deposited

INSIDE SURFACE ⇨

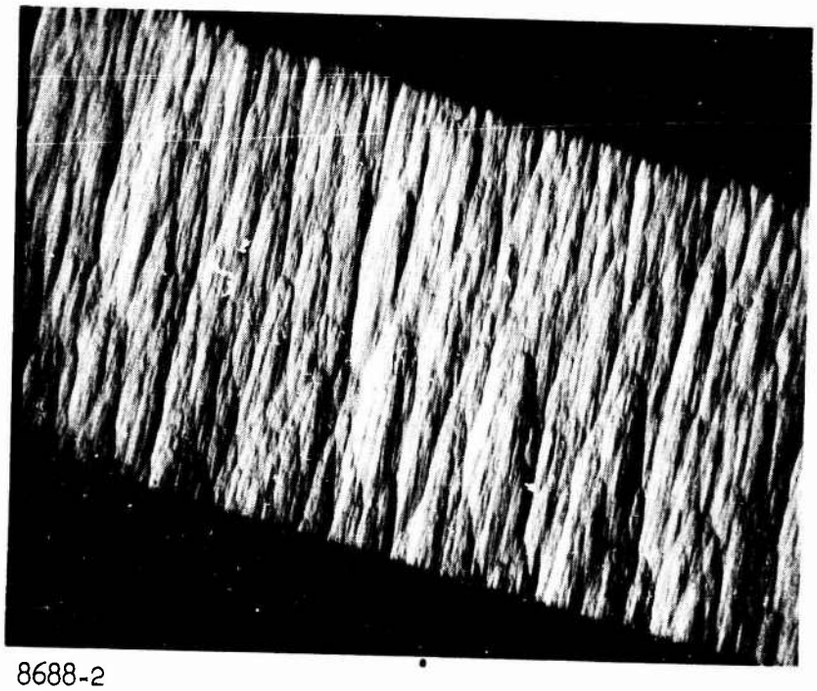

8688-2

B. C100-5-10 Chamber, after Test Firing, Run 177

FIGURE 50. (U) Microstructures of C100-5-3 and C100-5-10 Chambers (50X)

VII. CONCLUSIONS

(C) The major conclusions resulting from the test firing of free standing pyrolytic graphite thrust chambers are as follows:

1. Throat erosion rates were less than 0.10 mil/sec during test firings with LF_2/GH_2 and LF_2/BA1014.

2. Erosion of the chamber near the injector face was greater than in the throat, probably because of local concentrations of unreacted oxidizer.

3. Erosion of the pyrolytic graphite chamber near the injector face was controlled successfully when hydrogen film cooling from the injector was used. The hydrogen film cooling also reduced the erosion at the throat.

4. An attempt to control erosion near the injector by using BA1014 film cooling was unsuccessful. Other fuels such as hydrazine or MMH, which do not contain water, might be better for film cooling the pyrolytic graphite.

5. Oxidation of the outside of the pyrolytic graphite chamber by the atmosphere must be eliminated in order to demonstrate the maximum possible firing duration.

6. Throat erosion rates during test firings with $N_2O_4/0.5N_2H_4$-0.5UDMH were about 0.08 mil/sec when using an injector with 12 percent fuel film cooling. Attempts to reduce erosion by additional film cooling were unsuccessful.

7. There was no evident change in the microstructure of a pyrolytic graphite chamber which reached a temperature of 5700°F during 100 seconds of test firing.

8. A structural problem exists in the throat region of pyrolytic graphite free standing chambers due to high residual stresses. This problem was evidently responsible for failures of 40:1 altitude chambers during test firings and during vibration tests.

VIII. REFERENCES

1. Marquardt Report 6106, "(U) Free Standing Pyrolytic Graphite Thrust Chambers for Space Operation and Attitude Control. Phase I: Analysis and Preliminary Design", AFRPL-TR-66-95, 15 June 1966. UNCLASSIFIED.

2. Marquardt Report 5907, "(U) Final Report, Pyrolytic Graphite Rocket Thrust Chamber Development", 31 July 1962. UNCLASSIFIED.

3. Binford, J. S., Jr., and H. Eyring, "(U) Kinetics of Steam-Carbon Reaction", AD 294334, Tech. Note No. XII, Contract AF 33(638)-20839, Chem. Div., University of Utah, August 1955. UNCLASSIFIED.

UNCLASSIFIED

Security Classification

DOCUMENT CONTROL DATA - R&D

(Security classification of title, body of abstract and indexing annotation must be entered when the overall report is classified)

1. ORIGINATING ACTIVITY *(Corporate author)*

The Marquardt Corporation
Van Nuys, California

2a. REPORT SECURITY CLASSIFICATION

CONFIDENTIAL

2b. GROUP

4

3. REPORT TITLE

Free Standing Pyrolytic Graphite Thrust Chambers for Space Operation and Attitude Control Phase II: Small Scale Testing (U)

4. DESCRIPTIVE NOTES *(Type of report and inclusive dates)*

Final Report -- Phase II

5. AUTHOR(S) *(Last name, first name, initial)*

Campbell, J.G.
Haas, M.L.
Coulbert, C.D.

6. REPORT DATE	7a. TOTAL NO. OF PAGES	7b. NO. OF REFS
May 1967	118	3

8a. CONTRACT OR GRANT NO.	9a. ORIGINATOR'S REPORT NUMBER(S)
AF 04(611)-10790	TMC Report 6118
b. PROJECT NO. AFSC 3058	
c. AF Program Element Code: 6.24.05.18.4.	9b. OTHER REPORT NO(S) *(Any other numbers that may be assigned this report)* AFRPL-TR-67-98
d.	

10. AVAILABILITY/LIMITATION NOTICES In addition to the security requirements which must be met, this document is subject to special export controls and each transmittal to foreign governments or foreign nationals may be made only with prior approval of AFRPL (RPPR-STINFO), Edwards, California 93523.

11. SUPPLEMENTARY NOTES	12. SPONSORING MILITARY ACTIVITY
	Air Force Rocket Propulsion Laboratory Research and Technology Division Air Force Systems Command Edwards Air Force Base, California

13. ABSTRACT

(U) The results of test firing evaluation of forty-seven 100-pound thrust, free standing, pyrolytic graphite thrust chambers for application to high energy upper stage and attitude control liquid rocket engines are reported. The propellant combinations were LF_2/BA1014, LF_2/GH_2, and $N_2O_4/0.5N_2H_4$-0.5UDMH. The majority of the test firings were conducted at a chamber pressure of 100 psia; some tests were made at 300 psia. Chamber erosion rates and test firing durations are reported. Varying amounts of fuel film cooling were used in an attempt to control erosion of the PG chambers near the injector. The temperatures of the outside surface of a number of PG chambers were measured photographically by extended range film. Three PG chambers with 40:1 expansion nozzles were vibrated to study their structural integrity under boost vehicle vibration environments and a structural problem was found to exist at the nozzle throat due to high axial residual stresses on the outside surface of the chambers.

DD FORM 1 JAN 64 1473 0101-807-6800

UNCLASSIFIED

Security Classification

14. KEY WORDS	LINK A		LINK B		LINK C	
	ROLE	WT	ROLE	WT	ROLE	WT
THRUST CHAMBERS						
PYROLYTIC GRAPHITE						
SPACE OPERATION						
ATTITUDE CONTROL						

INSTRUCTIONS

1. ORIGINATING ACTIVITY: Enter the name and address of the contractor, subcontractor, grantee, Department of Defense activity or other organization *(corporate author)* issuing the report.

2a. REPORT SECURITY CLASSIFICATION: Enter the overall security classification of the report. Indicate whether "Restricted Data" is included. Marking is to be in accordance with appropriate security regulations.

2b. GROUP: Automatic downgrading is specified in DoD Directive 5200.10 and Armed Forces Industrial Manual. Enter the group number. Also, when applicable, show that optional markings have been used for Group 3 and Group 4 as authorized.

3. REPORT TITLE: Enter the complete report title in all capital letters. Titles in all cases should be unclassified. If a meaningful title cannot be selected without classification, show title classification in all capitals in parenthesis immediately following the title.

4. DESCRIPTIVE NOTES: If appropriate, enter the type of report, e.g., interim, progress, summary, annual, or final. Give the inclusive dates when a specific reporting period is covered.

5. AUTHOR(S): Enter the name(s) of author(s) as shown on or in the report. Enter last name, first name, middle initial. If military, show rank and branch of service. The name of the principal author is an absolute minimum requirement.

6. REPORT DATE: Enter the date of the report as day, month, year; or month, year. If more than one date appears on the report, use date of publication.

7a. TOTAL NUMBER OF PAGES: The total page count should follow normal pagination procedures, i.e., enter the number of pages containing information.

7b. NUMBER OF REFERENCES: Enter the total number of references cited in the report.

8a. CONTRACT OR GRANT NUMBER: If appropriate, enter the applicable number of the contract or grant under which the report was written.

8b, 8c, & 8d. PROJECT NUMBER: Enter the appropriate military department identification, such as project number, subproject number, system numbers, task number, etc.

9a. ORIGINATOR'S REPORT NUMBER(S): Enter the official report number by which the document will be identified and controlled by the originating activity. This number must be unique to this report.

9b. OTHER REPORT NUMBER(S): If the report has been assigned any other report numbers *(either by the originator or by the sponsor)*, also enter this number(s).

10. AVAILABILITY/LIMITATION NOTICES: Enter any limitations on further dissemination of the report, other than those imposed by security classification, using standard statements such as:

(1) "Qualified requesters may obtain copies of this report from DDC."

(2) "Foreign announcement and dissemination of this report by DDC is not authorized."

(3) "U. S. Government agencies may obtain copies of this report directly from DDC. Other qualified DDC users shall request through _____."

(4) "U. S. military agencies may obtain copies of this report directly from DDC. Other qualified users shall request through _____."

(5) "All distribution of this report is controlled. Qualified DDC users shall request through _____."

If the report has been furnished to the Office of Technical Services, Department of Commerce, for sale to the public, indicate this fact and enter the price, if known.

11. SUPPLEMENTARY NOTES: Use for additional explanatory notes.

12. SPONSORING MILITARY ACTIVITY: Enter the name of the departmental project office or laboratory sponsoring *(paying for)* the research and development. Include address.

13. ABSTRACT: Enter an abstract giving a brief and factual summary of the document indicative of the report, even though it may also appear elsewhere in the body of the technical report. If additional space is required, a continuation sheet shall be attached.

It is highly desirable that the abstract of classified reports be unclassified. Each paragraph of the abstract shall end with an indication of the military security classification of the information in the paragraph, represented as *(TS)*, *(S)*, *(C)*, or *(U)*.

There is no limitation on the length of the abstract. However, the suggested length is from 150 to 225 words.

14. KEY WORDS: Key words are technically meaningful terms or short phrases that characterize a report and may be used as index entries for cataloging the report. Key words must be selected so that no security classification is required. Identifiers, such as equipment model designation, trade name, military project code name, geographic location, may be used as key words but will be followed by an indication of technical context. The assignment of links, roles, and weights is optional.